The Impact of Trees on Temporal Variability in Urban Carbon and Water Budgets

A DISSERTATION
SUBMITTED TO THE FACULTY OF THE GRADUATE SCHOOL
OF THE UNIVERSITY OF MINNESOTA
BY

Emily Beth Peters

IN PARTIAL FULFILLMENT OF THE REQUIREMENTS
FOR THE DEGREE OF
DOCTOR OF PHILOSOPHY

Advisor: Joseph P. McFadden

June 2010

Acknowledgements

I would like to thank the many people who graciously helped me create this thesis. Most importantly, I thank Joe McFadden for his consistent support, excitement about my research, and valuable scientific conversations. I thank my committee members, Tim Griffis, Sarah Hobbie, and Rebecca Montgomery, for providing important insight and advice that greatly strengthened this thesis. I especially thank my adopted lab groups, the Hobbie and Montgomery labs, for providing exceptional advice on data analysis, scientific writing, and presentation techniques. Thanks to Ahmed Balogun, Leslie Brandt, Cinzia Fissore, Ben Freeman, Cheyne Hadley, Rebecca Hiller, Vicki Kalkirtz, Rebecca Koetter, Mark McPhail, Claudia Neuhauser, Julia Rauchfuss, Scott Shatto, Yana Sorokin, Tracy Twine, Harriet Van Vleck, and Jindong Wu for advice and field assistance that greatly improved the quality of my work. I would also like to thank John Baker, Peter Curtis, Michele Holbrook, Jeremiah Jazdzewski, Michael Loranty, Heather McCarthy, Diane Pataki, and Gary Newman for advice on field techniques and instrumentation; and Mark Holland, Aaron Rendahl and the Statistical Consulting Clinic for statistical advice.

This work was only possible because ~350 homeowners in Roseville, Saint Paul, Lauderdale, and Falcon Heights, Minnesota; Marge and Carl Jensen; Barbara and Rand Clausen; Eduardo Christ and Commonwealth Terrace Commons; Brian Heck, Heather Butkowski and the City of Lauderdale; and Les Potts, Doug Lauer, Tom Warnke and the University of Minnesota Landcare granted me permission to conduct repeated field sam-

pling on their property. I thank Joe McFadden and Rebecca Hiller for eddy covariance data from the turfgrass and KUOM field sites; Rebecca Montgomery for instrumentation to conduct sap flow and leaf gas-exchange measurements; Brian Horgan and Andy Holeman for advice and access to the University of Minnesota Turfgrass Research, Outreach, and Education Center; Larry Oberg for technical advice and access to the KUOM broadcast tower; Dave Ruschy for data from the University of Minnesota climate station; and Gary Reuter and the honeybee lab for supplying power to the Saint Paul sap flow site. I am grateful to Amy Caldwell, Ben Cooper, Charley Ertz, Greg Krogstad, John Lloyd and Rainbow Tree Care; Bernie Jabs, Cy Kosel, Scott Kruse, and the City of Saint Paul; Gordy Carleson, Mike Fredlund, Andy Long, Matthew Mednick, Gary Myhre, Leif Ruona, Ralph Sievert, Randy Windsperger, and the City of Minneapolis; and Jay Schroeder, Mark Stennes, Steve Sylvester and S&S Tree and Horticultural Specialists for providing aerial lift trucks and personnel time that allowed me to access urban tree canopies.

This work was financially supported by a Dayton Research Fellowship, a National Science Foundation Integrative Graduate Education and Research Trainingship, a University of Minnesota Interdisciplinary Doctoral Fellowship, an Ecological Society of America Urban Ecosystem Ecology Section Travel Grant, a Department of Ecology, Evolution and Behavior Travel Grant, and a grant to Joe McFadden from NASA Earth Science Division (NNG04GN80G).

Finally, I thank my family, Dave and Lisa Peters, Robert Broneak, and Anna Peters, for their emotional support and emergency field assistance.

Dedication

This dissertation is dedicated to my parents, Dave and Lisa Peters, whose curiosity about the world inspires me.

Abstract

Urbanization is responsible for some of the fastest rates of land-use change around the world, with important consequences for local, regional, and global climate. Vegetation can represent a significant proportion of many urban and suburban landscapes and modifies climate by altering local exchanges of heat, water vapor, and CO_2. To assess the contribution of plant functional types to urban ecosystem processes of water loss and carbon gain in a suburban neighborhood of Minneapolis–Saint Paul, Minnesota, USA, I investigated 1) the microclimate effects of different forest types over time, 2) the relative importance of environmental and biological controls on urban tree transpiration and canopy photosynthesis, and 3) the relative importance of trees and turfgrass on the spatial and seasonal variation in suburban evapotranspiration. Regardless of plant functional type, I found that seasonal patterns of soil and surface temperature were controlled by differences in stand-level leaf area index, and that sites with high leaf area index had soil and surface temperatures 7°C and 6°C lower, respectively, than sites with low leaf area index. Plant functional type differences in canopy structure and growing season length largely explained why evergreen needleleaf trees had significantly higher annual transpiration (307 kg H_2O m^{-2} yr^{-1}) and canopy photosynthesis (1.02 kg C m^{-2} yr^{-1}) rates per unit canopy area than deciduous broadleaf trees (153 kg H_2O m^{-2} yr^{-1} and 0.38 kg C m^{-2} yr^{-1}, respectively), offering an approach to scale up the tree component of urban water and carbon budgets. Turfgrass represented the largest contribution to annual evapotranspiration

in recreational and residential land-use types (87% and 64%, respectively), due to a higher fractional cover and greater daily water use than trees. Component-based estimates of suburban evapotranspiration underestimated measured water vapor fluxes by 3%, providing a useful approach to predict the seasonal patterns of evapotranspiration in cities. These finding have implications for the management of urban ecosystem services related to climate, carbon sequestration, and hydrology, and for predicting the impacts of climate change on urban ecosystems.

Table of Contents

Acknowledgements i

Dedication iii

Abstract iv

List of Tables ix

List of Figures x

Chapter 1
Introduction 1

Chapter 2
Influence of seasonality and vegetation type on suburban microclimates 8
- Summary 8
- Introduction 9
- Methods 12
  - Study area and site selection 12
  - LAI and microclimate measurements 14
  - Percent tree and ground cover measurements 17
  - Data analysis 18
- Results 19
  - Seasonal patterns of LAI and microclimate 19
  - Seasonal effects of LAI on microclimate 21
  - Site differences in LAI and microclimate 21
- Discussion 22
  - Seasonal patterns of LAI and microclimate variables 22
  - Site differences in mid-season microclimate and ground cover 27
  - Using tree cover to predict site differences in mid-season LAI 29
- Conclusions 31

Chapter 3
Biological and environmental controls on tree transpiration in a suburban landscape 42
- Summary 42
- Introduction 43
- Methods 47
  - Study sites 47

Field measurements 49
Data analysis 54
Results 55
Environmental conditions 55
Sap flux density 56
Transpiration 59
Discussion 60
Sap flux density differences among tree types 60
Responses to environmental drivers 61
Transpiration differences among tree types 64
Conclusions 67

Chapter 4
Seasonal contributions of vegetation types to suburban evapotranspiration 84
Summary 84
Introduction 85
Methods 88
Site information 88
Measuring suburban evapotranspiration and its component fluxes 90
Meteorological measurements 97
Scaling up component fluxes 98
Results 102
Land cover 102
Environmental conditions 102
Ecosystem evapotranspiration 103
Component evapotranspiration fluxes 104
Comparing component-based and eddy covariance-measured E_{total} 105
Comparing E_{total} fom two suburban land-use types 106
Discussion 108
Suburban evapotranspiration 108
Scaling component-based fluxes 109
Contributions of trees and turfgrasses to suburban E_{total} 114
Land-use comparisons 115
Conclusions 118

Chapter 5
Conclusion 131
Research summary 132
Implications for future research 133
Conclusion 135

References 136

Appendix 1
Estimating canopy photosynthesis using leaf gas-exchange and sap flow measurements 149
Introduction 149
Methods 150
Results 153
Discussion 154

List of Tables

Table 2-1. Forest characteristics of 29 suburban study sites, ground by vegetation type 32

Table 3-1. Fractional contribution of nine tree genera to the total stem count, canopy area, and basal area (cross-sectional area measured at 1.4 m) of trees >5 cm DBH in a forest inventory of a suburban neighborhood of Minneapolis–Saint Paul, Minnesota 69

Table 3-2. Site, plant functional type, xylem anatomy, shade tolerance, mean projected canopy area, mean leaf area index, mean sapwood depth, mean diameter at 1.4 m (DBH), and mean height by tree species per year 70

Table 3-3. Average maximum, mean, and minimum air temperature for day and night periods during the 2007 and 2008 growing seasons (DOY 165-250) 72

Table 3-4. Parameters for the exponential saturation model $J_S = a(1 - \exp(-bD_Z))$ for six genera in June and September 2008 73

Table 3-5. Growing season means of daily sap flux density per unit sapwood area, transpiration per unit canopy area, transpiration per unit leaf area, and annual sums of E_C for six genera in 2008 74

Table 4-1. Cover types by percentage of the flux footprint area, residential land-use area, and recreational land-use area 120

Table A1-1. Number of trees measured, site, and parameters from the linear regression model, $y = ax$, between leaf-level photosynthesis and stomatal conductance for nine tree species 156

List of Figures

Figure 2-1. Environmental conditions during the 2006 growing season at the open turfgrass references site 33

Figure 2-2. Seasonal patterns during the 2006 growing season of measured stand-level leaf area index, soil temperature, and infrared surface temperature of the ground cover of five suburban vegetation types..... 34

Figure 2-3. Mean mid-season stand-level leaf area index, soil temperature at 10 cm depth, and infrared surface temperature of five suburban vegetation types 36

Figure 2-4. Relationships between modeled stand-level leaf area index, relative soil temperature, and relative surface temperature during the 2006 growing season..... 37

Figure 2-5. Comparing satellite-derived and field-based tree cover measurements as predictors of modeled mid-season LAI 38

Figure 2-6. Comparing modeled mid-season LAI and field-based tree cover measurements as predictors of mid-season soil temperature, and mid-season surface temperature 39

Figure 2-7. Comparing modeled mid-season LAI and field-based tree cover measurements as predictors of turfgrass cover, bare soil cover, broad-leaved weed cover, and turfgrass + broad-leaved weed cover..... 40

Figure 3-1. Photosynthetically active radiation, mean daily air temperature, mean daytime vapor pressure deficit, soil water content, and precipitation in a suburban neighborhood of Minneapolis–Saint Paul, Minnesota. 75

Figure 3-2. Daily sums of sap flux density per unit sapwood area for seven tree genera measured in a suburban neighborhood of Minneapolis–Saint Paul, Minnesota..... 77

Figure 3-3. Average diurnal patterns of sap flux density per unit sapwood area for three groups of trees in a suburban neighborhood of Minneapolis–Saint Paul, Minnesota..... 79

Figure 3-4. Daily sums of sap flux density per unit sapwood area in response to day length normalized mean daytime vapor pressure deficit in a suburban neighborhood of Minneapolis–Saint Paul, Minnesota..... 80

Figure 3-5. Daily sums of sap flux density per unit sapwood area in response to daily sums of photosynthetically active radiation in a suburban neighborhood of Minneapolis–Saint Paul, Minnesota 81

Figure 3-6. Daily sums of transpiration per unit canopy area in evergreen needleleaf and deciduous broadleaf plant functional types in a suburban neighborhood of Minneapolis–Saint Paul, Minnesota 82

Figure 3-7. Total annual transpiration per unit canopy area in evergreen needleleaf and deciduous broadleaf plant functional types in a suburban neighborhood of Minneapolis–Saint Paul, Minnesota 83

Figure 4-1. Land cover classification derived from 2.4-m resolution QuickBird imagery for a 1 km radius surrounding the KUOM tall tower in a suburban neighborhood of Minneapolis–Saint Paul, Minnesota. 121

Figure 4-2. Environmental conditions in a suburban area of Minneapolis–Saint Paul, MN from 1 January 2007 to 31 December 2008 123

Figure 4-3. Daytime sums of ecosystem evapotranspiration per month measured at the 40 m level of the KUOM tower over a suburban area of Minneapolis–Saint Paul, Minnesota 124

Figure 4-4. (a) Average daily sums of measured evapotranspiration per cover area for non-irrigated turfgrass, evergreen needleleaf trees, and deciduous broadleaf trees per month across the 2008 growing season in a suburban area of Minneapolis–Saint Paul, Minnesota. (b) Average summertime (June to August) daily sums of evapotranspiration per cover area in 2008 for measured and modeled vegetation components 125

Figure 4-5. Comparison of half-hourly measured and scaled component sums of ecosystem evapotranspiration in a suburban area of Minneapolis–Saint Paul, Minnesota 126

Figure 4-6. Comparison of half-hourly measured and scaled component sums of ecosystem evapotranspiration in a suburban area of Minneapolis–Saint Paul, Minnesota during spring (April and May), summer (June to August), and fall (September to November) 127

Figure 4-7. Average daytime ecosystem evapotranspiration per month measured over two land-use types, recreational and residential, in a suburban area of Minneapolis–Saint Paul, Minnesota 128

Figure 4-8. (a) Annual precipitation and annual evapotranspiration of scaled component fluxes, trees, turfgrass, and open water, from the residential and recreational land-use ar-

eas. The average proportional contribution of vegetation components to ecosystem evapotranspiration from (b) residential and (c) recreational land-use areas per month .. 129

Figure A1-1. Relationships between leaf-level photosynthesis and stomatal conductance for nine tree species in a suburban neighborhood of Minneapolis–Saint Paul, Minnesota 157

Figure A1-2. Daily sums of canopy photosynthesis per unit canopy area for six tree genera in a suburban neighborhood of Minneapolis–Saint Paul, Minnesota 158

Figure A1-3. Annual sums of canopy photosynthesis per unit canopy area in evergreen needleleaf and deciduous broadleaf plant functional types in a suburban neighborhood of Minneapolis–Saint Paul, Minnesota 159

Chapter 1

Introduction

Half the world's population currently lives in urban areas, a proportion that is projected to increase to 60% by 2030 (United Nations 2005). This rapid population growth in urban areas is driving one of the fastest rates of land-use change around the world, with important consequences for local, regional and global climate (Pielke et al. 2002, Grimmond 2007). The clearing of agricultural or natural ecosystems for the built-up structures, impervious surfaces, and managed vegetation of urban development directly and indirectly impacts climate by altering the surface-energy balance (Oke 1982) and carbon cycle (Pataki et al. 2006a). While urban areas represent major sources of CO_2 and alter hydrology, they are also ecosystems with significant vegetation cover (Rowntree 1984) that exert direct control over land–atmosphere exchanges of water and carbon through the physiological processes of transpiration, photosynthesis, and respiration. In addition, plants indirectly control these land–atmosphere fluxes through biophysical properties, such as albedo, surface roughness, and leaf area index (LAI) or vegetation density, that drive changes in local microclimates (Smith and Johnson 2004, Tanaka and Hashimoto 2006). To manage a variety of ecosystem services in urban areas, including reduced surface temperature (Oke 1989, Leuzinger et al. 2010), increased energy efficiency (McPherson et al. 2005), mitigation of storm water runoff (Mitchell et al. 2008, Wang et al. 2008), and increased carbon sequestration (Nowak and Crane 2002), cities are increas-

ingly promoting the use of trees (*i.e.* recent "million trees" campaigns in Los Angeles and New York). Efforts to predict and manage these ecosystem services at the scale of whole neighborhoods or cities, however, are complicated by our limited understanding of how species vary in their microclimate effects, rates of water use and carbon uptake over time.

While a substantial amount of research has been done on the microclimate effects, water use, and carbon uptake of plants in natural ecosystems, the altered environmental conditions in urban and suburban areas limit the extrapolation of these measurements (Clark and Kjelgren 1990, Cregg and Dix 2001, Gregg et al. 2003). Elevated air temperature and vapor pressure deficit caused by the urban heat island effect relative to surrounding areas can alter the water use and carbon uptake of urban trees (Whitlow and Bassuk 1988, Whitlow et al. 1992, Kjelgren and Montague 1998, Mueller and Day 2005, Bush et al. 2008). Microclimate variability is relatively high in urban areas due to the spatial heterogeneity of surface types with different energy balances and heat storage capacities, and results in high rates of advectively-enhanced evapotranspiration from vegetated areas (Oke 1979, Spronken-Smith et al. 2000). Large amounts of impervious surface and compacted soils alter local hydrological processes and soil water content (Craul 1985), another important control on plant physiological processes (Kramer 1987, Lagergren and Lindroth 2002, Holscher et al. 2005). Moreover, the species composition of urban and suburban ecosystems can differ considerably from forests in surrounding areas, with built-up areas having generally higher frequencies of invasive and non-native species as well as human-cultivated varieties (McKinney 2002, Hahs et al. 2009, Walker et al. 2009).

Plant functional types (*e.g.* evergreen needleleaf trees or deciduous broadleaf trees) provide a potentially useful approach for examining the direct and indirect climate effects of vegetation in urban and suburban areas, as they represent major differences in physiology, biophysical properties, and leaf phenology among plant species (Reich et al. 1998). For example, evergreen needleleaf trees tend to have lower leaf-level transpiration rates and a longer leaf lifespan than deciduous broadleaf trees (Givnish 2002). Although rarely parameterized for urban ecosystems, hydrologic and land-surface models also use plant functional types to represent land–atmosphere exchanges of energy, water, and carbon in natural and agricultural ecosystems (Foley et al. 1998, Bonan et al. 2003). In addition, plant functional types can now be uniquely classified in urban landscapes using high-resolution satellite imagery (Tooke et al. 2009), allowing the extrapolation of local measurements to neighborhood and city scales. While previous studies have shown that vegetation cover and composition influence microclimate characteristics (Bonan 2000, Byrne et al. 2008, Huang et al. 2008), ecosystem evapotranspiration (Grimmond and Oke 1999, Offerle et al. 2006), and CO_2 fluxes (Moriwaki and Kanda 2004) in urban areas, no work has previously examined the combined effects of different plant functional types on the seasonality of urban microclimates, evapotranspiration, and carbon uptake.

The goal of my research is to fill current gaps in our understanding of how trees impact the temporal variability in urban carbon and water budgets. In my dissertation, I focus on a first-ring suburban neighborhood in Minneapolis–Saint Paul, Minnesota in north-central United States. Urban and suburban land use represents a significant percentage (over 14%) of the Upper Midwest region of the United States and suburban, low-

density residential land use, in particular, is increasing more rapidly than any other land-use type in the region (Radeloff et al. 2005). This area experiences cold, dry winters and warm, humid summers, and is sensitive to changes in climate due to its northern continental location. Local vegetation is also representative of regionally distinct plant functional types and species, potentially allowing the extrapolation of my results to other developed areas in the Upper Midwest region.

In Chapter 2, I examine how distinct urban forest types influence microclimate effects over time using a field-based observational study. I measured stand-level LAI, soil temperature, infrared surface temperature, and soil water content over a full growing season to determine how seasonal patterns of leaf development and microclimate are influenced by plant functional type. I also determined how seasonal changes in LAI modulate urban forest microclimates. I evaluated the ability of two tree canopy metrics, percent tree cover and LAI, to explain the variation in mid-summer microclimates among suburban vegetated areas. In addition, I evaluated the ability of satellite-derived and field-based estimates of tree cover to predict and scale up the variation in urban biophysical properties.

In Chapter 3, I examine the relative importance of biological and environmental controls on urban tree transpiration using a comparative sap flux study. I made continuous sap flux measurements across two growing seasons to determine how suburban tree species vary in their water use in response to environmental drivers, including vapor pressure deficit, photosynthetically active radiation, and soil moisture. I tested for differences in transpiration between evergreen needleleaf and deciduous broadleaf plant func-

tional types, as well as for differences among other tree classification schemes (*e.g.* by genus, xylem anatomy, and shade tolerance). I also evaluated the ability of different tree classification schemes to scale up and predict the tree transpiration component of urban and suburban water budgets.

In Chapter 4, I examine how plant functional types influence the spatial and seasonal variation in suburban evapotranspiration rates using a field-based observational study. I used measurements from a 40 m eddy covariance system to determine the magnitude and seasonal patterns of suburban ecosystem evapotranspiration. Using independent measurements of tree transpiration from Chapter 3 along with turfgrass evapotranspiration from a 1.35 m portable eddy covariance system, I scaled up tree and turfgrass evapotranspiration rates and evaluated how well these component-based estimates matched measured ecosystem evapotranspiration. In addition, I examined how the magnitude and seasonality of ecosystem evapotranspiration varies between residential and recreational land-use types and how tree and turfgrass component fluxes influence these seasonal patterns of ecosystem evapotranspiration.

In Appendix 1, I examine how urban tree species vary in their rates of carbon uptake over time using a field-based observational study. I calculated canopy photosynthesis rates using leaf gas-exchange and sap flow (Chapter 3) measurements to determine how urban tree species vary in their rates of canopy photosynthesis across the growing season. I also evaluated the ability of plant functional types to scale up and predict the tree component of urban and suburban carbon budgets.

In this dissertation, it is my aim is to quantify the spatial and temporal controls on how trees influence exchanges of water vapor and CO_2 between the land and the atmosphere in urban ecosystems. Through a series of field-based observational studies, I will assess how plant functional types both indirectly and directly control these land–atmosphere fluxes through their effects on microclimate, evapotranspiration, and canopy photosynthesis. By utilizing theories and techniques from ecosystem ecology, micrometeorology, and plant physiology, this work will contribute to a greater understanding of how plants control the climate and hydrology of urban and suburban ecosystems. This work provides information that contributes to the development of urban land-surface models by providing parameters specific to urban landscapes. Finally, this work is also expected to provide improvements for predicting carbon and water budgets in urban areas, particularly with changes in land-use and climate, for the improved management of urban ecosystem services.

from Paul, Melinda, Springer US <Melinda.Paul@springer.com>
to e.peters2000@gmail.com
cc "Leon de, Mhanilet" <Mhanilet.deLeon@springer.com>
date Tue, Jun 1, 2010 at 3:23 PM
subject RE: Permission Request

Dear Emily Peters,

Permission is granted provided that full acknowledgement is given to the original source of publication.

Thank you for your contribution to Urban Ecosystems.

With kind regards,

Melinda (Lindy) Paul
Springer
Senior Editor
Environmental Science
233 Spring St | New York, NY 10013-1578
tel (781) 347-1835
melinda.paul@springer.com

----- Original Message-----
From: e.peters2000@gmail.com
Sent: Sat 5/22/2010 1:28 AM
To: Leon de, Mhanilet
Subject: Permission Request

Dear Dr. Deleon

I would like to include a reprint of my paper (see below) in my PhD dissertation. The University of Minnesota, where I am a student, requires a letter from the publisher granting me permission to reprint the work. I was wondering if I could get permission to include my paper in my dissertation, and if I could receive a letter granting such permission.

Sincerely,

Emily Peters

Peters, E. B., and J. P. McFadden. 2010. Influence of seasonality and vegetation type on suburuban microclimates. Urban Ecosystems, doi: 10.007/s11252-010-0128-5.

Chapter 2

Influence of seasonality and vegetation type on suburban micro-climates*

* *With Joseph McFadden.* Reproduced with permission from Urban Ecosystems from: Peters, E. B., and J. P. McFadden. 2010. Influence of seasonality and vegetation type on suburban microclimates. Urban Ecosystems, doi:10.007/s11252-010-0128-5.

Summary

Urbanization is responsible for some of the fastest rates of land-use change around the world, with important consequences for local, regional, and global climate. Vegetation, which represents a significant proportion of many urban and suburban landscapes, can modify climate by altering local exchanges of heat, water vapor, and CO_2. To determine how distinct urban forest communities vary in their microclimate effects over time, we measured stand-level leaf area index, soil temperature, infrared surface temperature, and soil water content over a complete growing season at 29 sites representing the five most common vegetation types in a suburban neighborhood of Minneapolis-Saint Paul, Minnesota. We found that seasonal patterns of soil and surface temperatures were controlled more by differences in stand-level leaf area index and tree cover than by plant functional type. Across the growing season, sites with high leaf area index had soil temperatures that were 7°C lower and surface temperatures that were 6°C lower than sites with low leaf area index. Site differences in mid-season soil temperature and turfgrass ground cover

were best explained by leaf area index, whereas differences in mid-season surface temperature were best explained by percent tree cover. The significant cooling effects of urban tree canopies on soil temperature imply that seasonal changes in leaf area index may also modulate CO_2 efflux from urban soils, a highly temperature-dependent process, and that this should be considered in calculations of total CO_2 efflux for urban carbon budgets. Field-based estimates of percent tree cover were found to better predict mid-season leaf area index than satellite-derived estimates and consequently offer an approach to scale up urban biophysical properties.

Introduction

Vegetation alters local, regional, and global climate in part by controlling the exchanges of energy, water and carbon between land and the atmosphere (Foley et al. 2003). Plants exert direct control over land–atmosphere exchanges of water and carbon through the physiological processes of transpiration, photosynthesis, and respiration. In addition, plants indirectly control these land–atmosphere fluxes through biophysical properties, such as albedo, surface roughness, and leaf area index (LAI) or vegetation density, that drive changes in local microclimates (Smith and Johnson 2004, Tanaka and Hashimoto 2006).

In urban and suburban areas, vegetation cover has been shown to be important for explaining spatial differences in urban and suburban evapotranspiration rates (Grimmond and Oke 1999, Spronken-Smith 2002), net CO_2 exchange (Soegaard and Møller-Jensen

2003, Moriwaki and Kanda 2004), and microclimate characteristics (Bonan 2000, Byrne et al. 2008, Huang et al. 2008). For example, Spronken-Smith (2002) found that residential neighborhoods in Christchurch, New Zealand with high vegetation cover had greater evapotranspiration rates than did neighborhoods with less vegetation cover. Grimmond and Oke (1999) showed that the variability among North American cities in evapotranspiration rates was related to differences in the percent cover of vegetated surfaces, in addition to differences in precipitation and irrigation inputs. Determining the causes of spatial variation in CO_2 fluxes in cities is relatively more complex, and depends on housing density and traffic volume (Nemitz et al. 2002a, Coutts et al. 2007); however Moriwaki and Kanda (2004) showed that tree cover played an important role in driving the summertime CO_2 sink observed in a residential area of Tokyo, Japan. Previous studies have also found that vegetation cover and composition influence urban microclimate characteristics, such as air temperature, soil temperature, and surface temperature (Bonan 2000, Byrne et al. 2008, Huang et al. 2008). These ideas have been extended by several recent studies showing that the density of vegetation or LAI plays an important role in explaining the spatial variation in urban surface temperatures as well (Hardin and Jensen 2007, Jenerette et al. 2007). LAI provides a measure of the total amount of leaf surface area that can exchange heat, water, and CO_2 with the atmosphere, whereas percent cover provides only a measure of the presence or absence of vegetation. Percent vegetation cover, however, is a relatively easier metric to assess in urban areas using a variety of methods, including field-based inventories, aerial photographs, and satellite imagery (Walton et al. 2008).

Land surface models, which represent land–atmosphere exchanges of energy, water and carbon, are rarely parameterized for urban and suburban ecosystems, in part because these landscapes are so spatially complex (Pielke and Avissar 1990). Accounting for the direct and indirect climate effects of distinct urban ecological communities and plant compositions would greatly advance the development of these models. Plant functional types (*e.g.* evergreen needle-leaved trees or deciduous broad-leaved trees) offer a way to organize ecologically distinct groups of plants that represent major differences in physiology, biophysical properties, and leaf phenology (Reich et al. 1998), and are currently used to model the direct and indirect climate effects of vegetation in natural and agricultural ecosystems (Foley et al. 1998). Leaf phenology, or seasonal variation in LAI, is one of the most important ways by which different types of plants can influence the physical environment over time (Arora and Boer 2005). For example, evergreen trees have relatively constant leaf area throughout the year, while deciduous trees show much greater seasonal variability in leaf area. These seasonal differences in LAI influence the amount of solar radiation intercepted by the canopy, and transpiration and photosynthesis rates, over the course of the growing season.

In this study, we examined how distinct urban forest communities vary in their microclimate effects over the course of the growing season. We measured both the vegetation type differences and seasonal patterns of stand-level LAI, soil temperature, infrared surface temperature, and soil water content over a full growing season in a suburban residential neighborhood of Minneapolis–Saint Paul, Minnesota. Our objectives were to: 1) determine how seasonal patterns of leaf development and microclimate are influenced by

plant functional type; 2) determine how seasonal changes in LAI modulate urban forest microclimates; 3) evaluate the ability of percent tree cover and LAI to explain the variation in mid-season microclimates and percent ground cover among suburban vegetated areas; and 4) evaluate the ability of satellite-derived and field-based estimates of tree cover to predict and scale up the variation in urban biophysical properties in a suburban neighborhood.

Methods

Study area and site selection

In the Upper Midwest region of the United States, urban and suburban land use represents a significant percentage (over 14%) of the regional land surface. Suburban, low density residential land use, in particular, is increasing more rapidly than any other land-use type in the region (Radeloff et al. 2005). Our study area was located in a first-ring suburban neighborhood in the Minneapolis–Saint Paul metropolitan area in east-central Minnesota. The landscape (approximately 9 km^2) was a single-family residential area located at the border of Saint Paul and the suburbs of Roseville, Falcon Heights, and Lauderdale. Vegetated surfaces represented over 50% of the landscape, consisting of isolated trees, forested patches, and open turfgrass lawns.

We used true color aerial orthophotos with 0.15 m resolution (State of Minnesota 2006) to identify potential study sites that had dimensions of approximately 30 m × 30 m and were representative of the five most common vegetation types in the area (Table 1).

These five vegetation types consisted of three distinct plant functional types, deciduous broad-leaved trees, evergreen needle-leaved trees, and cool-season turfgrass lawns. We included two categories of deciduous tree cover because we observed a wide range of cover among the deciduous sites. We divided the deciduous sites into those having sparse or low cover (DL), with ≤ 40% tree cover, and those having high cover (DH), with ≥ 60% tree cover. Using two levels of deciduous tree cover allowed us to evaluate the relative importance of plant functional type versus percent tree cover in influencing urban bio-physical properties. We did not find a wide range of tree cover in areas dominated by evergreen species, so we could not employ a full-factorial experimental design. We selected sites that were approximately 30 m × 30 m in area because that size was large enough to minimize edge effects in ground-based optical LAI measurements but small enough to encompass relatively homogenous stands of the different vegetation types. The area of the sites also corresponds approximately to the pixel sizes of satellite remote sensing imagery that is commonly used for mapping urban features over extensive areas (*e.g.*, 30-m Landsat or 20-m SPOT). Based on a spring field survey, we verified the vegetation composition of potential sites and eliminated those sites with significant discontinuities in vegetation type, steep slopes that would complicate optical LAI measurements, or obstacles such as large fences. We selected sites where the ground cover was dominated by turfgrass because that was the most common ground cover type in the area. We did not stratify sites based on land management practices (*e.g.*, fertilization, irrigation, mowing, or pruning) because our 30 m × 30 m sites encompassed the land of multiple owners and because our replicate sites in each vegetation type were intended to broadly represent the

landscape as a whole. For each of the 29 selected sites, we obtained permission to access the property through personal communication with homeowners.

LAI and microclimate measurements

During the 2006 growing season, from leaf-out in April until leaf senescence in November, we measured a suite of biophysical variables weekly at each site. All measurements were collected at the geographic center of the site. Stand-level LAI (leaf area per plot area) was measured using an optical plant canopy analyzer (model LAI-2000, LI-COR, Lincoln, Nebraska, USA) on days when sky conditions were overcast or on clear sky days when the solar angle was low to avoid direct sunlight hitting the sensor. Because our LAI measurements reflect stand-level values, they represent the combined effects of the canopy density of tree-covered areas and the percent tree cover at each site. To prevent interference with the measurements, a 270° view cap was used to block the 90° horizontal angle of the sensor's view that was nearest to the operator. Each LAI measurement consisted of one above-canopy reading and the mean of four below-canopy readings taken in the cardinal directions at a distance of 1 m from the center point of each site, and at a height of 1 m above the ground. The above-canopy readings recorded the background light conditions and were collected in nearby open areas, such as sports fields or large parking lots without obstructions blocking the sky view. The LAI-2000 optical sensor consists of five detectors arranged in concentric rings, each with a different field of view. To ensure that the field of view of each LAI measurement was within the boundaries of each site, we used only the four inner rings (0 to 58° from zenith). Tree canopies were the

dominant source of leaf area to these stand-level LAI measurements, as understory vegetation was rarely present above the 1-m measurement height.

Seasonal LAI dynamics at each site were modeled by fitting two piecewise logistic curves to the LAI measurements (Zhang et al. 2003). At sites with evergreen tree canopies, both measured and modeled LAI were corrected for leaf clumping using a correction factor of 1.6, according to the manufacturer's recommendations for the LAI-2000. At sites with deciduous tree canopies, modeled and measured LAI were corrected for the influence of stems and branches, or wood area index (WAI), which varies seasonally with leaf development and senescence (Breda 2003). The modeled LAI curves were used to establish a WAI correction factor (α) that varied from zero during the middle of the growing season to unity outside the growing season (Dufrene and Breda 1995). The WAI was defined as the leaf-off LAI measurement collected at each site in November 2006. LAI at deciduous sites was corrected using $LAI_{corr} = LAI - (\alpha\ WAI)$. At sites with mixed tree canopies, measured and modeled LAI were divided into two pools, evergreen LAI and deciduous LAI, based on the proportion of evergreen and deciduous tree cover. The proportion of each tree cover type was estimated using a leaf-off aerial photograph with a 0.15 m resolution (State of Minnesota 2006) and separately digitizing the evergreen and deciduous tree canopies within an 18-m radius of each site's center point, which corresponded to the average field of view of the LAI measurements. The evergreen and deciduous LAI pools were separately corrected using the methods described above for pure evergreen and pure deciduous stands, then summed to calculate the corrected LAI at mixed sites.

On each sampling day, we collected microclimate measurements between 08:00 and 17:00 h by taking the mean of four readings in the cardinal directions at a distance of 1 m from the center point of each site. Soil temperature at 10 cm depth was measured using a thermister temperature probe (model Acorn Temp 5, Oakton, Vernon Hills, Illinois, USA, accuracy ± 0.2ºC). Surface temperature of the ground cover was measured using an infrared radiometer (model IRTS-P, Campbell Scientific, Inc., Logan, Utah, USA, accuracy ± 0.3ºC) held 0.5 m directly above the surface. Soil water content was measured at 5 cm depth using a frequency-domain reflectometer (model ML2x ThetaProbe, Delta-T Devices, Ltd., Cambridge, England, accuracy ± 1%). Because soil and surface temperature vary throughout the day with changes in solar radiation and weather, our spot measurements collected at different times of day could not be directly compared among sites. Instead, we used continuous temperature measurements at a nearby climate station to normalize all of the spot measurements so that they could be compared among the sites. We analyzed all temperatures as the difference between each spot measurement at each site and the temperature recorded at the same time point at the climate station. The climate station was located within our study area (<1 km from all measured sites) in an open turfgrass lawn, which was representative of low-maintenance lawns in the area—it was not irrigated and it was mowed approximately once per week with clippings left to decompose on the surface. The temperature of the upper 5 to 10 cm soil layer was continuously measured using two linear platinum resistance temperature probes (model STP-1, REBS, Inc., Seattle, Washington, USA, accuracy ± 0.5ºC). Air temperature was continuously measured 1.4 m above the ground using a sonic anemometer (model CSAT3,

Campbell Scientific, Inc., accuracy ± 0.025ºC). The sonic temperature was corrected following Schotanus et al. (1983) to calculate the actual air temperature. Half-hour averages of the reference temperature measurements were recorded using a datalogger (model CR1000, Campbell Scientific, Inc.). We present results as relative soil temperature (site soil temperature minus reference soil temperature) and relative surface temperature (site surface temperature minus reference air temperature). Although soil temperature measurements collected at 10 cm depth were referenced against soil temperature averaged over 5 to 10 cm depth, and surface temperature measurements were referenced against air temperature, these relative temperatures remove the effects of diurnal changes in solar radiation and weather and provide a meaningful way to compare the microclimate effects of vegetation type.

Percent tree and ground cover measurements

Field-based measurements of percent tree cover were made following the U.S. Forest Service Forest Inventory and Analysis (FIA) urban forest inventory pilot protocols (USDA Forest Service 2005) and represent a visual estimate to the nearest 5%. Each estimate was made from under the tree canopy on a 7.3 m radius (167 m^2) plot centered at each study site's center point. Satellite-derived estimates of percent tree cover at each site were obtained from a land-cover classification of a QuickBird (2.4 m resolution) multispectral image acquired on July 26, 2006 that had an accuracy of 87% for the tree class (J. Wu, personal communication). The center point of each study site was geo-referenced using post-processed coordinates from a global positioning system (model GS20, Leica

Geosystems AG, Heerbrugg, Switzerland) and overlaid on the land-cover map in a geographic information system (ArcMap, version 9.2, ESRI, Redlands, California, USA). Percent tree cover was calculated from the number of pixels that were classified as tree-covered within an 18 m buffer around each site's center point, approximating the field of view of our LAI measurements.

Ground cover was measured once in August 2006 at each site using a 60 cm × 60 cm aluminum quadrat with 121 point-intersections. At each point-intersection, ground cover was categorized as turfgrass, broad-leaved weed, or bare soil. Percent ground cover of each type was determined as the mean of four readings in the cardinal directions at a distance of 1 m from the center point of each site.

Data analysis

Statistical analyses were performed using the R statistical language (version 2.7.1, R Development Core Team). Seasonal patterns of LAI and microclimate variables were analyzed using linear mixed effects models with vegetation type and day of year (DOY) as fixed factors, and site as a random factor. The mid-season period of the growing season was defined as DOY 166 to 251, when the LAI at individual sites was neither increasing nor decreasing over time. Coefficients of variation and mid-season means of LAI and microclimate variables were analyzed using analysis of variance (ANOVA) tests. Significant ANOVAs ($\alpha = 0.05$) were followed by a Tukey's Honestly Significant Difference (HSD) post-hoc test ($\alpha = 0.05$) to perform multiple comparisons of means. The effects of LAI on microclimate variables across the growing season were analyzed

using stepwise backward elimination of linear mixed effects models (Akaike Information Criterion $\Delta < 3$) with vegetation type and LAI as fixed effects, and site as a random factor. The effects of mean mid-season LAI and percent tree cover on mean mid-season variables were analyzed using simple linear-regression. Open vegetation classes by definition have a stand-level LAI = 0 and thus were not included in any analyses involving LAI.

Results

Seasonal patterns of LAI and microclimate

The 2006 growing season (April to November) was warmer and drier than the local 30-year climate averages (National Climatic Data Center 2004). During June and July, air temperature was 2.5˚C warmer than the 30-year average and rainfall was 5.4 cm below average. During our measurements from April to November, air temperature at the reference turfgrass site ranged from a low of –8˚C to a high of 37˚C, and soil temperature ranged from 2˚C to 33˚C (Figure 2-1). Most of the large precipitation events (over 10 mm) occurred in July and August (Figure 2-1).

Over the course of the growing season, stand-level LAI differed significantly among the four forested vegetation types (Figure 2-2a, $F_{3,19} = 6.44$. $P = 0.004$). The coefficient of variation of LAI across the growing season was significantly different among vegetation types ($F_{3,19} = 17.51$, $P = 0.0001$) and lower at evergreen sites (c.v. = 16%) than at deciduous low (43%), deciduous high (40%), or mixed sites (34%). All sites

reached maximum LAI by DOY 166 and leaf senescence began on average by DOY 266. Mean mid-season LAI differed significantly among vegetation types (Figure 2-3a, $F_{3,19}$ = 6.06, P = 0.005) and, on average, mid-season LAI was highest at mixed sites (4.2 m^2 m^{-2}) and lowest at deciduous low sites (1.2 m^2 m^{-2}). Mid-season LAI at mixed sites, however, was not significantly different from evergreen or deciduous high sites.

Relative soil temperature differed significantly among the five vegetation types over the course of the growing season (Figure 2-2b, $F_{4,25}$ = 20.68, P < 0.0001). Soil temperature at all sites was lower than at the turfgrass reference site throughout the growing season. This was true even for our open lawn sites, which we attributed to small differences in the depths sampled by the buried soil temperature sensors at the reference site compared to our spot measurements at the other sites. In addition, the soil at the turfgrass reference site was very dry during mid-summer from lack of irrigation and low rainfall, whereas irrigation practices were variable across the open study sites. Mid-season soil temperatures differed significantly among vegetation types (Figure 2-3b, $F_{4,25}$ = 18.24, P < 0.0001) and, on average, mid-season soil temperatures at deciduous high, evergreen, and mixed sites were 2.8˚C cooler than at deciduous low and open sites.

Relative infrared surface temperature differed significantly among the five vegetation types over the course of the growing season (Figure 2-2c, $F_{4,25}$ = 8.07, P = 0.0003). Mean mid-season infrared surface temperature also differed significantly among vegetation types (Figure 2-3c, $F_{4,25}$ = 5.73, P = 0.002) and, on average, mid-season surface temperatures at deciduous high and mixed sites were 4.6˚C cooler than deciduous low sites.

Soil water content did not differ significantly among vegetation types over the course of the growing season ($F_{4,25} = 0.48$, $P = 0.75$).

Seasonal effects of LAI on microclimate

Over the course of the growing season, relative soil and surface temperature were negatively correlated with stand-level LAI (Figure 2-4). The slopes and intercepts of the response of relative soil temperature to increasing LAI were not significantly different among deciduous and mixed sites, but were significantly different among evergreen sites and deciduous/mixed sites (Figure 2-4a). The best-fit mixed-effects model, determined using the Akaike Information Criterion, for relative soil temperature at deciduous and mixed sites was $y = -1.15\ LAI + 0.50$, while the best-fit model for relative soil temperature at evergreen sites was $y = -3.07\ LAI + 7.72$. The slopes and intercepts of the response of relative surface temperature to increasing LAI, however, were not significantly different among vegetation types (Figure 2-4b). The best-fit mixed-effects model for relative surface temperature at all sites was $y = -0.95\ LAI + 2.98$.

Site differences in LAI and microclimate

Across all sites, mid-season LAI was positively correlated with both satellite-derived estimates of percent tree cover (Figure 2-5a, $R^2 = 0.16$, $P = 0.06$) and field-based measurements of percent tree cover (Figure 2-5b, $R^2 = 0.43$, $P < 0.001$). Satellite-derived percent tree cover varied over a narrower range than did the field-based measurements and it poorly predicted site differences in mid-season LAI.

Mid-season relative soil and surface temperatures across all sites were negatively correlated with both mid-season LAI (Figure 2-6a, $R^2 = 0.58$, $P < 0.001$ and Figure 2-6c, $R^2 = 0.35$, $P = 0.004$, respectively) and field-measured percent tree cover (Figure 2-6b, $R^2 = 0.33$, $P = 0.005$ and Figure 2-6d, $R^2 = 0.47$, $P < 0.001$, respectively). However, mid-season LAI better predicted mid-season relative soil temperature (Figs. 6a,b) while percent tree cover better predicted mid-season relative surface temperature (Figs. 6c,d). Turfgrass cover and turfgrass + broad-leaved weed cover were both negatively correlated with mid-season LAI (Figure 2-7a, $R^2 = 0.56$, $P < 0.001$ and Figure 2-7g, $R^2 = 0.53$, $P = 0.001$, respectively) and field-measured tree cover (Figure 2-7b, $R^2 = 0.16$, $P = 0.07$ and Figure 2-7h, $R^2 = 0.39$, $P = 0.002$, respectively). Broad-leaved weed cover was not correlated with mid-season LAI (Figure 2-7e, $R^2 = 0.01$, $P = 0.62$) or field-measured tree cover (Figure 2-7f, $R^2 = 0.08$, $P = 0.21$). Conversely, bare soil cover was positively correlated with both mid-season LAI (Figure 2-7c, $R^2 = 0.54$, $P < 0.001$) and field-measured tree cover (Figure 2-7d, $R^2 = 0.39$, $P = 0.002$). Across all sites, ground cover was better predicted by mid-season LAI than by percent tree cover.

Discussion

Seasonal patterns of LAI and microclimate variables

The five vegetation types represented in this study showed distinct seasonal patterns of canopy leaf development and microclimate effects. These seasonal variations in

urban biophysical properties were more strongly related to differences in percent tree cover and canopy density than to plant functional type.

We found that the five vegetation types represented in this study had distinctly different seasonal patterns of relative soil and surface temperature, yet did not differ in their seasonal patterns of soil water content. Over the course of the growing season, sites with greater tree cover and higher LAI had consistently cooler soil and surface temperatures than did open or low tree cover sites, regardless of plant functional type (Figs. 2b, c). Consistent with this finding, the only significant differences among vegetation types in mid-season relative soil and surface temperatures were between the low tree cover, low LAI sites and high tree cover, high LAI sites (Figure 2-3b, c). These differences in relative soil temperatures were largest during the middle of the growing season and minimal at the beginning and end of the growing season, while differences in relative surface temperature were most noticeable during the first half of the growing season. It is more likely that the seasonal dynamics of soil water content are controlled by precipitation events and irrigation practices, which were not sampled systematically in this study. These ideas are consistent with previous studies that have discussed the importance of irrigation as a driver of spatial patterns of soil moisture in urban and suburban landscapes (Scharenbroch et al. 2005, Byrne et al. 2008).

As expected, plant functional types differed in their seasonal LAI dynamics, most markedly with deciduous-dominated sites showing larger variation in LAI across the growing season than evergreen sites (Figure 2-2a). However, plant functional types did not explain the large differences in mid-season LAI among sites (Figure 2-3a), suggesting

that structural characteristics such as percent tree cover, stand density, or species composition are more important for explaining stand-level variability in urban LAI. Consistent with this, the only significant difference we found in mid-season LAI among the vegetation types was between the deciduous low and all other high tree cover sites (Figure 2-3a).

Our stand-level LAI measurements obtained with an optical plant canopy analyzer were similar to those found in another urban study from Terre Haute, Indiana (Hardin and Jensen 2007). LAI values at our suburban study sites were also similar to, or slightly lower than, those observed in temperate and boreal forests with tree species similar to those in our study area (Chen et al. 2006, Lindroth et al. 2008). This result is consistent with studies showing that the aboveground biomass of open-grown urban trees can be 20% less than forest-grown trees of the same diameter (Nowak 1994). Stand-level LAI values are also likely reduced in urban and suburban areas because of landscaping practices that maintain park-like spacing between trees and prevent natural succession and canopy closure.

Microclimate variables showed strong functional responses to changes in LAI across the growing season (Figure 2-4). Regardless of vegetation type, surface temperature decreased by ~1˚C for every unit (m^2 m^{-2}) increase in LAI (Figure 2-4b). In other words, surface temperatures under dense tree canopies (*e.g.*, sites with LAI = 6 m^2 m^{-2} in Figure 2-4b) were reduced up to 6˚C, relative to sparse canopies with near-zero LAI. Soil temperature also declined with increasing LAI. When compared to sparse tree canopies with near-zero LAI, soil temperatures under dense tree canopies (*e.g.*, LAI = 6 m^2 m^{-2})

were reduced up to 7˚C. However, the slope and intercept of this relationship was significantly different for evergreen-dominated versus deciduous-dominated sites (Figure 2-4a). For every unit increase in LAI, soil temperature decreased by ~3.1˚C at evergreen-dominated sites and by ~1.2˚C at deciduous-dominated sites. A possible explanation for the difference at the evergreen sites is that they had much less variation in LAI over the course of the growing season than did the deciduous and mixed sites. All sites with high tree cover (DH, EG, MX) showed a similar range of relative soil temperature (Figure 2-2b) due to seasonal changes in solar radiation. Because those changes in relative soil temperature are seasonally correlated with changes in LAI across the growing season, the small LAI range at evergreen sites resulted in a steeper decline in relative soil temperature with every unit increase in LAI. Alternatively, if our study area had included evergreen sites representing a larger range of LAI, we may have observed a similar soil temperature response to increasing LAI as in other vegetation types. Our interpretation is that while the difference in response of the evergreen sites was statistically significant, it may not have been ecologically significant, especially in light of the fact that we found no vegetation type differences in the relationship between relative surface temperature and LAI (Figure 2-4b).

The cooling effects of urban vegetation are well documented and are currently used as environmental design tools to reduce urban heat islands and home energy use (McPherson 1994). Previous field studies have found soil and surface temperatures of residential lawns to be several degrees cooler during the summer than other common ground cover types, such as bark, mulch (Byrne et al. 2008), and native grasses (Bonan

2000). This is largely because of the increased evaporative cooling by transpiring, and often well-irrigated, turfgrasses. Our results support these previous studies and they extend our understanding of how these cooling effects vary among urban vegetation types and over time with canopy leaf development. We found that tree canopies have a greater cooling effect on soils and the surface compared to open turfgrass lawns, which is likely due to the canopy intercepting solar radiation and shading the surface. Trees also have deeper roots and greater leaf area than turfgrasses, leading to greater evapotranspiration. Evapotranspiration from trees, however, occurs at the top of the canopy and does not necessarily mix throughout the vertical volume of air to significantly modify the local temperature surrounding an individual stand of trees (Oke 1989).

The differences in soil temperature we observed among our vegetation types could also have important implications for carbon cycling in urban areas. Because soil respiration rates increase exponentially with soil temperature between 0 and 40ºC (Lloyd and Taylor 1994), our results suggest that CO_2 efflux from urban soils may be modulated by seasonal changes in canopy density as well as plant functional type (Figure 2-4a). In natural systems, it has been shown that an increase in canopy density mediates soil respiration rates by reducing net radiation at the surface, causing lower soil temperatures (Smith and Johnson 2004, Tanaka and Hashimoto 2006). If we apply Smith et al.'s (2004) temperature-response equations from a woodland-grassland study to our suburban ecosystem with a mean summer soil temperature of 25˚C, the average soil respiration rate under a dense urban tree canopy (*e.g.* LAI = 6 m^2 m^{-2}) would be 56% lower than in an open turfgrass lawn (1.85 versus 4.17 μmoles CO_2 m^{-2} s^{-1}, respectively). Our results sug-

gest that the significant cooling effects of urban tree canopies on soil temperature should be accounted for in urban carbon budgets (Pataki et al. 2006b, Churkina 2008). The greatest potential for reduced CO_2 emissions from lower soil respiration rates would be in sites where urban tree canopies occur over grass or bare soil ground covers, rather than impervious surfaces.

Site differences in mid-season microclimate and ground cover.

We evaluated two stand-level metrics, LAI and percent tree cover, for their ability to explain spatial differences in mid-season microclimate, as well as mid-season ground cover composition, under the urban forest canopy. Overall, we found that mid-season LAI was a better predictor of both mid-season microclimate and ground cover variables than percent tree cover.

While we found mid-season LAI to be a better predictor of mid-season soil temperature (Figure 2-6a, b), we also found that percent tree cover was a better predictor of mid-season surface temperature (Figure 2-6c, d). Because surface temperature is most affected by the direct beam solar radiation penetrating a canopy at a given moment in time, it depends more on the extent and distribution of the canopy (indicated by percent tree cover) than the density of leaves per unit ground area (indicated by stand-level LAI). As a result, over the range of tree cover from 0 to 100%, the mean mid-season surface temperature was reduced by 6˚C on average. In contrast, soil temperature is a more integrated measure of a site's energy balance and is more strongly influenced by the total leaf

area per unit ground area. A greater mid-season LAI by five units (m^2 m^{-2}) consequently reduced the average mid-season soil temperature across the sites by an average of 4˚C.

Mid-season LAI was also a better predictor of site differences in percent ground cover than was percent tree cover (Figure 2-7). The percent cover of turfgrass, in particular, showed the strongest correlation with mid-season LAI (Figure 2-7a, $R^2 = 0.56$). Although turfgrass species are adapted to a variety of light environments, in general turfgrass is less shade tolerant than many broad-leaved weed species (Fry and Huang 2004), which showed no trend with increasing LAI or percent tree cover (Figs. 7e, f). In high light environments, turfgrass can out-compete weed species, but turfgrass is less competitive in low light conditions (Fry and Huang 2004). Additionally, human management prevents competition from broad-leaved weeds through the use of herbicides, which are often applied to open canopy, high light lawns. The cover of turfgrass in urban and suburban areas has been much less frequently quantified (Milesi et al. 2005) than has tree cover, which is relatively easily assessed using forest inventories, aerial or satellite imagery (Nowak et al. 2008). Our results suggest that it would be possible to produce a first-order estimate of the density of turfgrass ground cover by using the more readily available data on urban tree canopies, although the predictive equations would likely need to be developed regionally to account for differences in climate and horticultural practices. Ultimately, this information could be used to account for understory vegetation cover in models of urban land–atmosphere exchanges of energy, water, and carbon (Rivalland et al. 2005).

Using tree cover to predict site differences in mid-season LAI.

In this study, we evaluated the relative performance of two different measures of percent tree cover for predicting site differences in mid-season LAI. Measuring LAI in urban ecosystems is considerably more difficult than in natural forest systems because of numerous methodological constraints, including optical interference from buildings, a limited number of urban-specific allometric equations for trees, and spatially heterogeneous and isolated tree canopies (Peper and McPherson 2003). Although we found stand-level LAI was a better predictor of mid-season microclimates and ground cover than percent tree cover (Figs. 6, 7), percent tree cover is an easily measured and more commonly used metric for evaluating the extent and distribution of urban forests, as well as the ecosystem services they provide (Nowak et al. 2008, Wang et al. 2008). We found that field-based estimates of percent tree cover were better than satellite-derived estimates at predicting the site-to-site variations in LAI in our suburban study area (Figure 2-5). The satellite-derived land-cover map produced a narrower range of tree cover values compared to the field-based inventory using U.S. Forest Service urban forest inventory protocols (USDA Forest Service 2005). Although the field-based measures are more subjective, they take into account gaps within individual tree canopies that are too small to resolve in even high-resolution satellite imagery such as QuickBird (2.4 m). There was still considerable variation around the best-fit linear regression model (Figure 2-5b) and, in general, LAI at evergreen sites was under-predicted by 30%, while LAI at deciduous sites was over-predicted by 40%. The model fit was largely driven by the strong positive relationship between stand-level LAI and field-measured tree cover at levels of <50% tree cover.

At sites having >50% tree cover, there was considerable scatter in the relationship and field-measured percent tree cover poorly predicted mid-season LAI. This saturating effect of LAI with field-measured percent tree cover was likely due to the fact that both stand density and species composition contribute to a site's LAI. At sites with low percent tree cover, stand density had the greater influence on stand-level LAI. In contrast, at sites with high percent tree cover, differences in the canopy structure of different plant functional types and species was more important in determining stand-level LAI.

Developing relationships between percent tree cover and mid-season LAI would be a useful step toward scaling up urban biophysical properties and providing the information required to implement complex urban land-surface models. Our results suggest that satellite imagery with a pixel size on the order of 2.4 m is unable to resolve the detailed tree canopy information needed to scale up urban forest biophysical properties. However, metropolitan-scale comparisons of different methods for estimating tree cover have found that high-resolution aerial photography (60 cm ground resolving distance) produces similar estimates to field-based urban forest inventories (Nowak et al. 1996, Walton et al. 2008). This suggests that next-generation, high resolution satellite imaging systems, such as GeoEye-1 (1.65 m multispectral and 0.41 m panchromatic resolution at nadir), could be used to produce maps of urban forest canopy characteristics that would be adequate to model LAI, soil temperature, surface temperature, and ground cover over relatively large urban areas.

Conclusions

Urban forest vegetation types showed distinct seasonal patterns of stand-level LAI, soil temperature, and surface temperature, which were largely explained by differences in tree cover and changes in LAI, rather than by plant functional type. Over the course of the growing season, sites with higher percent tree cover and greater LAI reduced soil temperatures by up to 7˚C and surface temperatures by up to 6˚C, relative to sites with near-zero LAI. Because of low variability in LAI over the growing season, soil temperature at evergreen sites was more greatly reduced with every unit increase in LAI than at deciduous-dominated sites. Additionally, we found that site differences in mid-season soil temperature and turfgrass ground cover were better predicted by mid-season LAI, while mid-season surface temperature was better predicted by percent tree cover. The significant cooling effects of urban tree canopies on soil temperature imply that seasonal changes in canopy density may also modulate the CO_2 efflux from urban soils and should be included in urban carbon budgets. To scale up, we found that field-based estimates of tree cover were better than 2.4 m resolution satellite imagery for predicting the mean mid-season LAI values that were important for determining temperatures under the urban forest canopy, but that higher resolution aerial imagery or next-generation satellite sensors may provide a practical approach for larger metropolitan areas and regions.

Table 2-1. Forest characteristics of 29 suburban study sites, grouped by vegetation type. Data are means ±1 standard deviation. The species listed represent >60% of the trees counted in each vegetation type and are listed alphabetically.

Vegetation type	Label	Number of Sites (n)	Tree Cover (%)	Basal Area (m^2 ha^{-1})	Tree Height (m)	DBH (cm)	Tree Species
Open turfgrass lawns	OP	7	0	0	NA	NA	NA
Deciduous tree canopy, low cover	DL	5	21 (±11)	6 (±10)	7 (±4)	11 (±10)	*Acer ginnala* *Magnolia spp.*
Deciduous tree canopy, high cover	DH	7	83 (±7)	146 (±91)	11 (±5)	19 (±18)	*Acer negundo* *Acer saccharinum* *Fraxinus pennsylvanica* *Quercus alba*
Evergreen tree canopy	EG	5	56 (±21)	147 (±69)	14 (±3)	33 (±11)	*Picea glauca* *Pinus nigra*
Mixed deciduous and evergreen tree canopy	MX	5	71 (±16)	48 (±19)	11 (±4)	24 (±12)	*Acer platanoides* *Betula papyrifera* *Picea glauca* *Tsuga canadensis*

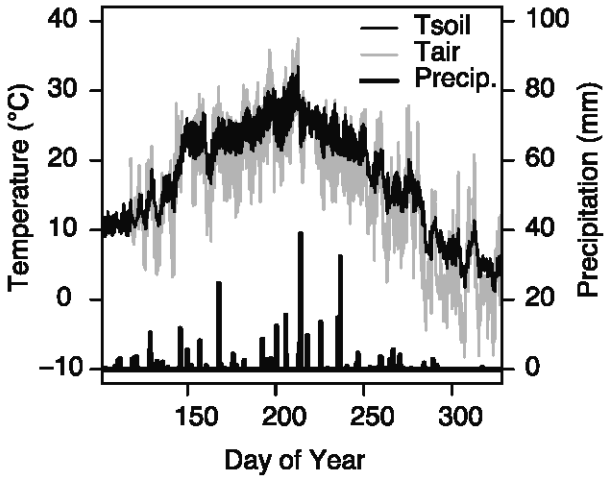

Figure 2-1. Environmental conditions during the 2006 growing season at the open turfgrass reference site. Air temperature was measured 1.4 m above the surface and soil temperature was measured over the upper 5–10 cm deep soil layer.

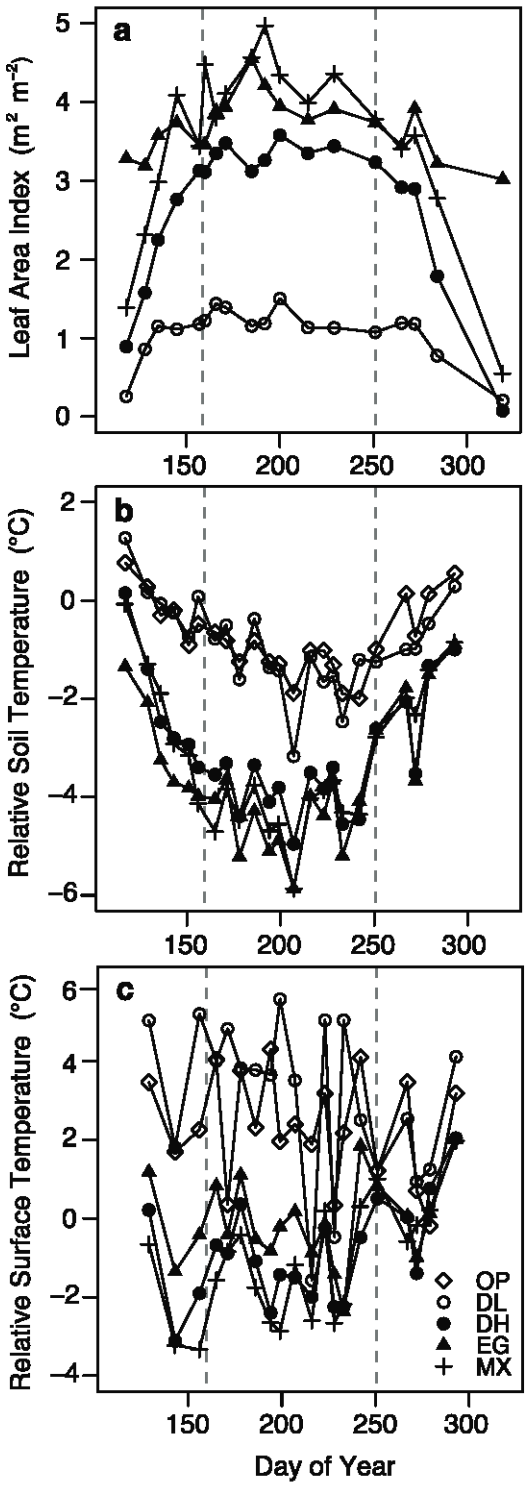

Figure 2-2. Seasonal patterns during the 2006 growing season of measured **(a)** stand-level leaf area index, **(b)** soil temperature at 10 cm depth, and **(c)** infrared surface tem-

perature of the ground cover of five suburban vegetation types: open turfgrass lawns (OP), deciduous tree canopy with low cover (DL), deciduous tree canopy with high cover (DH), evergreen tree cover (EG), and mixed deciduous and evergreen tree cover (MX). Each symbol represents the mean of all sites of a given vegetation type. The spot temperature measurements at the sites are expressed relative to the temperature recorded at the same time point at a climate station located in an open turfgrass area. The dashed vertical lines at Julian days 166 and 251 mark the mid-season period.

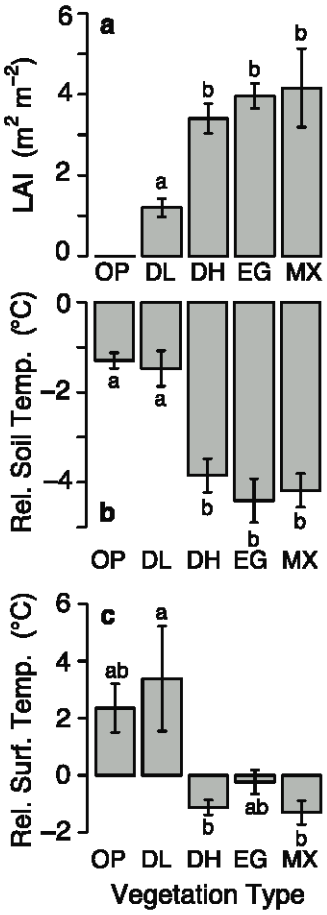

Figure 2-3. Mean mid-season **(a)** stand-level leaf area index, **(b)** soil temperature at 10 cm depth, and **(c)** infrared surface temperature of five suburban vegetation types: open turfgrass lawns (OP), deciduous tree canopy with low cover (DL), deciduous tree canopy with high cover (DH), evergreen tree cover (EG), and mixed deciduous and evergreen tree cover (MX). Error bars represent ±1 standard error. Lowercase letters indicate significantly different means based on a Tukey HSD multiple comparisons test. Mid-season is defined as the period between Julian days 166 and 251.

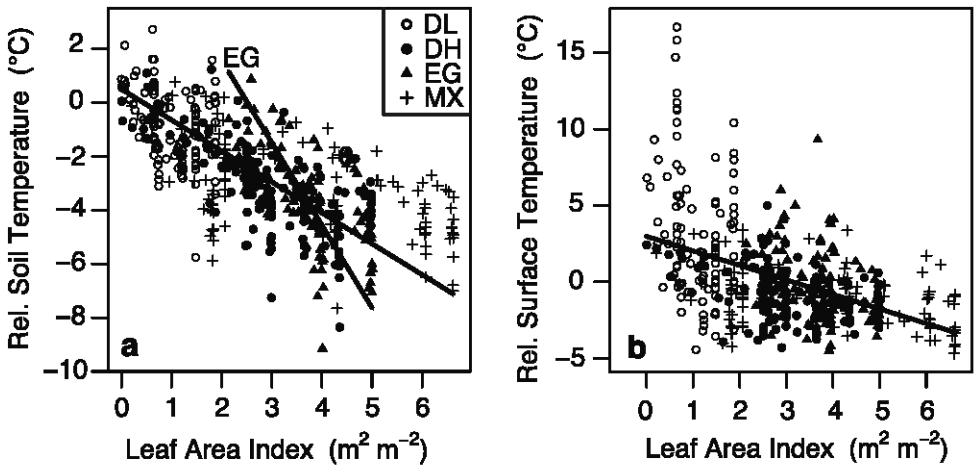

Figure 2-4. Relationships between modeled stand-level leaf area index and **(a)** relative soil temperature, and **(b)** relative surface temperature during the 2006 growing season. Each symbol represents a measurement at a single time point at an individual study site. Lines represent the best model fit after stepwise backwards elimination of linear mixed-effects models, where site is a random factor.

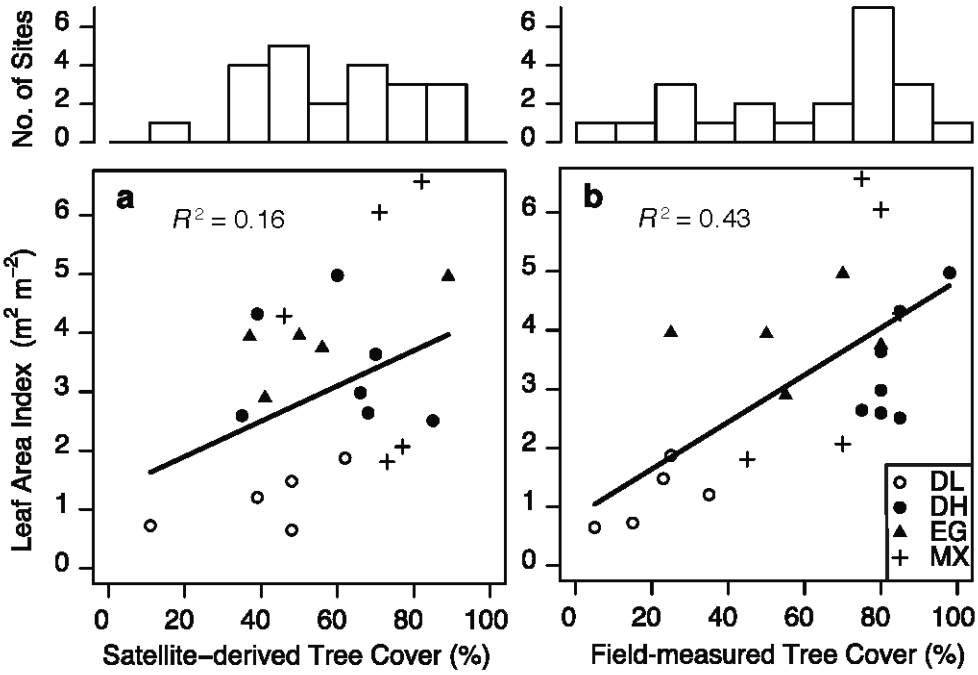

Figure 2-5. Comparing **(a)** satellite-derived and **(b)** field-based tree cover measurements as predictors of modeled mid-season LAI. Each symbol represents an individual study site. Histograms show the tree cover distribution determined by each method.

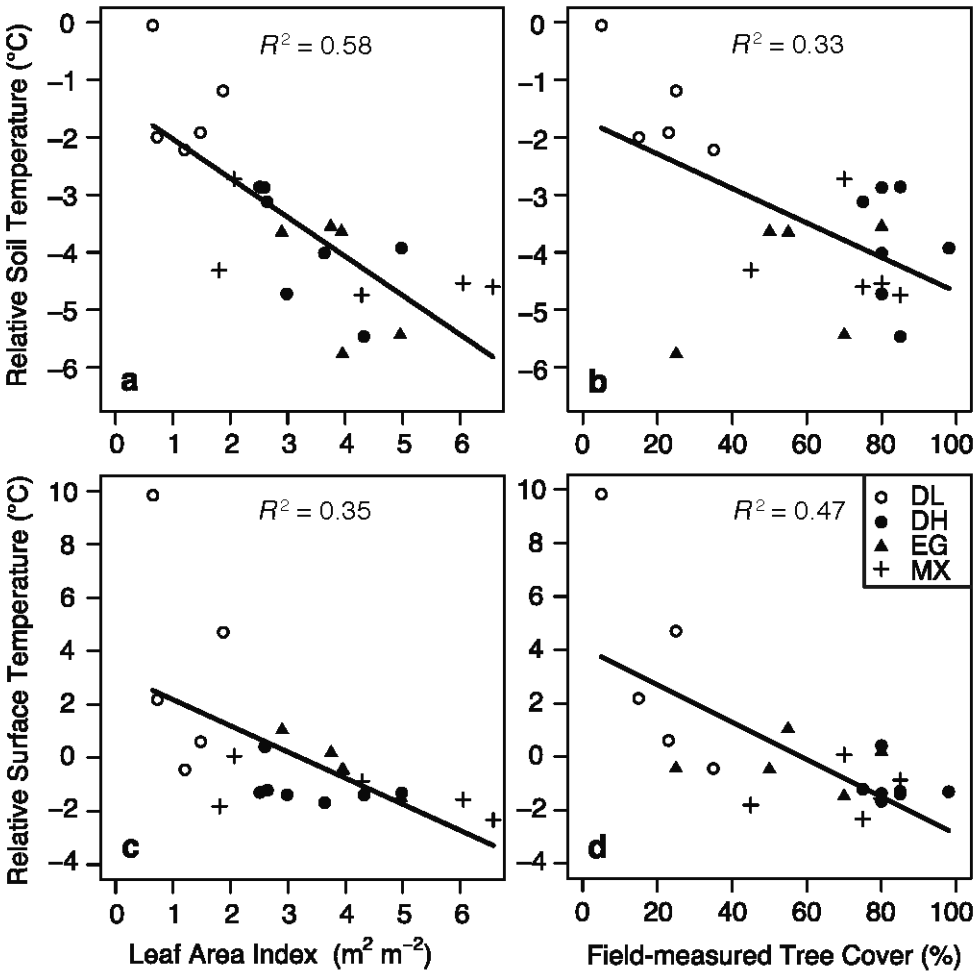

Figure 2-6. Comparing modeled mid-season LAI and field-based tree cover measurements as predictors of **(a), (b)** mid-season soil temperature, and **(c), (d)** mid-season surface temperature. Each symbol represents an individual study site.

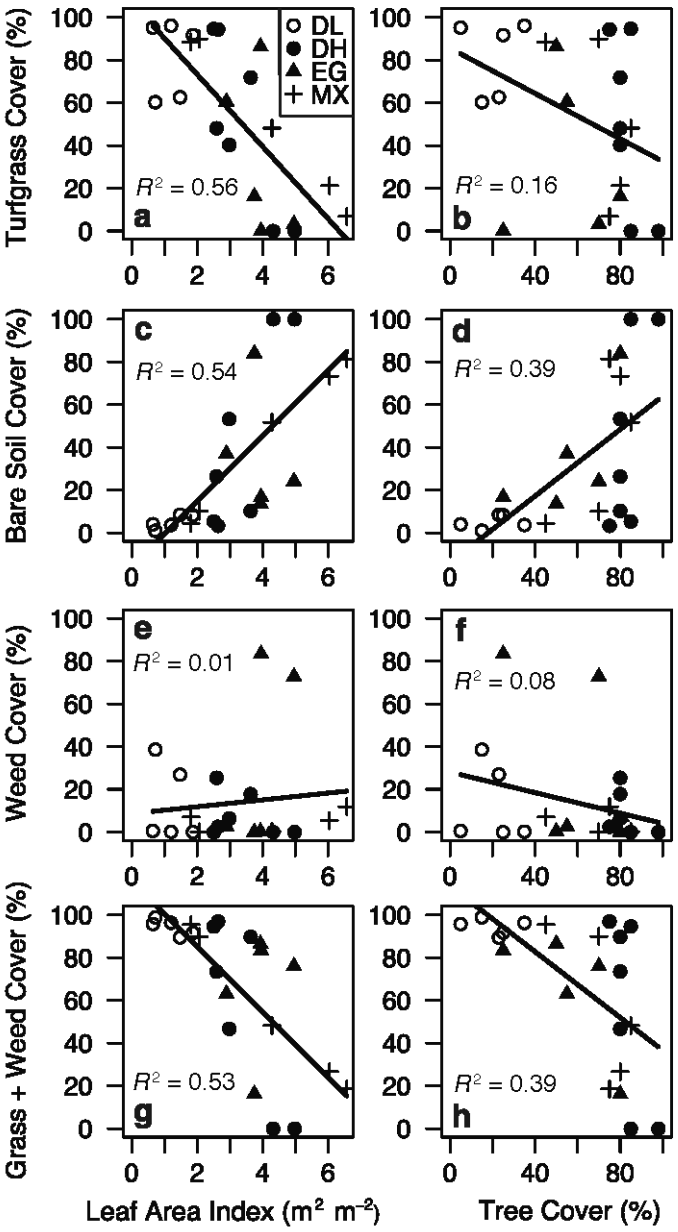

Figure 2-7. Comparing modeled mid-season LAI and field-based tree cover measurements as predictors of **(a), (b)** turfgrass cover, **(c), (d)** bare soil cover, **(e), (f)** broad-leaved weed cover, and **(g), (h)** turfgrass + broad-leaved weed cover. Each symbol represents an individual study site.

from jgr-biogeosciences <jgr-biogeosciences@agu.org>
to Emily Peters <pete1679@umn.edu>
date Mon, May 24, 2010 at 1:40 PM
subject RE: Reprint permission request

Dr. Peters,
You may use the paper in your dissertation as long as it is cited properly.
http://www.agu.org/pubs/authors/tou.shtml

Thank you very much.

Brendan Tully
Editor's Assistant

----- Original Message-----
From: e.peters2000@gmail.com [mailto:e.peters2000@gmail.com] On Behalf Of Emily Peters
Sent: Friday, May 21, 2010 1:33 PM
To: jgr-biogeosciences
Subject: Reprint permission request

Hello,
I would like to include a reprint of my paper (see below) in my PhD dissertation. The University of Minnesota, where I am a student, requires a letter from the publisher granting me permission to reprint the work. I was wondering if I could get permission to include my paper in my dissertation, and if I could receive a letter granting such permission.

Sincerely,

Emily Peters

Peters, E. B., J. P. McFadden, and R.A. Montgomery. In revision. Biological and environmental controls on tree transpiration in a suburban landscape. Journal of Geophysical Research-Biogeosciences.

Chapter 3

Biological and environmental controls on tree transpiration in a suburban landscape*

* *With Joseph McFadden and Rebecca Montgomery.* Reproduced with permission from the American Geophysical Union from: Peters, E. B., J. P. McFadden, and R. A. Montgomery. *In press*. Biological and environmental controls on tree transpiration in a suburban landscape. Journal of Geophysical Research – Biogeosciences.

Summary

Tree transpiration provides a variety of ecosystem services in urban areas, including amelioration of urban heat island effects and storm water management. Tree species vary in the magnitude and seasonality of transpiration due to differences in physiology, response to climate, and biophysical characteristics, thereby complicating efforts to manage evapotranspiration at city scales. We report sap flux measurements during the 2007 and 2008 growing seasons for dominant tree species in a suburban neighborhood of Minneapolis–Saint Paul, Minnesota, USA. Evergreen needleleaf trees had significantly higher growing season means and annual transpiration per unit canopy area (1.90 kg H_2O m^{-2} day^{-1} and 307 kg H_2O m^{-2} yr^{-1}, respectively) than deciduous broadleaf trees (1.11 kg H_2O m^{-2} day^{-1} and 153 kg H_2O m^{-2} yr^{-1}, respectively) due to a smaller projected canopy area (31.1 and 73.6 m^2, respectively), a higher leaf area index (8.8 and 5.5 m^2 m^{-2}, respectively), and a longer growth season (8 and 4 months, respectively). Measurements also

showed patterns consistent with species' differences in xylem anatomy (conifer, ring-porous, and diffuse-porous). As the growing season progressed, conifer and diffuse-porous genera had increased stomatal regulation to high vapor pressure deficit, while ring-porous genera maintained greater and more constant stomatal regulation. These results suggest evaporative responses to climate change in urban ecosystems will depend in part on species composition. Overall, plant functional type differences in canopy structure and growing season length were most important in explaining species' differences in mid-summer and annual transpiration, offering an approach to predict the evapotranspiration component of urban water budgets.

Introduction

Tree transpiration represents an important component of total evapotranspiration in many terrestrial ecosystems (Zhang et al. 2001, McLaren et al. 2008, Oishi et al. 2008, Paco et al. 2009). In urban and suburban areas, tree transpiration also provides ecosystem services (McPherson et al. 2005), such as reduced surface temperatures (Oke 1989, Leuzinger et al. 2010, Peters and McFadden 2010) and mitigation of storm water runoff (Mitchell et al. 2008, Wang et al. 2008). Cities are increasingly promoting the use of trees for managing ecosystem services (*e.g.* the recent "million trees" campaigns in Los Angeles, New York, and other cities); however efforts to predict and manage urban evapotranspiration rates are complicated by our limited understanding of how different urban tree species vary in water use. Tree species vary in both the magnitude and seasonality of transpiration due to differences in physiology, response to climate, and biophysical char-

acteristics (Wullschleger et al. 2001, Catovsky et al. 2002, Givnish 2002, Pataki and Oren 2003, Bovard et al. 2005, Tang et al. 2006, Bowden and Bauerle 2008). At landscape and regional scales, species composition is an important factor controlling the magnitude and seasonality of evapotranspiration (New et al. 1999, Zhang et al. 2001, Ewers et al. 2002). To manage ecosystem services from trees, we will ultimately need to quantify their aggregated evapotranspiration at neighborhood or city scales, which necessitates the difficult task of scaling up species' differences in transpiration.

Tree classification schemes that explain major differences in species' water use can simplify efforts to scale up the transpiration component of ecosystem water budgets. For example, differences in wood structure, or xylem anatomy type, have been shown to explain large differences in seasonal sap flux patterns among temperate tree species (Wullschleger et al. 2001, Bush et al. 2008). In conifer species, water transport occurs through relatively small, uniformly sized xylem conduits called tracheids. Although the xylem of diffuse-porous and ring-porous species also contains tracheids, most water transport occurs through larger vessel cells. Vessels formed early in the growing season in ring-porous species are larger and have a higher capacity to conduct water than vessels formed later in the growing season, while vessels formed in diffuse-porous species are relatively uniform in size. Due to these large earlywood vessels, ring-porous species tend to have greater risk of cavitation, increased stomatal regulation, and reduced sap flux as compared to diffuse-porous species (Hacke et al. 2006, Taneda and Sperry 2008). Other studies, however, show that vulnerability to cavitation can be related to plant rooting

depth, with shallowly rooted trees having greater vulnerability to embolism than deeply rooted trees (Cregg 1994, Sobrado 1997).

There is also evidence that tree water use varies with successional stage or shade tolerance (Abrams 1988, Hornbeck et al. 1997, Asbjornsen et al. 2007). Early-successional, generally shade-intolerant species tend to have lower stomatal resistances and higher leaf-level transpiration rates. Additionally, hydrologic and land-surface models commonly use plant functional types (*e.g.* evergreen needleleaf) that categorize plants according to major differences in physiology, biophysical characteristics and leaf habit (Foley et al. 1998, Bonan et al. 2003). Temperate evergreen needleleaf trees, for example, tend to have lower leaf-level transpiration rates, higher leaf area index, longer leaf lifespan, and longer active growing seasons than temperate deciduous broadleaf trees. While there are many studies in forest ecosystems that investigate how best to categorize and scale up species' differences in water use, this information is relatively lacking for urban and suburban ecosystems.

Altered environmental conditions in urban and suburban areas caused by the urban heat island effect and impervious surfaces may limit the extrapolation of measurements made in natural ecosystems (Clark and Kjelgren 1990, Cregg and Dix 2001, Gregg et al. 2003). The urban heat island causes elevated air temperature and vapor pressure deficit in urban and suburban areas relative to surrounding areas. Some of the earliest studies explicitly quantifying water relations of urban trees found that water deficits in New York City street trees were driven by periods of high atmospheric demand rather than low water supply (Whitlow and Bassuk 1988, Whitlow et al. 1992). More recently,

Bush et al. (2008) found exaggerated differences in sap flux density between diffuse and ring-porous tree species due to the high vapor pressure deficits in Salt Lake City, Utah. Urban and suburban areas also have large amounts of impervious surface and compacted soils that alter local hydrological processes and soil water content (Craul 1985), another important control on transpiration (Kramer 1987, Lagergren and Lindroth 2002, Holscher et al. 2005). Moreover, the species composition of urban and suburban ecosystems can differ considerably from forests in surrounding areas. Urban areas generally have higher frequencies of invasive and non-native species as well as human-cultivated varieties (McKinney 2002, Hahs et al. 2009, Walker et al. 2009).

Here we report results of continuous sap flux measurements during the 2007 and 2008 growing seasons on the dominant tree species in a suburban neighborhood of Minneapolis–Saint Paul, Minnesota in the north-central USA. Our objectives were to: 1) determine how suburban tree species vary in their water use in response to environmental drivers, including vapor pressure deficit, photosynthetically active radiation, and soil moisture; 2) test for significant differences in sap flux and transpiration rates between evergreen needleleaf and deciduous broadleaf plant functional types, and examine whether other ways of classifying urban tree species (*e.g.*, by genus, xylem anatomy, or shade tolerance) could also reveal consistent patterns of sap flux and transpiration at diurnal, seasonal and annual time scales; and 3) evaluate the ability of different tree classification schemes to scale up and predict the tree transpiration component of urban and suburban water budgets.

Methods

Study Sites

Our study sites were located in a first-ring suburban neighborhood in the Minneapolis–Saint Paul metropolitan area in east-central Minnesota, USA (44º59'N, 93º11'W). The neighborhood experienced rapid residential development in the 1950s and, prior to that time, farms and nurseries were the prominent land-use types. The area had a cold temperate climate with a mean annual temperature of 7.4ºC and mean annual precipitation of 747 mm. Due to its location near the center of the metropolitan area, the study area was influenced by the urban heat island effect that has been documented for Minneapolis–Saint Paul (Winkler et al. 1981, Todhunter 1996, Sen Roy and Yuan 2009). The study area had >20% tree cover and turfgrass lawns were the most common ground cover type based on an urban forest inventory we conducted in 2005–2006 following the U.S. Forest Service Forest Inventory and Analysis (FIA) protocol (USDA Forest Service 2005). Of the 1032 trees surveyed, 84 species were identified, with 9 genera representing over 80% of all trees (Table 3-1). The dominant canopy species, *Acer saccharinum*, *Fraxinus pennsylvanica*, *Picea glauca*, *Picea pungens*, *Populus deltoides, Quercus alba*, *Quercus macrocarpa*, and *Ulmus americana* each represented between 4% and 12% of the total cross-sectional trunk area measured at 1.4 m above ground level (*i.e.* basal area).

We selected four sites with stands of trees suitable for sap flux measurements within a 7 km^2 area. The sites were selected to include tree species and sizes that were as representative as possible of the urban FIA inventory, but subject to several logistical

constraints of the urban environment (*e.g.,* landowner permission, site suitability and safety, maximal extent of signal cables, and access to power). In 2007 we measured two sites, the Grove site, which was dominated by evergreen needleleaf tree species, and the Commonwealth Terrace Commons (CTC) site, which was dominated by deciduous broadleaf species. The Grove site was located on a single-family residential parcel and it included three *Picea glauca*, one *Pinus strobus* and four *Picea pungens* trees growing on loam soils (40% sand, 41% silt, 19% clay). The CTC site was located in a multi-family residential parcel and it included two *Fraxinus pennsylvanica* and five *Quercus rubra* trees growing on sandy loam soils (58% sand, 25% silt, 17% clay). In 2008 we measured two different study sites, Saint Paul and Lauderdale, which both had a mixture of evergreen needleleaf and deciduous broadleaf tree species, allowing us to rule out potential confounding effects between site and plant functional type. The Saint Paul site was located in a residential parcel and it included two *Fraxinus pennsylvanica*, two *Tilia americana*, two *Juglans nigra*, two *Ulmus thomasii*, two *Picea glauca*, and two *Pinus sylvestris* trees growing on loam soils (41% sand, 44% silt, 15% clay). The Lauderdale site was located in a 1.5 ha neighborhood park and it included two *Fraxinus pennsylvanica*, two *Ulmus pumila*, two *Picea abies*, and two *Pinus nigra* trees growing on loam soils (46% sand, 42% silt, 12% clay). In total, over the two years of the study, we measured sap flux on 37 trees, representing seven different genera, two plant functional types, three xylem anatomy types, and a range of shade tolerances (Table 3-2). The conifer xylem anatomy type represented the same species as the evergreen needleleaf plant functional type.

Shade tolerance was assigned according to species rankings in Niinemets and Valladares (2006).

In this suburban study area, the trees were grown under generally more park-like conditions with open canopies and a turfgrass ground cover, unlike street trees in a more densely developed urban area. The lower branches of many trees were pruned, but canopies were mature and healthy with no obvious signs of disease or damage. Although difficult to assess without below ground excavation, it was unlikely root systems were severely restricted by impervious surfaces, as the nearest roads and sidewalks occurred beyond the drip-line of all trees and often at distances >10 m from each tree. As is common in urban areas, surface soils at all sites were moderately compacted with an average bulk density of 1.43 g cm^{-3}. Although tree roots can penetrate compaction levels as high as 1.6 g cm^{-3} (Bartens et al. 2008), root growth could have been restricted in our study trees. Management regimes were considered low-maintenance at all sites with regular mowing, but little or no irrigation and no fertilizer use according to personal communications with the landowners. Total nitrogen and organic carbon contents of soils were lowest at the Grove site, highest at the CTC site, and ranged from 0.15% to 0.26% and 1.6% to 3.0%, respectively, across sites.

Field Measurements

Making physiological measurements on trees in an urban ecosystem presents numerous technical and logistical challenges, including the need to obtain permission from multiple landowners and limitations on activities such as tree coring and destructive sam-

pling. These constraints limited our ability to evaluate some sources of spatial variation in sap flow within trees, including axial, circumferential, and radial variation. We attempted to assess and reduce those sources of spatial variation that are known to contribute disproportionately large errors when scaling up tree transpiration, as discussed below.

From May to November, 2007 and from April to November, 2008, we measured sap flux density per unit conducting sapwood area (J_S) on our study trees using Granier-type heat dissipation probes (Granier 1987, Lu et al. 2004). We made sap flux measurements at a single height of 1.4 m on each tree. Although J_S is known to vary axially with height on the bole, choosing a measurement height that has been standard in many other studies allowed us to more directly compare J_S rates among the trees in this study as well as with measurements from the literature. Sensors were installed on the north and south sides of each tree to sample across a wide range in canopy exposure to solar radiation, a potential source of circumferential variation in J_S (Lu et al. 2004). As younger sapwood (less than 30 years old) often contributes a disproportionately large amount to whole-tree sap flux (Melcher et al. 2003, Ford et al. 2004, Gebauer et al. 2008), sensors were inserted radially into the sapwood only to a depth of 2 cm. To prevent thermal interference, the heated probe of each sensor was installed 10 cm above the unheated probe. To provide waterproofing and thermal insulation, we sealed the sapwood–air interface of the sensor with silicone and covered the sensors in reflective bubble wrap. Temperature differences between the heated and unheated sensors were taken every 15 s and half-hour averages were computed and stored in data loggers (CR1000, Campbell Scientific Inc., Logan, UT, USA). J_S in g H_2O m^{-2} s^{-1} was calculated following Granier (1987) as:

$$J_S = 119\left(\frac{\Delta T_M - \Delta T}{\Delta T}\right)^{1.231} \qquad (1)$$

where ΔT_M (ºC) is the maximum nighttime temperature difference between the heated and unheated sensors, and ΔT is the mean temperature difference between sensors during each half-hour measurement interval. While it has been suggested that Granier-type sensors should be calibrated for each new species to which they are applied (Lu et al. 2004), this was not practical in our study due to the destructive harvesting necessary for the calibration process. Many studies, however, have shown that the original calibration coefficient is relatively independent of wood anatomy or tree species (Catovsky et al. 2002, Lu et al. 2004). We used the software package BaseLiner (version 2.4.1, Hydro-Ecology Group, Duke University) to calculate ΔT_M and J_S. To allow for seasonal changes in thermal properties of wood, ΔT_M was calculated as the maximum temperature difference measured over each 24 h cycle. As this method can lead to an underestimate of nocturnal J_S, we only calculated ΔT_M when nighttime vapor pressure deficit remained below 1 kPa (Oishi et al. 2008). On days when nighttime vapor pressure deficit exceeded 1 kPa, ΔT_M was estimated by linear interpolation. Due to short sapwood depth and sensor contact with heartwood, we corrected sap flux estimates from *Quercus rubra* (Table 3-2) following Clearwater et al. (1999) and Oishi et al. (2008).

To express transpiration per unit canopy area (E_C), each tree's daily sum of J_S in g H_2O cm^{-2} day^{-1} was multiplied by the ratio of cross-sectional sapwood area to projected canopy area and adjusted for radial variation in sap flow. Projected canopy area was de-

termined by measuring canopy width in two orthogonal directions on each tree. The cross-sectional sapwood area of each tree was determined by measuring sapwood depth on two increment cores collected at a height of 1.4 m on the north and south sides of each tree during the winters following sap flux measurements. Following Lu et al. (2004), active xylem was distinguished from heartwood and non-active sapwood based on visual inspection immediately after cores were removed from the tree. Heartwood and non-active sapwood did not appear as translucent as water-filled active xylem when cores were held up to the light. Many studies emphasize the importance of accounting for radial variation in J_S when scaling to whole-trees, as it can lead to significant overestimates of transpiration if a constant J_S rate is assumed across the entire sapwood depth (Ford et al. 2004, Gebauer et al. 2008). While it was not feasible to directly measure J_S at multiple depths in our study, we did apply generalized radial trend relationships for gymnosperms and angiosperms developed by Pataki et al. (In review) when scaling J_S to E_C. Although there is still variability associated with using these radial trend relationships, the error introduced was random rather than the systematic overestimate that would result from assuming a constant J_S rate across the entire sapwood depth.

Transpiration per unit leaf area (E_L) was calculated by dividing E_C by the maximum, mid-summer leaf area index (LAI) of each tree. In August 2008, the LAI of each tree at the Lauderdale and Saint Paul sites was measured using an optical plant canopy analyzer (model LAI-2000, LI-Cor, Lincoln, Nebraska, USA) on days when sky conditions were overcast to avoid direct sunlight hitting the sensor. The mean LAI of each tree was calculated from ten LAI measurements taken around the bole at a height of 1 m

above the ground and a distance of 1 m away from the bole. To prevent interference with the measurements, a 270° view cap was used to block the 90° horizontal angle of the sensor's view that was nearest to the operator. The LAI-2000 optical sensor consists of five detectors arranged in concentric rings, each with a different field of view. To ensure that the field of view of each LAI measurement was within the tree canopy of interest, we used only the two inner rings (0–28° from zenith). While Villalobos et al. (1995) showed that reducing rings can lead to an overestimate of LAI for larger isolated trees, Ryu et al. (2010) showed that differences among different optical LAI estimation techniques were smallest when using the inner three rings of the LAI-2000. The LAI of evergreen needleleaf trees was corrected for leaf clumping using a correction factor of 1.6, according to the manufacturer's recommendations for the LAI-2000.

LAI was calculated using an isolated canopy model with computed crown distances in the LI-Cor FV2200 software, which is based on the vertical profile of each crown and does not assume a horizontally homogeneous canopy. Although the isolated canopy model is better suited for analyzing individual trees than the homogeneous canopy model, Broadhead et al. (2003) showed that the isolated canopy model still underpredicted LAI of orchard-grown olive trees by 30%. We modeled each crown as a cylinder using measurements of tree height, height-to-crown, and mean crown radius that were collected on each tree in July 2008. This cylindrical crown model may also lead to an underestimation of LAI, as it could represent too large of a volume over which leaf area is distributed, particularly in evergreen needleleaf trees. Despite the uncertainty associated with measuring LAI of individual trees, we expect that our measurements provide an ac-

curate representation of the relative LAI differences among our study trees, as shown for LAI-2000 measurements in other urban studies (Peper and McPherson 2003).

We measured a suite of micrometeorological variables at each study site, including air temperature and relative humidity (model HMP45C, Campbell Scientific Inc., Logan, UT, USA) at two-thirds canopy height, and volumetric soil water content at 10 cm depth (model ECH2O, Decagon Devices, Inc., Pullman, WA, USA). The soil water content measurements were calibrated relative to a set of gravimetric measurements made in the same soil type at the University of Minnesota climate station. These calibrations were conducted by oven-drying soil cores of a known volume that were collected across a two-week period. Photosynthetically active radiation (PAR) (LI-190, LI-Cor, Inc., Lincoln, NE, USA) was measured at a nearby climate station located on an open turfgrass lawn at the University of Minnesota Turfgrass Research, Outreach, and Education Center and precipitation data were obtained from the University of Minnesota climate station (both <1 km from our study sites). Micrometeorological data were collected every 15 s and half-hour averages were computed and stored on data loggers. Vapor pressure deficit was calculated from the humidity and air temperature measurements collected within the tree canopy at each study site.

Data Analysis

We tested for differences in sap flux and transpiration among plant functional types using linear mixed-effects models with multiple non-nested random effects. Plant functional type was treated as a fixed factor, and site and genus as non-nested, random

blocking factors. The significance level for all tests was $\alpha = 0.05$. Statistical tests for significant differences among genera, xylem anatomy type, and shade tolerance were not computed because our field experiment was designed only to formally test differences between the evergreen needleleaf and deciduous broadleaf plant functional types. Daytime (PAR > 0 μmol m^{-2} s^{-1}) mean vapor pressure deficit was normalized for day length (D_Z) following Phillips and Oren (1998). We used exponential saturation models to analyze the relationships between J_S and D_Z following Ewers et al. (2001). To calculate annual sums of E_C in 2008 we filled gaps in daily J_S by developing exponential saturation models of the relationship between daily sums of J_S and daytime mean vapor pressure deficit over a moving window of 21 days. Statistical analyses were performed using the R (version 2.8) statistical language (R Development Core Team 2010).

Results

Environmental Conditions

The seasonal patterns of daily cumulative PAR, air temperature, daytime vapor pressure deficit, soil moisture, and precipitation were similar during the two years of study, although spring air temperature and vapor pressure deficit were higher in 2007 than in 2008 (Figure 3-1). The middle of the growing season (*i.e.* 14 June – 7 Sept. [DOY 165– 250]) was on average warmer and wetter in 2007 compared to 2008, with mean air temperatures of 22.7 and 21.8ºC, respectively, and cumulative rainfalls of 245 and 127 mm, respectively. In addition, both day and night air temperatures were higher on aver-

age during the 2007 growing season (Table 3-3). In both years, most large (>10 mm) precipitation events occurred in July and August, but in 2007 those events were on average twice as large as in 2008 (Figure 3-1). Within a single year, sites differed significantly in volumetric soil water content averaged across the entire measurement period ($P < 0.001$ in both 2007 and 2008) due in part to differences in soil texture. The higher soil moisture and seasonal pattern at the Grove site was also due to occasional irrigation by homeowners using automatic sprinklers, whereas the other sites received no irrigation. To account for the site differences in soil texture and irrigation, the mixed-effects statistical models used in our analyses treat site as a random blocking factor.

Sap flux density

Seasonal patterns of sap flux density (g H_2O cm^{-2} day^{-1}) varied among the seven tree genera (Figure 3-2). For those genera sampled in both 2007 and 2008 (*i.e.*, *Picea*, *Pinus*, and *Fraxinus*), while some of the inter-annual variation in the magnitude of daily sums of J_S can be attributed to different study sites and trees, the seasonal patterns of daily J_S within each genera were consistent across the two years. At the beginning and end of both growing seasons, daily J_S varied among genera mainly due to plant functional type differences in leaf habit. Four deciduous genera (*Fraxinus*, *Ulmus*, *Tilia* and *Juglans*) had low values of daily J_S when trees were leafless in early spring (before DOY 140) and late fall (after DOY 300). In contrast, evergreen genera (*Picea* and *Pinus*) had high rates of daily J_S in early spring and did not have low rates of daily J_S until the daily mean air temperature dropped below 0ºC in late fall of 2008 (Figure 3-1, Figure 3-2).

Daily patterns of sap flux density in 2008 showed higher rates of J_S (g H_2O m^{-2} s^{-1}) across the entire day for evergreen species during April and May, with less pronounced but still significantly higher J_S in October and November, than deciduous species (Figure 3-3).

Although some genera were only measured at one site (*Tilia*, *Juglans*, and *Quercus*), patterns of J_S during the middle of the growing season (June to August) suggest that differences in xylem anatomy may play a role. In both conifer (*Picea* and *Pinus*) and diffuse-porous genera (*Tilia* and *Juglans*), daily J_S peaked in May or June and then decreased as the growing season progressed (Figure 3-2). In contrast, daily J_S in ring-porous genera (*Fraxinus*, *Ulmus*, and *Quercus*) was relatively uniform across the growing season (Figure 3-2). In June and July 2008, the daily patterns of J_S showed that diffuse-porous genera had on average higher rates of J_S across the day than did either conifer or ring-porous genera (Figure 3-3). However, by August all three xylem anatomy types showed similar diurnal patterns of J_S. The morning increase in J_S and evening decline in J_S occurred at similar times of day for all xylem anatomy types, although the timing of these diurnal events varied across the year with changes in day length.

In 2008, daily J_S showed a saturating response to increasing D_Z during the growing season (Figure 3-4). In conifer (*Picea* and *Pinus*) and diffuse-porous genera (*Tilia* and *Juglans*), daily J_S reached higher asymptotic maxima early in the growing season than late in the growing season, as highlighted by the decline in parameter *a* of the exponential saturation models in June and September (Figure 3-4, Table 3-4). In addition, daily J_S reached a maximum at higher values of D_Z in June than in September, indicating stomatal

closure was initiated at lower values of D_Z in September than in June. In contrast, the response of daily J_S to increasing D_Z did not change across the growing season in ring-porous genera (*Fraxinus* and *Ulmus*). Daily J_S reached similar maximum values (parameter *a*, Table 3-4) at similar values of D_Z in both June and September. Data for conifer and ring-porous genera sampled in 2007 were consistent with these results (data not shown).

Daily J_S showed two distinct responses to increasing daily sums of PAR in 2008 (Figure 3-5). In conifer (*Picea* and *Pinus*) and diffuse-porous genera (*Tilia* and *Juglans*), daily J_S had a linear response to increasing PAR, with a stronger correlation in conifer genera (*Picea* $R^2 = 0.93$, $P < 0.001$ and *Pinus* $R^2 = 0.90$, $P < 0.001$ vs. *Tilia* $R^2 = 0.85$, $P < 0.001$ and *Juglans* $R^2 = 0.72$, $P < 0.001$, respectively). In ring-porous genera (*Fraxinus* and *Ulmus*), daily J_S had a saturating response with PAR. Unlike the responses of daily J_S to increasing D_Z, the responses of daily J_S to increasing PAR generally did not vary across the 2008 growing season (June to September). *Tilia* was the only genus to show a decrease in the slope of the J_S to PAR relationship between June and September.

Over the middle of the 2008 growing season (DOY 165 – 250), when all genera had maximum LAI, daily J_S had a slight, but significant, positive response to increasing soil moisture in *Picea* ($R^2 = 0.37$, $P < 0.001$), *Pinus* ($R^2 = 0.18$, $P < 0.001$), and *Tilia* ($R^2 = 0.53$, $P < 0.001$). Daily J_S, however, was not significantly explained by soil moisture in *Juglans* ($R^2 = 0.002$, $P = 0.29$), *Fraxinus* ($R^2 = –0.007$, $P = 0.48$), and *Ulmus* ($R^2 = 0.004$, $P = 0.26$) genera. Volumetric soil water content ranged from 8% to 22% at the Lauderdale site and 12% to 28% at the Saint Paul site over this time period.

When averaged over the middle of the 2008 growing season (DOY 165 – 250), daily J_S was not significantly different among plant functional types ($P = 0.53$). Although our study was not designed to formally test for differences among genera, xylem anatomy, or shade tolerance, growing season means of daily J_S (Table 3-5) suggest that there were not large differences among these tree classification schemes (Table 3-2).

Transpiration

The magnitude and seasonal patterns of daily transpiration per unit canopy area (E_C), varied markedly between the evergreen needleleaf and deciduous broadleaf plant functional types (Figure 3-6). When averaged over the middle of the 2008 growing season, evergreen needleleaf trees transpired almost twice as much water per unit canopy area per day as deciduous broadleaf trees (1.90 and 1.11 kg H_2O m^{-2} day^{-1}, respectively, $P = 0.014$). This variation in daily E_C was largely due to plant functional type differences in canopy structure. Compared to deciduous broadleaf trees, evergreen needleleaf trees had higher LAI (5.5 and 8.8 m^2 m^{-2}, respectively, $P = 0.11$, Table 3-2) and significantly smaller projected canopy area (73.6 and 31.1 m^2, respectively, $P = 0.02$, Table 3-2). Not only did evergreen needleleaf trees have higher daily E_C values on average across all months of the 2008 measurement period, but they also remained active over a much longer growing season than the deciduous broadleaf trees. On average, the evergreen needleleaf trees sustained transpiration rates of over 0.5 kg H_2O m^{-2} day^{-1} for at least eight months in 2008, compared to only four months in deciduous broadleaf trees (Figure 3-6). Consequently, the differences we found between plant functional types in average

growing season daily E_C were further exaggerated at the annual scale. Cumulative annual E_C of evergreen needleleaf trees was on average 307 kg H_2O m^{-2} yr^{-1}, while the annual E_C of deciduous broadleaf trees was 153 kg H_2O m^{-2} yr^{-1} ($P = 0.003$, Figure 3-7). This estimate of total annual water loss from evergreen needleleaf trees is likely a slight underestimate because our spring measurements began after these trees were already physiologically active (Figure 3-2). In the middle of winter, however, air temperature is typically below freezing in this area and transpiration from evergreen needleleaf trees is likely to be minimal.

When averaged over the middle of the 2008 growing season (DOY 165 – 250), daily transpiration per unit leaf area (E_L) was not significantly different among plant functional types ($P = 0.57$). Daily E_L, when averaged over the middle of the 2008 growing season, also did not suggest any differences due to genera, xylem anatomy, or shade tolerance (Table 3-5), although our experimental design did not allow formal statistical tests for these differences.

Discussion

Sap flux density differences among tree types

Genera showed marked differences in both the magnitude and pattern of daily sap flux density, largely due to differences in leaf habit among plant functional types and suggestive of differences in xylem anatomy. Evergreen needleleaf trees are among the most cold tolerant of tree species, with some species capable of surviving temperatures as

low as –60ºC (Havranek and Tranquillini 1995). An evergreen leaf habit consequently allows trees to remain physiologically active over a longer growing season than trees with a deciduous leaf habit. Similar to the results of this study, Catovsky et al. (2002) found that *Tsuga canadensis*, an evergreen needleleaf species, had relatively high J_S when coexisting deciduous broadleaf species were leafless in a northeastern USA forest. We also found patterns of J_S during the middle of the growing season consistent with other studies that show differences in water use among xylem anatomy types. For example, Bush et al. (2008) found that ring-porous species growing in Salt Lake City, Utah showed relatively constant maximum J_S rates across the growing season, while diffuse-porous species showed steady declines in maximum J_S rates.

Although we did not observe species' differences in sap flux that could be explained by differences in shade tolerance, our study was not designed to formally test this idea and thus it warrants further study. It may be that shade tolerance is relatively more important for establishment and timing of growth than for regulating adult tree water use. Typically shade tolerance is a trait assessed in juvenile trees and can vary across the lifetime of a tree, with juveniles of a given species usually exhibiting greater shade tolerance than adults (Niinemets and Valladares 2006). Consequently, the species-specific shade tolerance rankings we used may not be particularly relevant for the fully mature, planted trees we studied.

Responses to environmental drivers

Seasonal patterns of daily J_S are generally thought to relate to species' differences in vulnerability to xylem cavitation and stomatal sensitivity to vapor pressure deficit. The variation in species' responses to vapor pressure deficit and PAR that we observed in a suburban ecosystem over the growing season lends support to these ideas. Consistent with the idea that ring-porous species are more vulnerable to cavitation because of their large earlywood vessels (Hacke et al. 2006, Taneda and Sperry 2008), we found that ring-porous genera appeared to exercise greater stomatal regulation at high D_Z and more constant stomatal regulation across the growing season. Reductions in sap flux via stomatal closure at high D_Z may protect the xylem of ring-porous species from cavitation, but potentially at the expense of photosynthesis and carbon gain. Although we did not directly measure photosynthesis in this study, the saturating response of J_S to increasing PAR in ring-porous species suggests that these species are limited in their ability to use high light conditions for photosynthesis. The growing season declines in maximum J_S, as well as D_Z at maximum J_S, that we observed for conifer and diffuse-porous species are also consistent with evidence that these xylem anatomy types can maintain relatively high hydraulic conductance at low xylem pressure, but do so at the risk of some drought-induced xylem cavitation over time (Hacke et al. 2006, Sperry et al. 2006, Willson and Jackson 2006, Taneda and Sperry 2008). The linear response of J_S to increasing PAR in conifer and diffuse-porous species suggests that these species permit greater carbon uptake and growth during high light, high vapor pressure deficit conditions. Because we did not directly measure cavitation in this study, alternative hypotheses that may explain the observed decline in J_S over the growing season include artifacts of sensors measuring a higher pro-

portion of less functional, older xylem as trees grow radially (Melcher et al. 2003), physiological changes associated with leaf senescence (Matile 2000), pectins, gums, resins, latex, or tylose formation blocking xylem over time (Neumann et al.), or changes in water uptake by roots (Snyder and Williams 2007).

Over the same range of vapor pressure deficit, our measured rates of J_S were similar to published values for the same tree species in natural forest ecosystems (Ewers et al. 2002, Lagergren and Lindroth 2002, Pataki and Oren 2003). This suggests that, under similar environmental conditions, water use measurements from forests could be extrapolated and applied to trees in a low-management, suburban ecosystem such as our study area. However, because urban areas tend to have a wider range of vapor pressure deficit than surrounding areas, these extrapolations should be made with caution. It is likely that we observed distinct water use patterns by xylem anatomy type because our J_S measurements spanned a wider range of vapor pressure deficit than is typical of natural temperate forests. Consistent with this, in Salt Lake City, Utah, Bush et al. (2008) found distinct seasonal patterns of sap flux between ring and diffuse-porous species across a wide range in vapor pressure deficit. In addition, the extrapolation of measurements from natural forests may be difficult because of non-overlapping species composition. To the best of our knowledge, this is the first study to measure J_S in *Fraxinus pennsylvanica*, *Juglans nigra*, *Picea pungens*, and *Pinus nigra,* which are common in urban areas of the north-central and northeastern United States. However, given that there were >80 tree species identified in our study area, it would be desirable to obtain measurements for additional common urban species in future studies.

Given expected changes in regional climate, plans to use trees as "green infrastructure" to manage ecosystem services related to evapotranspiration will require particular attention to species selection. With climate change, air temperature and vapor pressure deficit are expected to increase in many urban areas (Solomon et al. 2007). Co-occurring increases in atmospheric humidity, on the other hand, could result in no changes in urban vapor pressure deficit (Santer et al. 2007). Our results suggest that species composition will affect changes in evapotranspiration from urban ecosystems, along with changes in land use, management practices, and development. Our data suggest that water fluxes from areas with mostly ring-porous species, for example, may be relatively unchanged compared to areas dominated by conifer or diffuse-porous species. However, future study is required to confirm these trends. At the same time, increases in air temperature will also likely influence the seasonality of evapotranspiration rates due to changes in leaf phenology. Higher air temperatures in urban areas compared to rural areas have already been associated with earlier green-up of urban vegetation and changes in regional net primary productivity (Imhoff et al. 2004). Earlier bud break could lead to higher water fluxes in the spring, particularly in areas dominated by diffuse-porous tree species. On the other hand, in areas dominated by evergreen needleleaf species, water fluxes may increase across the year, as the number of days with a mean air temperature above 0ºC increases. Predicting ecosystem responses to climate change is a complex and challenging task. Therefore, we caution that these ideas should be considered hypotheses and investigated with future studies.

Transpiration differences among tree types

Canopy structure and growing season length played important roles in distinguishing species' differences in transpiration rates. Differences in canopy structure may be particularly exaggerated in urban areas due to disparities in pruning practices between coexisting evergreen needleleaf and deciduous broadleaf trees. While lower branches of deciduous broadleaf trees are often pruned and reduce the LAI per tree, these branches are frequently left in place on evergreen needleleaf trees and increase the LAI per tree. These differences in canopy structure, along with differences in projected canopy area and growing season length, yielded the significantly higher daily and annual transpiration rates of evergreen needleleaf trees on a per unit canopy area basis than deciduous broadleaf trees. Although relatively few studies express tree transpiration on a per unit canopy area basis, Catovsky et al. (2002) found that hemlock (*Tsuga canadensis*) trees had lower annual transpiration per unit canopy area than did deciduous broadleaf species in a northeastern USA forest. These contrasting results are likely because hemlock trees have lower LAI than most other evergreen needleleaf species (Waring et al. 1978).

To estimate the tree transpiration component of urban water budgets, differences between evergreen needleleaf and deciduous broadleaf trees in growing season length and canopy structure offer an approach for scaling up species differences in water use. Projected canopy area is also a logistically easy and nondestructive metric to assess in urban ecosystems compared to the more traditional metrics used to scale up tree transpiration in natural forest ecosystems, such as stand-level sapwood area per hectare or leaf area index (Granier et al. 1996, Ewers et al. 2002, Bovard et al. 2005, Tang et al. 2006,

Ford et al. 2007, McLaren et al. 2008, Oishi et al. 2008). While stands of trees do exist in urban areas, in general trees are more isolated and patchily distributed across urban landscapes, making it difficult to measure and extrapolate stand-level features (*e.g.* sapwood area per hectare). The distribution of trees in savanna ecosystems is similarly patchy, which is why in a Mediterranean oak savannah ecosystem, projected canopy area was also used for scaling up the tree transpiration component of a water budget (Paco et al. 2009). Additionally, logistical constraints may limit the ability to collect extensive data for urban ecosystems. For instance, the number of individual homeowner permissions needed to core privately owned trees for sapwood area measurements in urban areas could be quite extensive and difficult to obtain. The allometric equations often used to estimate stand-level sapwood area or leaf area in forest ecosystems may not be suitable for application in urban ecosystems because they can be highly site specific and remain under-developed for open-grown, urban trees (Peper and McPherson 2003). We compared our measurements of sapwood area to values calculated using published allometric equations for the same species in forest ecosystems (Lundblad and Lindroth 2002, Wullschleger and Hanson 2006, Gebauer et al. 2008) and found that the allometric equations on average overestimated our measurements by 26% ($y = 1.26x$, $R^2 = 0.86$, $P < 0.001$). However, for trees with a sapwood area less than 400 cm^2, the allometric equations overestimated our measured values by only 18% ($y = 1.18x$, $R^2 = 0.76$, $P < 0.001$). In contrast, projected canopy area can be easily assessed in urban areas using forest inventories and remote sensing imagery (Nowak et al. 1996, Walton et al. 2008). Tree cover maps and forest inventories already exist for many cities and thus are readily avail-

able for this type of scaling. A combination of high-resolution remote sensing products (*e.g.,* QuickBird and LiDAR) and techniques now allow deciduous and evergreen tree canopies and ground cover classes to be detected in urban areas (Tooke et al. 2009).

Regardless of the approach used to estimate tree canopy cover in urban areas, the spatial heterogeneity of urban microclimates will complicate efforts to scale up and predict the tree transpiration component of urban water budgets (Peters and McFadden 2010). For example, even the extrapolation of our measurements to street trees in the same city would potentially be complicated by the differences in environmental conditions experienced by trees grown over impervious surfaces compared to trees grown over turfgrass. When grown over asphalt, trees experience more desiccating atmospheric conditions that cause some species to show increased rates of water loss, whereas others show reduced stomatal conductance and lower transpiration rates (Cregg 1995, Kjelgren and Montague 1998, Mueller and Day 2005, Leuzinger et al. 2010).

Conclusions

Sap flux measurements in a suburban neighborhood in the north-central United States showed that the magnitude and seasonality of transpiration in common urban tree species differed significantly with plant functional type (evergreen needleleaf and deciduous broadleaf). The measurements also showed patterns of sap flux consistent with differences in xylem anatomy (conifer, ring-porous, and diffuse-porous) among tree species. As the growing season progressed, conifer and diffuse-porous genera had increased

stomatal regulation to high vapor pressure deficit, while ring-porous genera maintained greater and more constant stomatal regulation. The variation among tree species' responses to vapor pressure deficit suggests that evapotranspiration from urban forest ecosystems in response to climate change will depend in part on species composition. Evergreen needleleaf trees had significantly higher growing season means and total annual transpiration per unit canopy area (1.90 kg H_2O m^{-2} day^{-1} and 307 kg H_2O m^{-2} yr^{-1}, respectively) than deciduous broadleaf trees (1.11 kg H_2O m^{-2} day^{-1} and 153 kg H_2O m^{-2} yr^{-1}, respectively). This was because evergreen trees, in comparison to deciduous trees, had a smaller projected canopy area (31.1 and 73.6 m^2, respectively), a higher leaf area index (8.8 and 5.5 m^2 m^{-2}, respectively), and a longer growth season (8 and 4 months, respectively). These plant functional type differences in canopy structure and growing season length offer an approach to scale up species' differences in tree transpiration and predict the evapotranspiration component of urban and suburban water budgets for management of urban ecosystem services.

Table 3-1. Fractional contribution of nine tree genera to the total stem count, canopy area, and basal area (cross-sectional area measured at 1.4 m) of trees >5 cm DBH in a forest inventory of a suburban neighborhood of Minneapolis–Saint Paul, Minnesota. Genera are sorted by their fractional contribution to the total canopy area.

Genus	Stems (%)	Canopy area (%)	Basal area (%)
Acer	16	22	21
Quercus	6	14	16
Fraxinus	13	13	10
Ulmus	7	9	7
Picea	18	8	13
Populus	7	7	9
Gledistia	2	5	3
Pinus	7	5	8
Betula	5	4	2
Other genera	19	13	11

Table 3-2. Site, plant functional type, xylem anatomy, shade tolerance, mean projected canopy area, mean leaf area index (LAI), mean sapwood depth, mean diameter at 1.4 m (DBH), and mean height by tree species per year. Numbers in parentheses are one standard deviation of the mean.

Species	*n*	Site	Plant Functional Type	Xylem Anatomy	Shade Tolerance[a]	Canopy Area (m^2)	LAI (m^2 m^{-2})	Sapwood Depth (cm)	DBH (cm)	Height (m)
2007										
Fraxinus pennsylvanica	2	CTC	deciduous broadleaf	ring-porous	mid	101.6 (59.8)	—	10.0 (0.1)	49.1 (2.0)	19.4 (2.7)
Picea glauca	3	Grove	evergreen needleleaf	conifer	high	14.3 (6.8)	—	2.9 (1.3)	16.7 (5.5)	9.8 (3.4)
Picea pungens	4	Grove	evergreen needleleaf	conifer	high	11.8 (1.2)	—	4.3 (1.6)	16.8 (5.0)	9.6 (2.7)
Pinus strobes	1	Grove	evergreen needleleaf	conifer	mid	28.7 (NA)	—	6.6 (NA)	15.2 (NA)	10.3 (NA)
Quercus rubra	5	CTC	deciduous broadleaf	ring-porous	mid	85.1 (30.1)	—	1.8 (0.3)	42.9 (7.7)	20.8 (3.5)
2008										
Fraxinus pennsylvanica	4	Lauderdale Saint Paul	deciduous broadleaf	ring-porous	mid	75.9 (11.1)	4.1 (1.3)	8.8 (3.3)	38.6 (11.4)	17.7 (5.5)
Juglans nigra	2	Saint Paul	deciduous broadleaf	diffuse-porous	low	96.4 (71.0)	4.6 (0.2)	4.8 (0.04)	40.8 (25.1)	15.0 (4.0)
Picea abies	2	Lauderdale	evergreen needleleaf	conifer	high	46.3 (16.7)	9.1 (2.3)	3.0 (0.7)	49.7 (7.0)	20.8 (5.4)

Picea glauca	2	Saint Paul	evergreen needleleaf	conifer	high	26.0 (2.4)	11.3 (0.1)	5.9 (0.3)	29.9 (5.4)	13.0 (0.8)
Pinus nigra	2	Lauderdale	evergreen needleleaf	conifer	low	33.6 (1.0)	7.6 (0.4)	7.7 (1.8)	41.5 (6.3)	20.0 (1.7)
Pinus sylvestris	2	Saint Paul	evergreen needleleaf	conifer	low	18.4 (6.7)	7.1 (1.5)	8.6 (1.3)	21.0 (2.9)	9.1 (3.0)
Tilia americana	2	Saint Paul	deciduous broadleaf	diffuse-porous	high	28.1 (2.0)	10.2 (0.9)	7.7 (0.5)	22.8 (1.8)	12.8 (0.3)
Ulmus pumila	2	Lauderdale	deciduous broadleaf	ring-porous	mid	90.8 (70.6)	2.8 (0.4)	2.6 (0.9)	50.8 (12.6)	20.7 (4.7)
Ulmus thomasii	2	Saint Paul	deciduous broadleaf	ring-porous	mid	68.1 (36.3)	6.5 (0.8)	3.0 (0.1)	44.4 (7.0)	13.1 (0.7)

[a] (Niinemets and Valladares 2006)

Table 3-3. Average maximum, mean, and minimum air temperature (T_{air}) for day and night periods during the 2007 and 2008 growing seasons (DOY 165–250). Day was defined as time periods when incoming solar radiation was >10 W m^{-2}. Numbers in parentheses are one standard deviation of the mean.

	Maximum T_{air} (ºC)	Mean T_{air} (ºC)	Minimum T_{air} (ºC)
2007			
Day	27.2 (3.9)	24.0 (3.3)	18.2 (2.7)
Night	24.7 (3.4)	20.9 (2.6)	18.1 (2.6)
2008			
Day	26.5 (3.1)	23.3 (2.9)	17.1 (3.0)
Night	23.8 (3.1)	19.8 (2.7)	16.9 (3.0)

Table 3-4. Parameters for the exponential saturation model $J_S = a(1 - \exp(-bD_Z))$ for six genera in June and September 2008.

		June		September	
Genus	*n*	*a*	*b*	*a*	*b*
Fraxinus	4	159.1	1.5	139.4	1.7
Juglans	2	207.6	1.5	129.4	2.1
Picea	4	232.4	0.8	156.0	0.7
Pinus	4	186.5	1.1	141.8	0.8
Tilia	2	376.2	0.7	140.9	1.1
Ulmus	4	150.5	1.5	156.1	1.6

Table 3-5. Growing season means of daily sap flux density per unit sapwood area (J_S), transpiration per unit canopy area (E_C), transpiration per unit leaf area (E_L), and annual sums of E_C for six genera in 2008. Numbers in parentheses are ±1 standard error.

Genus	*n*	Growing Season Mean J_S (g cm^{-2} day^{-1})	Growing Season Mean E_C (kg m^{-2} day^{-1})	Growing Season Mean E_L (kg m^{-2} day^{-1})	Annual Sum E_C (kg m^{-2} yr^{-1})
Fraxinus	4	153.91 (20.78)	0.91 (0.34)	0.24 (0.09)	122.87 (50.02)
Juglans	2	186.26 (35.99)	0.76 (0.52)	0.19 (0.11)	97.20 (78.51)
Picea	4	158.67 (29.38)	1.80 (0.42)	0.18 (0.08)	294.81 (62.76)
Pinus	4	152.58 (29.38)	2.01 (0.42)	0.28 (0.09)	319.22 (62.76)
Tilia	2	210.97 (35.99)	1.87 (0.52)	0.23 (0.11)	240.75 (78.51)
Ulmus	4	148.19 (29.39)	1.18 (0.42)	0.31 (0.09)	171.51 (62.76)

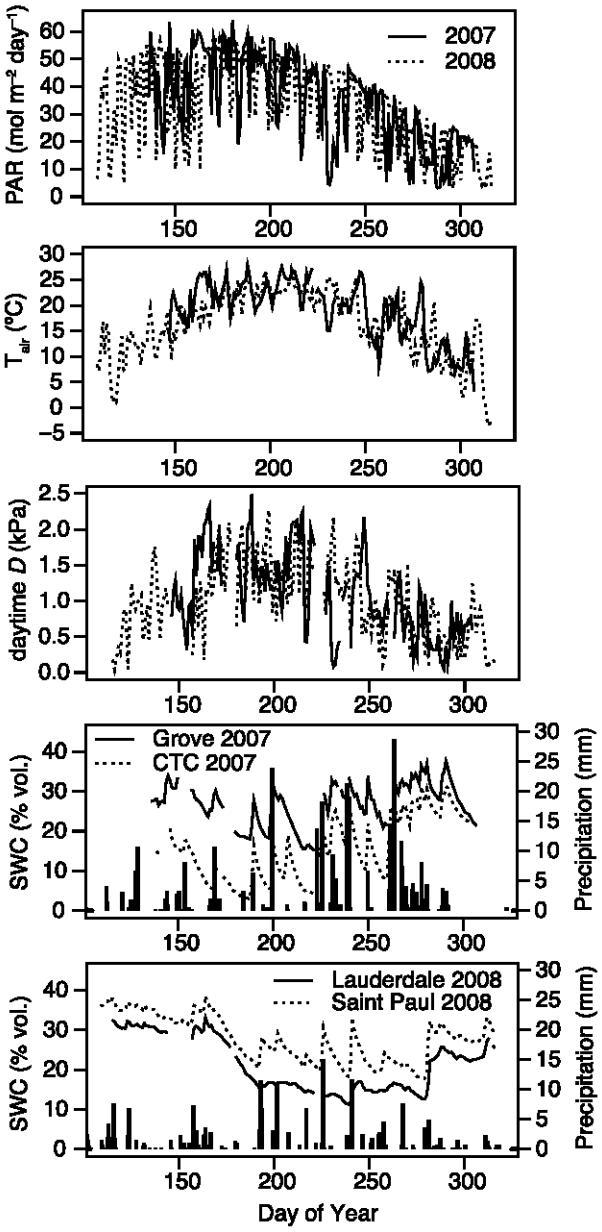

Figure 3-1. Photosynthetically active radiation (PAR), mean daily air temperature (T_{air}), mean daytime vapor pressure deficit (*D*), soil water content (SWC), and precipitation in a suburban neighborhood of Minneapolis–Saint Paul, Minnesota. PAR and precipitation were measured at climate stations in nearby open turfgrass lawns. T_{air} and *D* were measured at a total of four stands: Grove and CTC sites in 2007 and Lauderdale and Saint Paul

sites in 2008. Only the 2007 and 2008 means of T_{air} and D are shown because in 2007 significant site differences were small in magnitude (0.9ºC, $P < 0.001$ and 0.1 kPa, $P < 0.001$, respectively) and in 2008 sites were not significantly different ($P = 0.72$ and $P = 0.61$, respectively). Soil water content was measured at the same four stands.

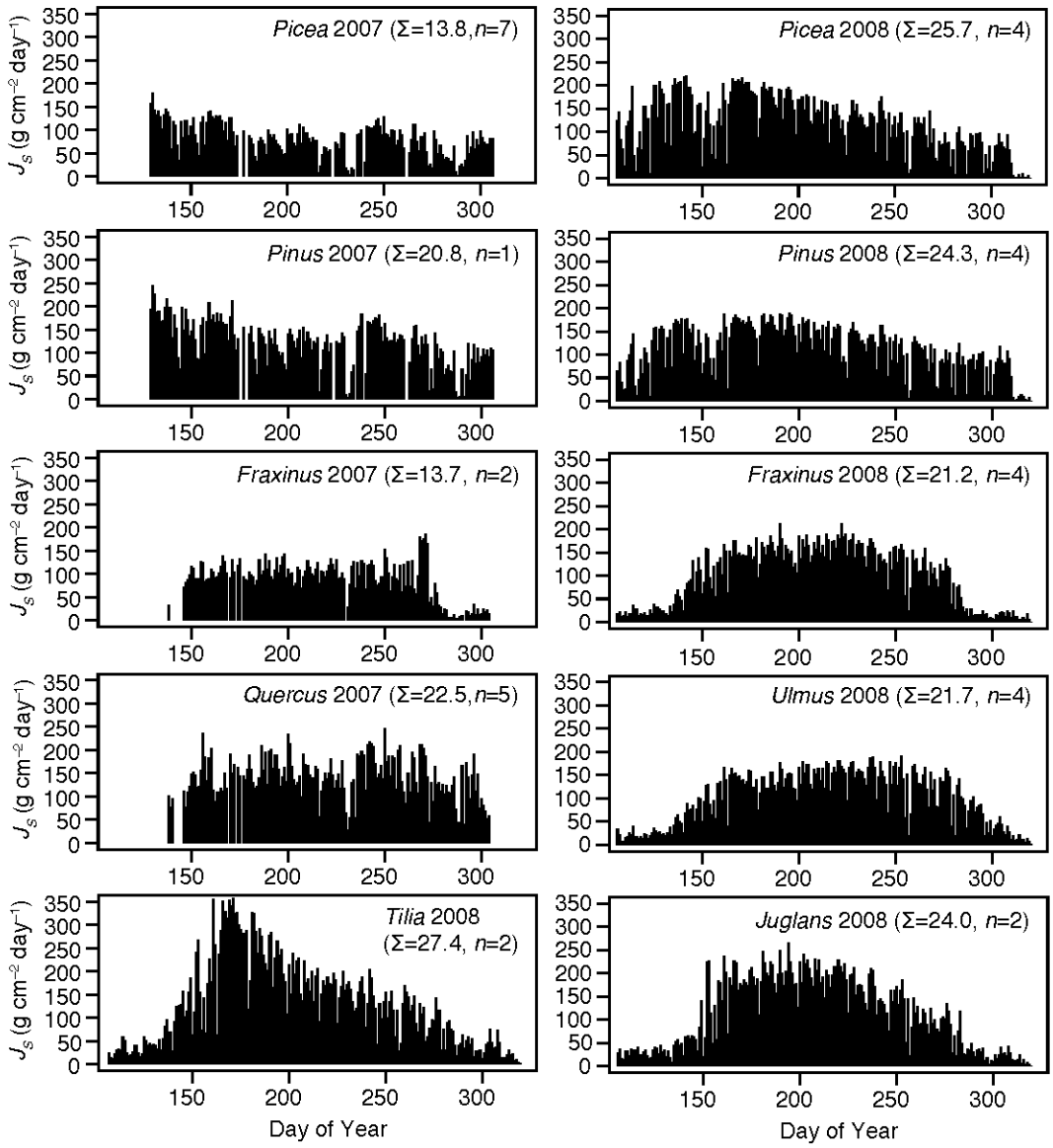

Figure 3-2. Daily sums of sap flux density per unit sapwood area (J_S) for seven tree genera measured in a suburban neighborhood of Minneapolis–Saint Paul, Minnesota. Each panel represents the mean of all trees per genus measured for a given year. Early spring (April) sap flux density observations are not available for 2007 because measurements did not commence until May. In 2007, measurements were made at the CTC and Grove sites. In 2008, measurements were made at the Lauderdale and Saint Paul sites. See Table

3-2 for the sites at which each genus was measured. Missing data represent days when equipment failed due to power interruptions. Numbers in parentheses are integrated sums of J_S in kg H_2O cm^{-2} across the measurement period and n number of trees measured, respectively.

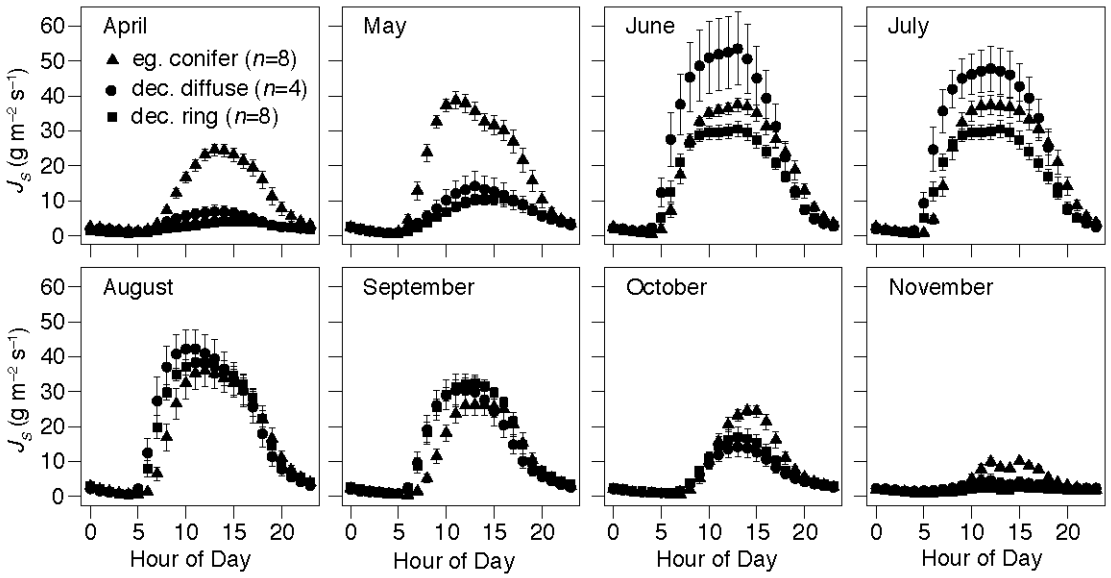

Figure 3-3. Average diurnal patterns of sap flux density per unit sapwood area (J_S) for three groups of trees in a suburban neighborhood of Minneapolis–Saint Paul, Minnesota: evergreen needleleaf conifer genera (triangles), deciduous broadleaf diffuse-porous genera (circles), and deciduous broadleaf ring-porous genera (squares). Data shown are from April to November 2008. Error bars represent ± 1 standard error. Numbers in parentheses are *n* number of trees measured per group.

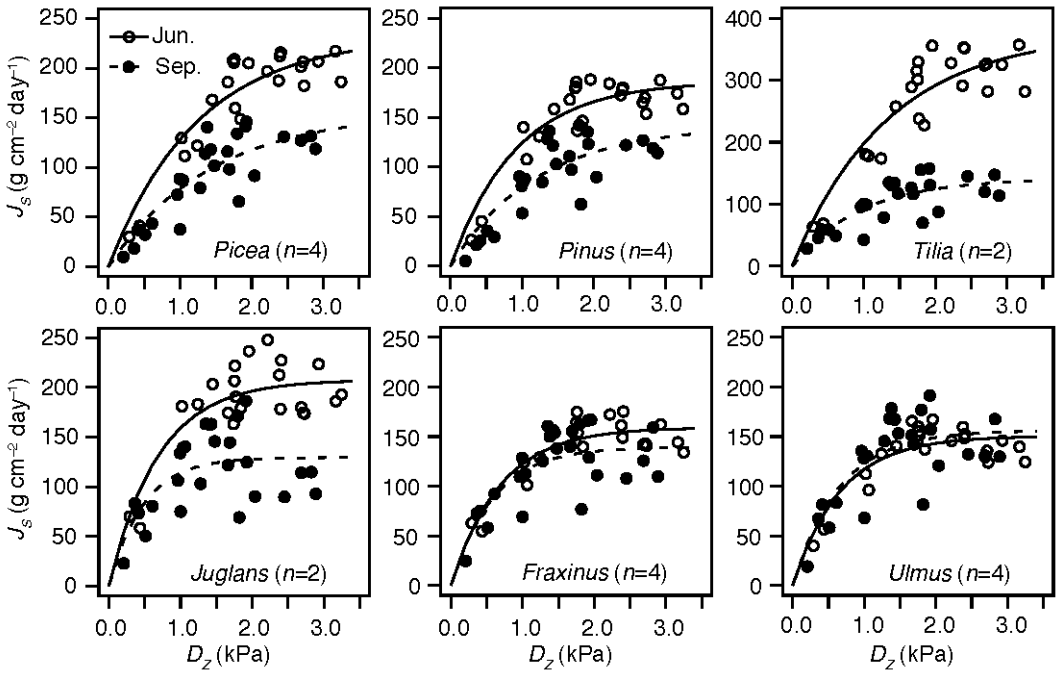

Figure 3-4. Daily sums of sap flux density per unit sapwood area (J_S) in response to day length normalized mean daytime vapor pressure deficit (D_Z) in a suburban neighborhood of Minneapolis–Saint Paul, Minnesota. Data shown are from June (open circles) and September (closed circles) in 2008. Each panel represents the mean of all trees measured per genus with *n* number of trees shown in parentheses. Lines are exponential saturation curves of the form: $y = a(1 - \exp(-bx))$. Note the different vertical axis for *Tilia*.

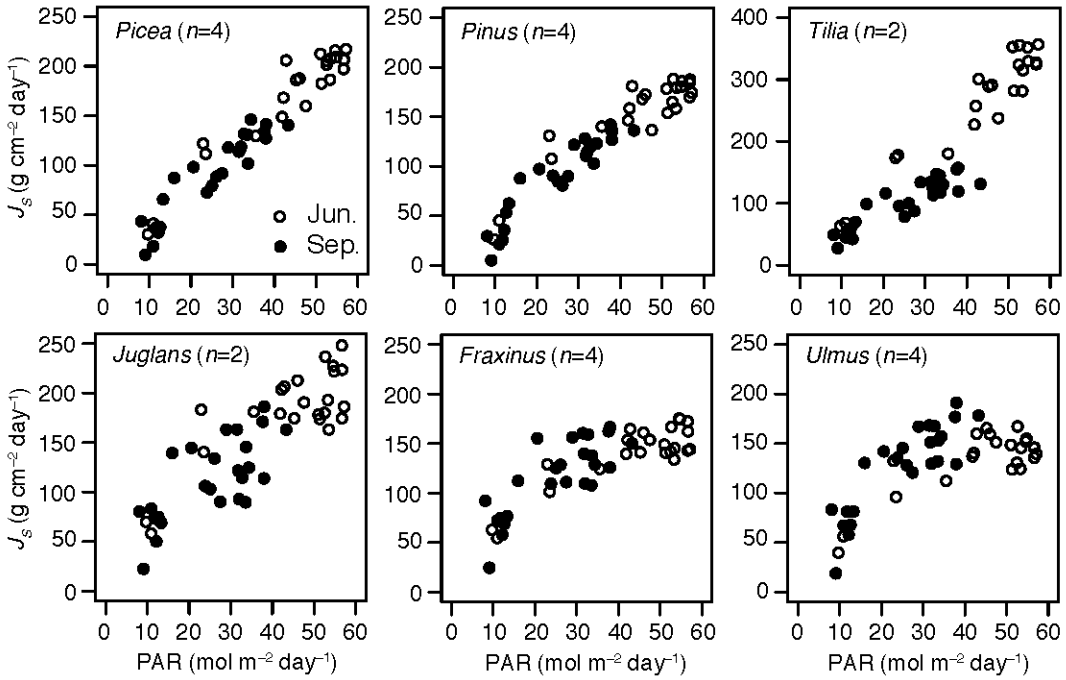

Figure 3-5. Daily sums of sap flux density per unit sapwood area (J_S) in response to daily sums of photosynthetically active radiation (PAR) in a suburban neighborhood of Minneapolis–Saint Paul, Minnesota. Data shown are from June (open circles) and September (closed circles) in 2008. Each panel represents the mean of all trees measured per genus with *n* number of trees shown in parentheses. Note the different vertical axis for *Tilia*.

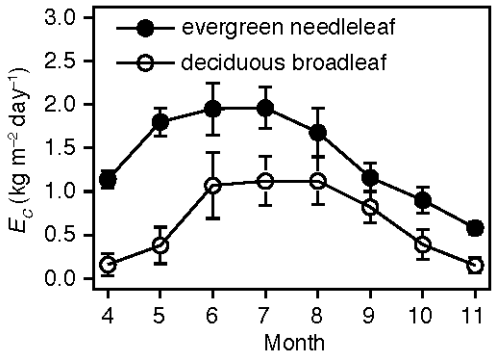

Figure 3-6. Daily sums of transpiration per unit canopy area (E_C) in evergreen needleleaf (closed circles) and deciduous broadleaf (open circles) plant functional types in a suburban neighborhood of Minneapolis–Saint Paul, Minnesota. Symbols represent monthly averages from April to November 2008. Error bars represent ±1 standard error.

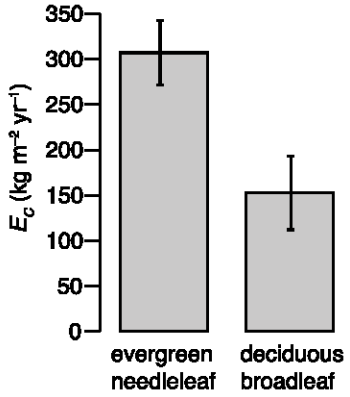

Figure 3-7. Total annual transpiration per unit canopy area (E_C) in evergreen needleleaf and deciduous broadleaf plant functional types in a suburban neighborhood of Minneapolis–Saint Paul, Minnesota. Cumulative water loss was summed from April to November 2008. Error bars represent ±1 standard error.

Chapter 4

Seasonal contributions of vegetation types to suburban evapotranspiration

Summary

Evapotranspiration is an important term of both energy and water balances in urban areas and is an important ecosystem service of urban vegetation. The spatial heterogeneity of urban surface types with different seasonal water use patterns (*e.g.* trees and turfgrass lawns) complicates efforts to predict and manage urban evapotranspiration rates, necessitating a surface type, or component-based, approach. In a suburban neighborhood of Minneapolis–Saint Paul, Minnesota, USA, we simultaneously measured ecosystem evapotranspiration and its main component fluxes using eddy covariance and heat dissipation sap flux techniques to assess the relative contribution of plant functional types (evergreen needleleaf tree, deciduous broadleaf tree, cool-season turfgrass) to seasonal and spatial variations in suburban evapotranspiration. Component-based evapotranspiration estimates agreed well with measured water vapor fluxes, although the imbalance between methods varied seasonally from an overestimate of 20% in spring to an underestimate of 11% in summer. Turfgrasses represented the largest contribution to total annual evapotranspiration in recreational and residential land-use types (87% and 64%, respectively), followed by trees (10% and 31%, respectively), with the relative contribution of

plant functional types dependent on fractional cover and seasonal differences in daily water use. Recreational areas had higher annual evapotranspiration than residential areas (467 versus 324 mm $year^{-1}$, respectively) and altered seasonal patterns of evapotranspiration due to greater turfgrass cover (74% versus 34%, respectively). Our results suggest that plant functional types offer a useful approach to predict the seasonal patterns of evapotranspiration among cities, as well as with changes in climate, land use, or vegetation composition that may disproportionately impact urban vegetation types.

Introduction

Evapotranspiration is an important term of both energy and water balances urban areas and consequently plays a key role in management decisions related to conservation of water resources, mitigation of urban heat islands, and reduction of storm water runoff. Managing these ecosystem services requires accurate assessments of urban evapotranspiration rates, and indeed water vapor fluxes have been measured from numerous cities representing different climates, geographical regions, and land-use types (Grimmond and Oke 1999, Nemitz et al. 2002b, Spronken-Smith 2002, Moriwaki and Kanda 2004, Offerle et al. 2006, Balogun et al. 2009). Collectively, these studies show that cities vary in magnitude and seasonality of evapotranspiration due to differences in climate, irrigation, and vegetation cover. For example, densely built-up city centers or downtown areas with high impervious surface cover tend to have lower evapotranspiration rates and smaller evaporative fractions (Nemitz et al. 2002b, Grimmond et al. 2004) than residential areas with short buildings and high vegetation cover (Grimmond et al. 1996, Moriwaki and

Kanda 2004, Grimmond et al. 2006, Balogun et al. 2009). Recent studies additionally suggest that plant growth form is another important factor controlling total evapotranspiration in urban areas, with turfgrass-dominated areas showing higher water fluxes than tree-dominated areas (Kotani and Sugita 2005, Offerle et al. 2006, Balogun et al. 2009). The spatial heterogeneity of urban landscapes, however, greatly complicates the extrapolation of these ecosystem-scale measurements to other urban and suburban areas, as vegetation composition varies widely within and between cities. The management of urban ecosystem services necessitates an approach to quantifying urban evapotranspiration rates according to the major land-surface types present, hereafter referred to as a component-based approach. Partitioning of ecosystem water fluxes among stand types or species has been previously investigated in natural ecosystems (Baldocchi et al. 2000, Oishi et al. 2008, Paco et al. 2009), yet this information is relatively lacking in urban ecosystems.

Plant functional types provide a potentially useful approach for partitioning the seasonal patterns of urban evapotranspiration, as they represent major physiological and biophysical differences among plant species (Reich et al. 1997) and they also can be uniquely identified in urban landscapes using high-resolution satellite imagery (Tooke et al. 2009). For example, evergreen needleleaf trees tend to have lower leaf-level transpiration rates than deciduous broadleaf trees (Givnish 2002), while both tree types tend to have deeper roots and access to additional sources of water compared to cool-season grasses (Jackson et al. 1996, Ludwig et al. 2004). Plant functional types also represent distinct seasonal patterns in physiological activity, or phenology, among plant species. For example, cool-season turfgrasses, which are ubiquitous across temperate urban land-

scapes (Milesi et al. 2005), are physiologically active primarily in the spring and fall (Zhang et al. 2007), while evergreen needleleaf and deciduous broadleaf trees show peak function in mid-summer (Givnish 2002). Many studies have quantified evapotranspiration rates of turfgrass (Feldhake et al. 1983, 1984, Zhang et al. 2007) and, to a lesser extent, of trees in urban areas (Whitlow and Bassuk 1988, Whitlow et al. 1992, Bush et al. 2008), yet no work has examined the combined effects of these plant functional types on the seasonality of urban evapotranspiration.

Here we report a two-year study in which we made independent measurements of total ecosystem evapotranspiration and its main component fluxes to better understand how vegetation influences the spatial and seasonal variation in suburban evapotranspiration. We measured ecosystem evapotranspiration using an eddy covariance system mounted 40 m above the landscape, tree transpiration using heat dissipation sap flow sensors, and turfgrass evapotranspiration using a 1.35 m portable eddy covariance system. Our main objectives were to: 1) determine the magnitude and seasonal patterns of suburban evapotranspiration; 2) evaluate how well scaled component-based estimates match measured ecosystem evapotranspiration rates; 3) determine how the magnitude and seasonality of ecosystem evapotranspiration varies between residential and recreational land-use types; and 4) examine the seasonal water use patterns of vegetation types and their influence on ecosystem evapotranspiration in recreational and residential land-use types.

Methods

Site information

Our study was conducted in a first-ring suburban neighborhood in the Minneapolis–Saint Paul metropolitan area in east-central Minnesota, USA (44º59'N, 93º11'W). Prior to rapid residential development in the 1950s, the prominent land-use types in the area were farms and nurseries. The area has a cold temperate climate with mean annual temperature of 7.4ºC and mean annual precipitation of 747 mm. Due to its location near the center of the metropolitan area, the study area was influenced by the urban heat island effect that has been documented for Minneapolis–Saint Paul (Winkler et al. 1981, Todhunter 1996, Sen Roy and Yuan 2009). The relatively flat terrain made this landscape suitable for eddy covariance measurements from the KUOM broadcast tower located in the center of our approximately 7 ha study area (Figure 4-1). The area immediately adjacent to the tower consisted of residential land use (single-family housing) to the northwest and northeast and recreational land use (golf course) to the southwest. Vegetated surfaces consisted primarily of forested patches, isolated trees, and open turfgrass lawns. Of the over 80 tree species identified in this area, the dominant canopy species were *Acer negundo* (boxelder), *Acer saccharinum* (silver maple), *Fraxinus pennsylvanica* (green ash), *Gleditsia tricanthos* (honey locust), *Picea glauca* (white spruce), *Populus deltoides* (cottonwood), *Quercus alba* (white oak), and *Ulmus americana* (American elm), with a mean tree height of 12 m.

We selected four sites with stands of trees suitable for sap flux measurements within our study area (Figure 4-1) (Peters et al. in press). Sites were selected to include

representative tree species and sizes with the total number of sites limited by numerous logistical constraints (*e.g.*, equipment, landowner permission, site suitability, signal cable lengths, and access to power). Trees at all sites were grown under park-like conditions with open-canopies and a turfgrass ground cover. The lower branches of many trees were pruned, but canopies were mature and healthy with no obvious signs of disease or damage. Root systems were not likely restricted by impervious surfaces, as the nearest roads and sidewalks occurred beyond the drip-line of all trees and often at distances >10 m from each tree. Surface soils at all sites were moderately compacted with an average bulk density of 1.43 g cm^{-3}, as is typical of urban soils (Craul 1985). Management regimes were considered low-maintenance at all sites and included regular mowing, but had little or no irrigation and no fertilizer use based on personal communication with the landowners.

We made eddy covariance measurements over a 1.5 ha turfgrass field that was located within the footprint of the KUOM tall tower (Figure 4-1). This site was representative of low-maintenance lawns in the area, as it was mowed to a height of 7 cm approximately once per week with clippings left to decompose on the surface and was not irrigated or fertilized. C_3 cool-season turfgrass species, *Poa pratensis* (Kentucky bluegrass), *Lolium perenne* (perennial ryegrass) and *Festuca arundinacea* (tall fescue), dominated this site. Surface soils at this site were slightly compacted with an average bulk density of 1.22 g cm^{-3}.

Measuring suburban evapotranspiration and its component fluxes

Latent (*LE*) and sensible (*H*) heat fluxes over the suburban landscape were measured from the 40 m level on the KUOM broadcast tower using an eddy covariance system consisting of a 3-D sonic anemometer (CSAT3, Campbell Scientific, Inc., Logan, Utah, USA) and a closed-path infrared gas analyzer (LI-7000, LI-Cor, Lincoln, Nebraska, USA). The measurement height was >2× the mean height of the trees, which overtopped the roofs of the houses. The sonic anemometer and the filtered air inlet for the gas analyzer were mounted on a 3 m boom that was oriented toward the northwest (315°). The gas analyzer and the data-acquisition system were housed in an insulated, thermostatically controlled, heated and ventilated rack-mount computer enclosure at the base of the tower. The water vapor channel of the gas analyzer was calibrated using a dew point generator (LI-640, LI-Cor, Lincoln, Nebraska, USA) in a nearby laboratory, with two different LI-7000 instruments cycled regularly between the lab and the tower. Air was sampled through a 9.5-mm I.D. pure FEP tubing at a rate of 23 SLPM and a by-pass flow rate of 7.5 SLPM through 4-mm I.D. pure PTFE tubing and was delivered to the gas analyzer using a system of needle valves, mass-flow meters, and two rotary vane vacuum pumps (Gast models 1023 and 211 for the main and the by-pass pumps, respectively, Benton Harbor, Michigan, USA). The digital data from the sonic anemometer was transmitted to the base of the tower using a pair of fiber optic media converters linked by multimode fiber optic cable to avoid RF interference from the broadcast tower. Data collected with the sonic anemometer and infrared gas analyzer were recorded at 10 Hz using in-house soft-

ware running on a utility-grade UNIX server at the base of the tower (V120, Sun Microsystems, Santa Clara, California, USA).

Thirty minute turbulent fluxes, including ecosystem evapotranspiration (E_{total}), were computed using a slightly modified version of *eth-flux* (Mauder et al. 2008). Following Vickers and Mahrt (1997), a filter was implemented to remove spikes in the sonic data likely caused by data communication. A maximum of five values exceeding ±6 standard deviations within a 300 s moving window were removed. This procedure was repeated three times for each 30 min block. The time lag due to the transport of air through the tubing was calculated using the peak of the cross-correlation function between the vertical wind velocity and the water vapor concentration. The mean lag for the water vapor signals was 11 s. All subsequent analyses were performed using the R (version 2.8) statistical language package (R Development Core Team 2010). The sonic temperature was corrected following Schotanus et al. (1983). High-frequency losses in the fluxes were corrected following Eugster and Senn (1995) using a damping-loss constant of 0.28 s^{-1}. Data were screened to remove periods when instruments were being serviced and wind directions were from the southeast (90 to 180º) to avoid interference from the tower structure. Land use associated with these wind directions was also atypical of the predominantly residential area because it was experimental crop plots cultivated by the University of Minnesota. Gaps in measurements from January 2007 to December 2008 represented 48% of the data, due to unfavorable wind directions (20%) from behind the tower (90–180º) and power outages (28%). We performed a minimal level of filtering to maximize the

amount of data. Due to the complexity of the suburban land surface and our focus on comparing scaled-up surface type fluxes to measured E_{total}, we did not gap-fill the tall tower data for the analyses presented here.

Measured E_{total} should balance against the sum of its component fluxes such that:

$$E_{total} = E_T + E_G + E_W \quad (1)$$

where E_T is evapotranspiration from trees, E_G is evapotranspiration from turfgrass lawns, and E_W is evaporation from open water (*e.g.* ponds and swimming pools). Each of these surface type fluxes was either independently measured or modeled as described below. Evaporation from bare soil and impervious surfaces was assumed to be negligible because bare soil represented a small fraction of the study area (~7%) and impervious surfaces effectively prevent evaporation from soils below.

E_T is composed of tree transpiration (T_T) and rainfall interception loss from tree canopies (I_T) such that:

$$E_T = T_T + I_T \quad (2)$$

In our study area, Peters et al. (in press) found species' differences in T_T per unit canopy area were largely explained by plant functional type differences in canopy structure and growing season length. Consequently, we used evergreen needleleaf and deciduous broadleaf plant functional types to estimate E_T at the ecosystem scale, such that:

$$E_T = E_{Teg} + E_{Tdec} \quad (3)$$

where E_{Teg} is evapotranspiration from evergreen needleleaf trees and E_{Tdec} is evapotranspiration from deciduous broadleaf trees.

T_{T} was measured using Granier-type heat dissipation sap flow (Granier 1987, Lu et al. 2004) on a total of 37 trees (17 trees in 2007 and 20 different trees in 2008) across four sites. Trees represented seven different genera (*Picea, Pinus, Quercus, Fraxinus, Ulmus, Tilia,* and *Juglans*) and two plant functional types (evergreen needleleaf and deciduous broadleaf) (Peters et al. in press). Measurement periods ran from May to November in 2007 and April to November in 2008. The software package BaseLiner (version 2.4.1, Hydro-Ecology Group, Duke University) was used to calculate sap flux density per conducting sapwood area. To minimize underestimates of nocturnal sap flow we calculated reference temperatures only on nights when vapor pressure deficit did not exceed 1 kPa (Oishi et al. 2008). T_{T} per unit canopy area was calculated as the product of each tree's sap flux density and the ratio of cross-sectional sapwood area to projected canopy area. Cross-sectional sapwood area was determined from multiple cores per tree using visual estimates apparent immediately after removal from the trunk (Lu et al. 2004). Adjustments were made for radial variation in sap flow according to Pataki et al. (In review).

I_{T} was estimated using a tree-based adaptation of the Rutter canopy interception model (Rutter et al. 1975, Valente et al. 1997). The crown of each tree was considered a

closed canopy and interception loss calculated on a canopy area basis. Following Wang et al. (2008), we modeled crown storage capacity of both evergreen needleleaf and deciduous broadleaf trees as a function of leaf area index (LAI) with a specific leaf storage of 0.2 mm. The seasonal pattern of LAI was modeled using piece-wise logistic equations fit to stand-level LAI measurements (LAI-2000, LI-Cor, Lincoln, Nebraska, USA) that were collected biweekly at sap flux sites from prior to leaf-out to after senescence in 2007 and 2008 (Peters and McFadden 2010). Maximum LAI values for evergreen needleleaf and deciduous broadleaf trees were determined from mid-summer LAI measurements on each study tree in 2008 (Peters et al. in press) and LAI ranges were determined from seasonal LAI patterns observed in homogeneous stands of evergreen needleleaf and deciduous broadleaf trees in 2006 (Peters and McFadden 2010). Modeled LAI of evergreen needleleaf trees ranged from a minimum of 7.75 m^2 m^{-2} in winter to a maximum of 8.8 m^2 m^{-2} in summer, while modeled LAI of deciduous broadleaf trees ranged from a minimum of 0 m^2 m^{-2} in winter to a maximum of 5.5 m^2 m^{-2} in summer. I_T was modeled every half-hour by calculating potential evapotranspiration (E_P) in kg H_2O m^{-2} s^{-1} using the Priestley-Taylor equation (Priestley and Taylor 1972):

$$E_P = \alpha \frac{\Delta(R_N - G)}{\lambda(\Delta + \gamma)} \qquad (4)$$

where α is a standard calibration constant of 1.26, R_N is net radiation in MJ m^{-2} s^{-1}, G is ground heat flux in MJ m^{-2} s^{-1}, λ is latent heat of vaporization in MJ kg^{-1}, Δ is the slope

of the saturation vapor pressure temperature curve in kPa ºC^{-1}, and γ is the psychrometric constant in kPa ºC^{-1}.

Through our analyses comparing measured and component-based estimates of E_{total}, we determined it was important to include irrigated and non-irrigated turfgrass vegetation types when scaling up E_{G} to the suburban ecosystem. Because most tree canopies in our study area have a turfgrass understory, we also included two understory turfgrass vegetation types in our estimate of E_{G}, such that:

$$E_G = E_{Gnirr} + E_{Girr} + E_{Gunder\_eg} + E_{Gunder\_dec} \qquad (5)$$

where E_{Gnirr} is evapotranspiration from non-irrigated turfgrass lawns, E_{Girr} is evapotranspiration from irrigated turfgrass lawns, $E_{\text{Gunder\_eg}}$ is evapotranspiration from turfgrass growing below evergreen needleleaf tree canopies, and $E_{\text{Gunder\_dec}}$ is evapotranspiration from turfgrass growing below deciduous broadleaf tree canopies.

E_{Gnirr} was measured using the eddy covariance method over a 1.5 ha turfgrass field located in the footprint of the KUOM tall tower. *LE* and *H* heat fluxes were measured using an eddy covariance system consisting of a 3-D sonic anemometer (CSAT3, Campbell Scientific, Logan, Utah, USA) and an open-path infrared gas analyzer (LI-7500, LI-Cor, Lincoln, Nebraska, USA) oriented toward the west (270°) at a height of 1.35 m above the ground on a portable meteorological tripod (905, Met One Instruments, Grants Pass, Oregon, USA). Wind velocity, air temperature, and scalar concentrations of water vapor were recorded at 20 Hz using a datalogger (CR5000, Campbell Scientific, Logan,

Utah, USA) and fluxes were computed over 30-minute periods by applying a time lag if needed, and calculating the covariance between the vertical wind speed and the water vapor concentration. The turbulence data processing followed the same procedures as for the tall tower except that the open-path gas analyzer data were corrected for changes in air density and sensible heat following Webb et al. (1980) and high frequency losses in the fluxes were corrected using Moore's (1986) transfer functions for line averaging and sensor separation. Gaps in measurements from January 2007 to December 2008 represented 42% of the data, due to unfavorable wind directions from behind the tower (0–180º), power outages, and unsatisfied quality criteria (Foken and Wichura 1996). Gaps in E_{Gnirr} fluxes were filled using multiple linear regression models of R_{N} and air temperature with two-week windows and separate daytime and nighttime fitted coefficients.

E_{Girr} was calculated using the Priestly-Taylor equation with α equal to 0.87. Also known as the crop coefficient, α ranges from 0.6 to 1.14 for non-stressed, cool-season grasses (Carrow 1995, Ervin and Koski 1998, Brown et al. 2001, Zhang et al. 2007).

$E_{\mathrm{Gunder\_eg}}$ and $E_{\mathrm{Gunder\_dec}}$ were modeled as linear functions of the solar radiation passing through each tree canopy (Feldhake et al. 1985, Eastham and Rose 1988). Radiation passing through the canopy (R_{V}) in W m^{-2} was calculated using the Beer-Lambert law (Campbell and Norman 1998) such that:

$$R_V = R_S e^{-kLAI} \qquad (6)$$

where R_S is incident solar radiation at the top of the canopy in W m^{-2} and k is an attenuation coefficient. LAI was modeled separately for evergreen needleleaf and deciduous broadleaf trees as described above. Following another urban study (Wang et al. 2008), we set k equal to 0.7 for both tree types. Calculated R_V was used to predict E_{Gunder_eg} and E_{Gunder_dec} from monthly linear regression models of measured E_{Gnirr} and R_S (R^2 ranged from 0.76 to 0.94 across the 2007 and 2008 growing seasons).

E_W, which included a few small ponds, water traps on the golf course, and residential swimming pools, was calculated using the Priestly-Taylor equation with α equal to 1.26.

Meteorological measurements

To assess the environmental conditions in which our study occurred, we measured a suite of meteorological variables. At the turfgrass site, R_N and R_S were measured at 2 m above the ground using a far-component net radiometer (model CRN1, Kipp and Zonen, Delft, Netherlands). G was measured at 5 cm depth at two locations at the turfgrass site using heat flux plates (HFT-3.1, Radiation and Energy Balance Systems, REBS, Seattle, Washington, USA). An integrating platinum resistance temperature probe (STP-1, REBS, Seattle, Washington, USA) was used to measure storage of heat in the upper 5 cm of soil, which was added to the measurements recorded by the heat flux plates. Volumetric soil water content was measured at 10 cm depth (ECH2O, Decagon Devices, Inc., Pullman, WA, USA) at the turfgrass site and calibrated relative to a set of gravimetric measurements made in the same soil type at the University of Minnesota climate station. These

calibrations were conducted by oven-drying soil cores of a known volume that were collected across a two-week period. We measured R_N (CNR1, Kipp and Zonen, Delft, Netherlands) from the KUOM broadcast tower at 150 m above ground. Precipitation data were obtained from the University of Minnesota climate station (<1 km from the KUOM tower site). Vapor pressure deficit (D) was calculated from the water vapor concentration and air temperature measurements at the KUOM tall tower and turfgrass sites.

Scaling up component fluxes

We assessed the land cover in the study area using satellite imagery, aerial photography, a Geographic Information System (GIS) land-use database (ArcMap, version 9.3, ESRI, Redlands, California, USA), and an urban forest inventory. A land cover classification was produced using QuickBird (2.4 m resolution) multispectral imagery acquired on 26 July 2006 and leaf-off, true color aerial imagery (0.15 m resolution) acquired by Ramsey County on 8 April 2003. Preparation of the QuickBird imagery included orthorectification using a 10 m digital elevation model, georectification using the Ramsey County survey control network, masking of water bodies using a GIS data layer, and normalized difference vegetation index (NDVI) thresholding to isolate the vegetated fraction of the image. The vegetation classes were then extracted using the following steps. First, an unsupervised isodata classification was used to separate areas covered by trees, turfgrass, and shadow. Second, the shadowed area was masked and re-classified using a supervised classifier. Third, the tree class was separated into deciduous broadleaf and evergreen nee-

dleleaf tree classes using a green and red normalized band ratio from the leaf-off color aerial imagery. Fourth, irrigated and non-irrigated turfgrass areas were separated using a minimum-distance supervised classification. Fifth, swimming pools were classified using a simple ratio of the blue to the near infrared bands of the QuickBird imagery, within the residential land-use area. We assessed the accuracy of the land cover classification using the subplot centers of 150 randomly selected field plots that we surveyed in 2005 and 2006 using the U. S. Forest Service Forest Inventory and Analysis (FIA) urban forest protocol (USDA Forest Service 2005). The overall per-pixel accuracy of the classification was 82%, with similar accuracies of ~80% for the deciduous tree, evergreen tree, and turfgrass classes, and 93% for the impervious surface class.

Footprint models have been widely used to estimate the source area of eddy covariance measurements of E_{total} (Schmid 1994, Kljun et al. 2004); however these models are restricted to measurements over extended homogeneous surfaces and were not designed for application in spatially complex urban landscapes (Vesala et al. 2008b). Although our study area contains considerable spatial heterogeneity in surface types, it does not violate these model assumptions as much as a densely built-up city center or downtown area because it has a relatively flat topography, a dense tree canopy that overtops most of the buildings, and lacks deep street canyons caused by tall buildings. Therefore, to allow for comparisons between measured E_{total} and scaled component fluxes, we used a parameterized version of a Lagrangian stochastic footprint model (Kljun et al. 2004) to estimate the crosswind integrated footprint of each half-hourly measurement of E_{total}. We ran the footprint model using a fixed boundary-layer depth of 1000 m and a roughness

length calculated from the eddy covariance measurements. As the Kljun et al. (2004) parameterization does not predict two-dimensional flux source areas, we used the following approach based on Barcza et al. (2009) to obtain a spatial sample of the fractional cover of land surface types within the source area. First, we used the footprint model to calculate distance from the tall tower to the maximal contribution point as well as the distances corresponding to every tenth percentile of the footprint for each half-hourly measurement of measured E_{total}. Second, we plotted the 10 points of the flux footprint along the mean wind direction on the land cover map in a GIS and calculated the fractional cover of each component class within a 1 ha circular area (radius = 56 m) around each point. Third, we calculated the average of the 10 sampled areas, each weighted by the crosswind-integrated footprint corresponding to that point, to obtain the final estimate of the fractional land cover that contributed to each half-hourly flux measurement. To estimate the fractional cover of turfgrass underneath the tree canopy, we calculated the difference between the percent turfgrass cover from field measurements on FIA plots (which included understory vegetation) and the percent turfgrass cover derived from the satellite data (which could not detect the understory). On average, 50% of the tree-covered area had a turfgrass understory and this value was used to represent the fractional cover of understory turfgrass for the entire footprint area.

For comparison with measured E_{total}, component fluxes were converted from a per cover area basis to a per ground area basis by multiplying E_{Teg}, E_{Tdec}, E_{Gnirr}, E_{Girr}, E_{Gunder_eg}, E_{Gunder_dec}, and E_W by the fractional cover estimates and summing the terms. Comparisons between measured and component-based E_{total} methods were restricted to half-

hour periods in 2007 and 2008 when friction velocity $u_* > 0.2$ m s^{-1} and scaled Monin-Obukhov length $z_m/L \geq -200$ and ≤ 1. We conducted an error analysis of the component-based estimates of E_{total} by propagating errors associated with the land cover classification, measured and modeled component fluxes (Taylor 1982). E_{Gnirr} was assumed to have a relative error of 20%, which is typical of eddy covariance measurements in general (Baldocchi et al. 1988). E_{Girr} was assumed to have a relative error of 16%, based on the published range of α reported for cool-season turfgrass species (Carrow 1995, Ervin and Koski 1998, Brown et al. 2001, Zhang et al. 2007). For both evergreen and deciduous trees, T_T was assumed to have a relative error of 40%, based on the measured variation in annual sums among individual trees. I_T was assumed to have a relative error of 40% and 23% for deciduous and evergreen trees, respectively, based on measured variation in LAI. Because E_W, E_{Gunder_dec}, and E_{Gunder_eg} were minor components of E_{total} and we did not have a strong quantitative basis for estimating their respective errors, they were excluded from this error analysis.

To compare measured E_{total} from a residential neighborhood and a recreational land-use area in a golf course, we delineated two regions of interest (Figure 4-1) based on the Ramsey County GIS database. We restricted land use comparisons to periods when the 10% flux contribution fell exclusively within one of the two land-use types during daytime conditions ($R_S > 10$ W m^{-2}). Annual E_{total} from recreational and residential land-use areas was determined by scaling component fluxes according to their respective land cover fractions shown in Table 4-1.

Results

Land cover

Open turfgrass lawns were the dominant land cover type in our suburban study area, representing 53% of the tall tower footprint, followed by 29% tree cover, and 15% impervious surface cover (Table 4-1). Of the tree-covered area, 86% was composed of deciduous broadleaf species and 14% of evergreen needleleaf species. A turfgrass understory was present in 52% of tree-covered areas. Vegetation cover varied considerably between the two dominant land-use types, such that turfgrass cover dominated the recreational area and tree cover dominated the residential area. The recreational area had 40% higher turfgrass cover, 54% more irrigated turfgrass cover, 23% less tree cover, and 13% less impervious surface cover than the residential area. The difference in percent cover of irrigated turfgrass between residential and recreational areas was confirmed with personal observations during the FIA field inventory that most homes did not have automatic irrigation systems.

Environmental conditions

The seasonal patterns of R_N, air temperature, and D were relatively similar between the two years of study, but there were several periods with higher D in the summer of 2007 compared to 2008. The seasonal patterns of rainfall and soil moisture varied considerably between 2007 and 2008 (Figure 4-2). Not only was total annual rainfall higher in 2007 (749 mm) and more similar to the 30-year average (747 mm) than 2008 (550

mm), the seasonal distribution of rainfall varied as well (National Climatic Data Center 2004). In 2007, the greatest amount of precipitation occurred in September (170 mm), whereas in 2008 it occurred in April (109 mm). August was the wettest month (103 mm) over the 30-year average (National Climatic Data Center 2004). Consequently, rainfall patterns in 2007 were relatively more similar to the long-term average than in 2008. Air temperature and *D* were also higher in late spring and early summer in 2007 compared to 2008. Soil moisture reached a growing season (April to November) low of 17% on average in May of 2007 compared to a low of 11% on average in August of 2008.

Ecosystem evapotranspiration

E_{total} from the suburban landscape, measured from the 40 m level on the KUOM tower, varied seasonally across the two years of study (Figure 4-3). On average, daytime ($R_S > 10$ W m^{-2}) sums of E_{total} were near zero in winter in both 2007 and 2008 and showed increased rates from April to October. In April and May, we observed higher daytime sums of E_{total} on average in 2007, but in July and August we observed higher daytime E_{total} on average in 2008. Daytime E_{total} peaked in June of 2007 at an average rate of 2.7 mm day^{-1} and in July of 2008 at an average rate of 3.1 mm day^{-1}. The prevailing northwest wind direction led E_{total} to be relatively more representative of residential than recreational land-use areas (Figure 4-1). We consider this systematic bias when interpreting these results.

In mid-summer (June to August), the eddy covariance system at the 40-m level of the tall tower had an energy budget closure of 70%. This imbalance did not vary with

wind direction or between residential and recreational land-use types. To estimate the energy budget closure at the tall tower we used G measured at the turfgrass site, which does not contain any impervious surfaces. Therefore, it is likely that G is an underestimate for the suburban landscape and may increase the energy imbalance. The average midday (11:00 – 15:00 h) evaporative fraction (LE/R_N) and Bowen ratio (H/LE) were 0.93 and 0.24, respectively, in mid-summer. We similarly observed a mid-summer energy budget closure of 75% with the 1.35 m portable eddy covariance system at the turfgrass site, but with a higher midday evaporative fraction (0.41) and lower Bowen ratio (0.37).

Component evapotranspiration fluxes

The magnitude and seasonal patterns of evapotranspiration varied considerably among the plant functional types represented in this study. Across the 2008 growing season (April to November), average daily E_{Gnirr} was higher than either E_{Teg} or E_{Tdec} on a per cover area basis (Figure 4-4). E_{Gnirr} and E_{Teg} were similar at the beginning and end of the growing season and both remained >1 kg H_2O m^{-2} day^{-1} on average for at least seven months in 2008, compared to only four months for E_{Tdec}. All three plant functional types showed maximum daily evapotranspiration rates in June. Mid-summer daily evapotranspiration in 2008 also varied among the four turfgrass components represented in this study (Figure 4-4b) with average daily E_{Girr} (3.10 kg H_2O m^{-2} day^{-1}) higher than E_{Gnirr} (2.99 kg H_2O m^{-2} day^{-1}), E_{Gunder_dec} (0.07 kg H_2O m^{-2} day^{-1}), and E_{Gunder_eg} (0.01 kg H_2O m^{-2} day^{-1}). Data for plant functional types measured and modeled in 2007 were consistent with these results (data not shown).

I_T represented 27% and 32% of annual E_{Tdec} and E_{Teg}, respectively. On summer days with rain events, daily E_{Tdec} and E_{Teg} were 44% and 22% higher, respectively, than on days without rain events. Although precipitation events were originally filtered out of the E_{Gnirr} measurements, gap-filled E_{Gnirr} showed a 22% decline on summer days with rain events. We were unable to separate evaporation and transpiration components of turfgrass because the eddy covariance measurements used at the turfgrass site represent only total evapotranspiration.

Comparing component-based and eddy covariance-measured E_{total}

Compared to component-based estimates of E_{total} with all open canopy turfgrass scaled as E_{Gnirr}, component-based estimates that included a modeled E_{Girr} vegetation type showed better agreement with measured E_{total}, particularly in summer when winds were from the southwest (R^2 = 0.66 and 0.73, respectively, Figure 4-5). Including E_{Girr} reduced the summer imbalance from an underestimate of 7% to 3% in the southwest quadrant, and had little effect on the imbalance in spring and fall or when winds were from the northwest or northeast. For the remainder of our analyses, all component-based estimates of E_{total} consequently included modeled E_{Girr}.

Overall, component-based estimates of E_{total} underestimated measured E_{total} by an average of 3%, with the component-based approach explaining 83% of the variation in measured fluxes when a linear regression model was fit through the origin ($y = 1.03x$, $P < 0.001$). 30-minute estimates of component-based E_{total} had a mean relative error of 21%. The imbalance between the two methods, however, varied seasonally with the compo-

nent-based approach resulting in a 20% overestimate of measured fluxes in spring, an 11% underestimate in summer, and a 9% overestimate in fall (Figure 4-6). The largest overestimates of measured E_{total} tended to occur when winds were from the southwest, while underestimates tended to occur when winds were from the northwest or northeast and during periods of high R_N (>800 W m^{-2}), high H fluxes (>175 W m^{-2}), and high D (>2 kPa). Accounting for T_T differences among xylem anatomy types (conifer, ring-porous, and diffuse-porous) instead of plant functional types reduced the overall imbalance such that measured E_{total} was overestimated by 1% and varied seasonally from a 25% overestimate in spring to a 6% underestimate in summer. The imbalance was also relatively unaffected by the method used to sample the land cover fractions associated with each half-hourly flux. Using only the maximum contribution point or the non-weighted mean of the 10 footprint contribution points changed the overall imbalance by –0.007% and +0.003%, respectively.

Comparing E_{total} from two suburban land-use types

Measured E_{total} varied in magnitude and seasonality between the two suburban land-use types represented in our study (Figure 4-7). Recreational areas had higher average daytime E_{total} than residential areas in the spring and fall, as well as during the drought conditions of June 2007. In addition, recreational areas had a lower average mid-day Bowen ratio in mid-summer than residential areas (0.69 and 1.08, respectively). Daytime E_{total} was relatively similar between the two land-use types in late summer (August and September) and winter.

Annual sums of E_{total}, which were based on the sum of scaled component fluxes, were higher on average from the recreational area (467 mm yr^{-1}) compared to the residential area (324 mm yr^{-1}) (Figure 4-8a). Despite large differences in total annual rainfall between 2007 and 2008, the inter-annual variation in annual E_{total} was relatively small for both residential and recreational land-uses. In 2007 and 2008, annual E_{total} from recreational areas represented 62% and 85% of annual precipitation, respectively, while annual E_{total} from residential areas represented 42% and 61% of annual precipitation, respectively. E_G was the largest component of annual E_{total} in both recreational and residential areas (87% and 64%, respectively), followed by E_T (10% and 31%, respectively), and E_W (3% and 5%, respectively). E_{Girr} was a much larger component of annual E_G in recreational than residential areas (83% vs. 23%, respectively), while E_{Tdec} was the dominant component of annual E_T in both land use types (95% and 83%, respectively) because deciduous trees were more abundant than evergreen trees in the suburban area we studied.

The contribution of different vegetation types to E_{total} in 2008, as determined from the sum of scaled component fluxes, varied seasonally in both land-use types (Figure 4-8b,c). E_{Girr} had the highest proportional contribution to E_{total} in July, while the maximum contribution from E_{Gnirr} occurred in spring (April and May) and fall (October and November). The largest contribution from E_{Tdec} occurred in August and September, while the highest contribution from E_{Teg}, albeit small, was in April and November, particularly in residential areas. Data for vegetation contributions in 2007 were consistent with these results (data not shown).

Discussion

Suburban evapotranspiration rates

Ecosystem evapotranspiration (E_{total}) observed in this study fell within the range of values represented for other suburban residential areas around the world (Grimmond and Oke 1999, Grimmond and Oke 2002, Spronken-Smith 2002, Moriwaki and Kanda 2004, Offerle et al. 2006, Vesala et al. 2008a, Balogun et al. 2009). The evaporative fraction (0.37) we observed was most similar to that measured in older suburban areas in North America, such as Chicago (Grimmond et al. 1994). Among suburban areas previously studied in North America, the fraction of available energy used for evaporation ranges from 0.22 to 0.46, with the highest values associated with recently developed exurban areas dominated by open turfgrass lawns and trees with small canopies and the lowest values associated with older suburbs dominated by mature tree canopies (Balogun et al. 2009). With 29% tree cover and 53% turfgrass cover, the footprint area of our study had a higher vegetation cover than is typical of North American cities (Nowak et al. 1996, Grimmond and Oke 2002). Although it has been suggested that advected energy from impervious surfaces can partially compensate for the decrease in vegetated surfaces in urban compared to rural ecosystems (Oke 1979), the E_{total} measured in this study remained less than values measured in temperate hardwood forests of North America. For example, growing season E_{total} rates >3 mm day^{-1} are commonly observed at hardwood forests in northern Wisconsin (Cook et al. 2004), Indiana (Schmid et al. 2000), Michigan

(Schmid et al. 2003), North Carolina (Oishi et al. 2008), and Tennessee (Wilson et al. 2001).

The seasonality of suburban E_{total} observed in this study was more similar to patterns found in temperate hardwood forests from southern latitudes than northern latitudes of North America. For example, in a mixed deciduous forest in Oak Ridge, Tennessee, Wilson et al. (2001) observed E_{total} rates that were significantly above zero from April to October, similar to patterns found in our study. Additionally, in a deciduous maple-beech to oak-hickory transition forest in south-central Indiana, Schmid et al. (2000) found increased E_{total} from May to October. In contrast, elevated E_{total} occurred only from May to September in an upland hardwood forest in northern Wisconsin (Cook et al. 2004), and from late May to September in a hardwood-boreal transition forest in the lower peninsula of Michigan (Schmid et al. 2003). These comparisons suggest that the urban heat island effect, in addition to the high percent cover of turfgrasses that are active in the spring and fall, may have played an important role extending the growing season at our suburban study site, relative to surrounding rural areas. This is consistent with analyses that find increases in annual net primary productivity in urban areas, particularly in cold regions, which have been attributed to extended growing seasons caused by the urban heat island effect (Imhoff et al. 2004).

Scaling component-based fluxes

Our comparison of measured and component-based estimates of E_{total} showed that component-based approaches can capture much of the seasonal and spatial variability in

suburban E_{total} with a similar accuracy (79%) to that of eddy covariance measurements (~80%) (Baldocchi et al. 1988). Similar to studies in forest ecosystems, we found that component-based estimates of E_{total} slightly underestimated measured values, particularly at high flux rates in summer (Hogg et al. 1997, Wilson et al. 2001, Bovard et al. 2005, Oishi et al. 2008). Unlike these forest studies, however, we found that component-based estimates tended to overestimate measured fluxes in spring and fall. Several potential sources of error may explain these discrepancies between methods, including 1) errors associated with the measurements or models used to estimate component fluxes, 2) a mismatch in the spatial footprints associated with the measured and scaled fluxes, 3) under-sampling species' differences in water use, and 4) the spatial heterogeneity of urban microclimates.

The measurements and models used to estimate components of E_{total} in this study all contribute some degree of uncertainty when scaling up E_{total}. Previous studies from forest ecosystems have found that heat dissipation sap flux techniques may underestimate transpiration, particularly during periods of high radiation (Hogg et al. 1997, Wilson et al. 2001, Bovard et al. 2005, Oishi et al. 2008), and could explain the component-based underestimates we observed during summer. The lack of energy balance closure observed at the tall tower and turfgrass sites, although typical of eddy covariance systems in general (Wilson et al. 2002), suggests a systematic underestimate of both E_{total} and E_G. While an underestimate of E_G may help explain the summer imbalances, it is contrary to explaining the overestimates observed in spring and fall. Depending on the seasonal variation in LAI among trees in our study area, the modeled seasonal LAI patterns also represent a source

of error in our estimates of I_T, E_{Gunder_eg}, and E_{Gunder_dec}. As comparisons between component-based and measured estimates of E_{total} were restricted to periods with high quality data and exclude most rainfall events, it is unlikely that the I_T component significantly contributed to the observed imbalances. The seasonal pattern of understory turfgrass evapotranspiration, however, is consistent with the observed imbalances. E_{Gunder_eg} and E_{Gunder_dec} were highest in spring and fall when tree LAI was low, and E_{Gunder_eg} and E_{Gunder_dec} were lowest in mid-summer when tree LAI was high (data not shown). It is also likely that using a constant coefficient equal to 0.87 in the Priestley-Taylor equation to model E_{Girr} led to an overestimate of E_{total} in spring and fall and an underestimate in summer. Studies show that α varies seasonally in non-stressed, cool-season grasses, with lowest values in spring and fall and highest values in summer (Ervin and Koski 1998, Brown et al. 2001, Zhang et al. 2007).

Even in urban areas with relatively flat topography, flux footprints are particularly difficult to assess due to the spatial heterogeneity of surface types and complex transport of scalars, and can lead to the mischaracterization of footprint areas when scaling up component fluxes (Vesala et al. 2008a, Vesala et al. 2008b). While we did not attempt to replicate the 2-D source area associated with each measured half-hourly value of E_{total}, we did find that component-based estimates of E_{total} were not greatly affected by different methods of sampling the land cover classification map. Consequently, we believe the misrepresentation of the footprint area to be a relatively minor source of error in our component-based estimates of E_{total}.

Species-rich ecosystems, such as ours, additionally complicate efforts to scale up measurements made on only a few individuals, species, or sites, as water use can be highly variable among tree (Oren et al. 1998, Pataki and Oren 2003, Kumagai et al. 2005) and turfgrass species and among management regimes (Zhang et al. 2007). Although the effect was relatively small, including T_T differences among xylem anatomy types resulted in a 4% reduction in the overall imbalance compared to using the coarser plant functional type categories. Management practices, including irrigation, fertilization, mowing height, and canopy shading can also significantly impact rates of water loss from turfgrass (Feldhake et al. 1983, Zhang et al. 2007). The large differences in daily evapotranspiration between our measured non-irrigated turfgrass and our modeled values of irrigated and understory turfgrass suggest that irrigation management effects were captured in seasonality, but fertilizer and mowing practices were not accounted for. Occasional irrigation by homeowners, particularly during periods of low soil moisture in mid-summer, was also not accounted for and may contribute to the observed underestimate of measured fluxes in summer. Evapotranspiration from unmeasured understory plants has additionally been suggested to contribute to observed imbalances in forest ecosystems (Bovard et al. 2005, Oishi et al. 2008). It is unlikely that evapotranspiration from common suburban understory vegetation types, such as woody shrubs, vegetable or flower gardens, contributed significantly to the E_{total} in our study area because their cover represented less than 2% of the landscape. Although the seven tree genera and one turfgrass lawn we studied provides a limited sampling of species' differences in water use, the relatively good match that we found between component-based and measured E_{total} sug-

gests that this group of plant functional types captured much of the species' variation in water use within the suburban landscape we studied.

Finally, microclimate variability in urban areas (Bonan 2000, Byrne et al. 2008, Peters and McFadden 2010) may lead to a relatively more important source of error in urban component-based estimates of E_{total} than in natural ecosystems. The spatial heterogeneity of urban surface types with different energy balances and heat storage capacities results in the advection, or lateral transport, of heat from paved surfaces with high sensible heat fluxes to vegetated surfaces with high latent heat fluxes (Oke 1979, Spronken-Smith et al. 2000). Advection can be an important energy source to irrigated urban parks and lawns, causing elevation of E_G rates by up to 35% (Oke 1979, Feldhake et al. 1983, Spronken-Smith et al. 2000). Trees grown over asphalt can transpire 30% more water than trees grown over turfgrass (Kjelgren and Montague 1998), while some tree species initiate stomatal closure and have reduced rates of water loss (Kjelgren and Montague 1998, Montague and Kjelgren 2004). In addition, sparsely planted trees can have T_T rates two to three times higher than those of densely planted trees (Hagishima et al. 2007) and windbreaks can reduce E_G rates by 25% (Danielson and Feldhake 1981). Our study trees had relatively open growth forms compared to forest-grown trees, yet they were all grown under generally more park-like conditions as compared to trees in more densely built-up urban areas. Consequently, our T_T measurements likely underestimate E_T rates of trees growing in complete isolation or near paved surfaces. This idea was further supported by the large underestimates of E_{total} we observed during periods of high net radiation, high sensible heat fluxes, and high vapor pressure deficit from northwest and north-

east wind directions. In contrast, the turfgrass site was a relatively large lawn that was less likely to have been exposed to advected sources of energy compared to smaller residential lawns surrounded by sidewalks, driveways, and streets. It is difficult to determine whether our E_G measurements provide a systematic overestimate or underestimate of water loss from residential yards. As microclimate effects are an important source of uncertainty in predicting component-based E_{total} in urban and suburban ecosystems, future studies should focus on how best to account for this variability when scaling.

Contributions of trees and turfgrasses to suburban E_{total}

The relative contribution of trees and turfgrass to annual E_{total} was driven largely by fractional cover and plant functional type differences in daily water use. Studies from forest ecosystems similarly show that the relative contribution of different tree species to E_{total} is driven both by species' abundances on the landscape, often measured as contributions to total basal area or leaf area, and by species-specific differences in water use (Wullschleger et al. 2001, Tang et al. 2006). Despite their higher rates of water use than deciduous broadleaf trees, evergreen needleleaf trees had a nearly negligible contribution to E_{total} in our study area due their relatively small fractional cover of the landscape. Turfgrass, however, due its high cover and high daily E_G rates across the growing season, represented the largest proportional contribution (87% and 64% in recreational and residential areas, respectively) to annual E_{total} in our study area. Pasture grasses in natural savannah ecosystems, by contrast, represent a much smaller component (20–44%) of E_{total} than trees (Baldocchi and Xu 2007, Paco et al. 2009). While these studies are from sa-

vanna ecosystems with similar percent tree cover to our study area, it is important to note they are from areas with a Mediterranean climate and very different species compositions.

The proportional contribution of different vegetation types to suburban E_{total} varied seasonally due to different patterns in physiological activity among plant functional types. While evergreen needleleaf and deciduous broadleaf trees both have maximum physiological function in the middle of summer in temperate ecosystems, the evergreen leaf habit and high cold tolerance allows evergreen needleleaf trees to remain physiologically active over a longer growing season than either deciduous broadleaf trees or cool-season turfgrasses (Havranek and Tranquillini 1995, Catovsky et al. 2002, Givnish 2002). Correspondingly, we observed the highest proportional contribution to E_{total} from deciduous broadleaf trees in late summer and, albeit small, the highest contributions from evergreen needleleaf trees in April and November when deciduous trees were leafless. Our observation of a mid-summer low in the contribution to E_{total} from non-irrigated turfgrass is consistent with the mid-summer dormancy of cool-season turfgrasses (Feldhake et al. 1984, Fry and Huang 2004, Zhang et al. 2007).

Land-use comparisons

Similar to other urban studies, we found that the magnitude of E_{total} varied between land-use types according to differences in the total cover and composition of vegetation (Grimmond and Oke 1999, Spronken-Smith 2002, Offerle et al. 2006, Vesala et al. 2008a, Frey et al. 2010). Seasonal patterns of E_{total} were also highly influenced by the

phenology of the dominant vegetation type. For example, the turfgrass-dominated recreational area not only showed higher annual E_{total} than the deciduous tree-dominated residential area, but it specifically showed higher rates of E_{total} in spring and fall when cool-season turfgrasses are most active. In addition, our study extends these previous findings to show that turfgrass management, particularly through irrigation inputs, is another important factor influencing the spatial and seasonal variability of suburban E_{total}. The relatively high evaporative fluxes we measured from the recreational area during drought conditions in 2007 suggest that increased irrigation during periods of low soil moisture can significantly alter E_{total} from urban areas. While homeowners also maintain irrigated turfgrass lawns, management intensity can vary widely among individual landowners (Larson et al. 2009). To predict suburban E_{total}, these results suggest it will be important to know not just the total vegetation cover in urban landscapes, but also the fractional cover of different vegetation types and turfgrass management practices. In addition, it is likely that changes in land-use, vegetation composition, or turfgrass management practices, particularly related to irrigation use, will lead to changes in total water fluxes from urban and suburban ecosystems.

Given the growing interest among cities in using "green infrastructure" to manage problems such as stormwater runoff and energy demand, it is important for urban planners and designers to consider the trade-offs among different potential landscape configurations (Mitchell et al. 2008). For example, in arid regions the water conservation benefits of low water-use species must be weighed against the cooling benefits of high water-use species (Larson et al. 2009, Shashua-Bar et al. 2009). In contrast, cities in mesic regions

with frequent rainfall events may value the storm water interception benefits of vegetation with large canopies relatively more than other ecosystem services related to E_{total} (Wang et al. 2008). Although we found that cool-season turfgrasses had higher rates of water loss than evergreen needleleaf and deciduous broadleaf trees per unit cover area, the overall cooling effect of turfgrass was not necessarily higher than that of trees. This is because trees also provide cooling by intercepting solar radiation and shading the ground beneath canopies (Peters and McFadden 2010). In the arid communal settlement of Midreshet Ben Gurion, Israel, for example, Shashua-Bar et al. (2009) found that turfgrass lawns shaded by tree canopies resulted in both a greater reduction in air temperature and a 50% reduction in water use compared to un-shaded turfgrass lawns.

By approximating runoff as the difference between measured precipitation and annual component-based E_{total}, we estimate runoff to represent 26% and 48% of annual precipitation on average from the recreational and residential areas in our study, respectively. While these estimates neglect irrigation inputs, changes in storage, and ground water recharge and should be used with caution, they are within the range of annual runoff fractions previously reported for watersheds in the Minneapolis–Saint Paul metropolitan area (Brezonik and Stadelmann 2002). These results are in agreement with studies showing that increased pervious surfaces in urban areas decrease direct runoff (Brezonik and Stadelmann 2002, Mitchell et al. 2008, Wang et al. 2008, Haase 2009). Although it is beyond the scope of our study to offer specific planting recommendations to cities interested in managing ecosystem services with green infrastructure, this study advances our ability to quantify the relative contributions of different vegetation types to suburban E_{to-}

$_{tal}$, an important step in evaluating decisions related to the seasonal management of urban water and energy budgets.

Despite the good agreement we found between component-based and measured E_{total} in the suburban ecosystem we studied, differences in species composition among cities make it complex to extrapolate our component measurements of evapotranspiration to other urban and suburban areas, particularly in more southern latitudes. For example, the turfgrass site in this study only represented cool-season turfgrass species, as warm-season species are not typically planted in the climate zone associated with Minnesota. Yet cool and warm-season turfgrasses have large differences in evapotranspiration, with cool-season species using up to 45% more water during the growing season compared to warm-season species (Feldhake et al. 1983, Zhang et al. 2007). Cities located in warmer climates with higher frequencies of warm-season turfgrasses will need to consider these species' differences in water use when scaling up and predicting urban E_{total}.

Conclusions

We quantified seasonal variations in evapotranspiration from a suburban landscape in the Upper Midwest region of the United States, with peak rates >3 mm day^{-1} in summer. The good agreement between our component-based and measured E_{total}, with an overall imbalance of 3%, suggests that the major plant functional types captured most of the spatial and temporal variability required to quantify urban E_{total}. Component-based estimates overestimated measured E_{total} in spring (20%) and fall (10%) and underesti-

mated measured E_{total} in summer (11%), likely due to errors associated with the irrigated turfgrass model and variability from microclimate effects. We found turfgrass was the major component to annual E_{total} from both recreational and residential land-uses types (87% and 64%, respectively) due to a high fractional cover (74% and 34%, respectively) and higher average rates of water use per cover area in mid-summer than deciduous broadleaf or evergreen needleleaf trees (1.4, 2.3, and 3.0 kg m^{-2} day^{-1}, respectively). The maximum contribution to E_{total} from non-irrigated turfgrass occurred in spring and fall, irrigated turfgrass in mid-summer, deciduous broadleaf trees in late summer, and evergreen needleleaf trees in early spring and late fall. Turfgrass-dominated recreational land-use areas had higher average annual E_{total} compared to deciduous tree-dominated residential areas (467 and 324 mm $year^{-1}$, respectively), as well as an altered seasonal pattern of E_{total} with higher fluxes in spring and fall, and during a mid-summer drought. These results suggest that a plant functional type approach could be used to estimate and compare E_{total} among different cities and to evaluate the effects of changes in land use, vegetation composition, or management practices on urban water and energy budgets.

Table 4-1. Cover types by percentage of the flux footprint area, residential land-use area, and recreational land-use area. Percent cover was determined from the land cover classification map shown in Figure 4-1 and does not include turfgrass under tree canopies. The footprint area was defined as the total area bounded by the 10% contour line (Figure 4-1).

Suburban landscape	Deciduous tree (%)	Evergreen tree (%)	Non-irrigated turfgrass (%)	Irrigated turfgrass (%)	Open water (%)	Impervious surfaces (%)
Footprint area	25	4	18	35	2	15
Residential area	37	6	25	9	2	22
Recreational area	19	1	11	63	2	5

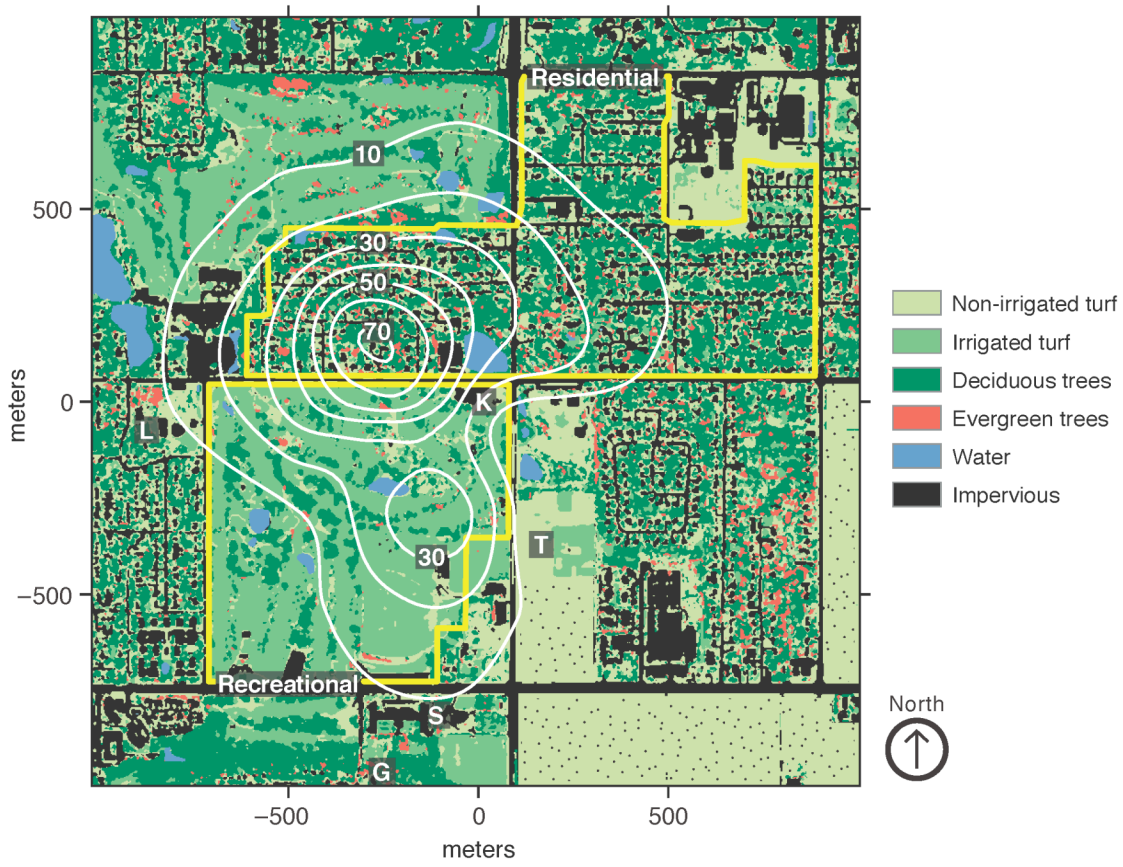

Figure 4-1. Land cover classification derived from 2.4-m resolution QuickBird imagery for a 1 km radius surrounding the KUOM tall tower (indicated by the letter **K** at the origin) in a suburban neighborhood of Minneapolis–Saint Paul, Minnesota. The mobile tower in the turfgrass field is indicated by the letter **T**. The Lauderdale (**L**), Saint Paul (**S**), and Grove (**G**) sap flux sites are indicated by the letters corresponding to their names. The CTC sap flux site was located in a residential area 1.3 km south of the map edge and is not shown. The white lines are isopleths representing the relative footprint contribution to the measured fluxes at the 40 m level of the tall tower from January 2007 to December 2008, as presented in Rebmann et al. (2005). Yellow lines delineate the residential and recreational land-use areas that were used to bin the data for the analyses

in Figure 4-7 and Section 3.6. Stippled areas in the SE corner of the map indicate low herbaceous vegetation in experimental crop plots.

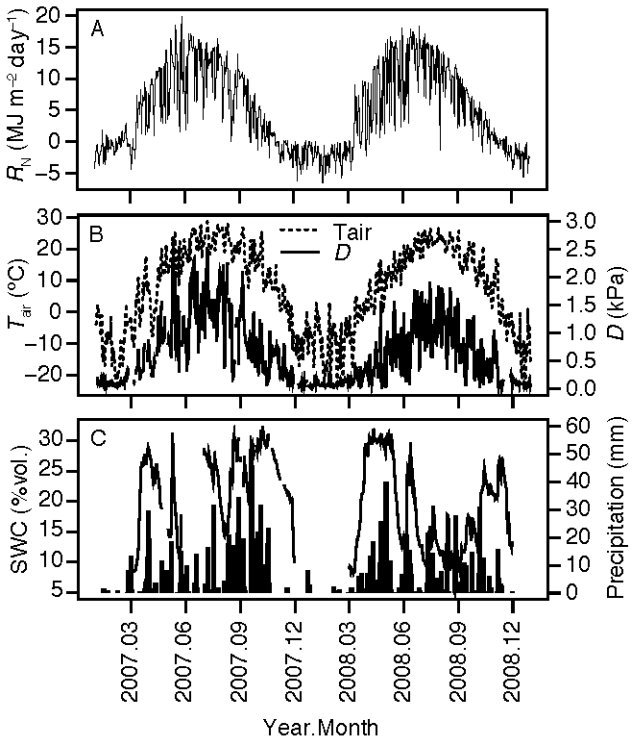

Figure 4-2. Environmental conditions in a suburban area of Minneapolis–Saint Paul, MN from 1 January 2007 to 31 December 2008. **(A)** Daily totals of net radiation (R_N) were measured at the 150 m level of the KUOM tower. **(B)** Mean daily air temperature (T_{air}) and mean daytime vapor pressure deficit (D) were measured at the 40 m level of the KUOM tower. **(C)** Soil water content (SWC) was measured at 10 cm depth at the turfgrass site. Gaps in soil water content data indicate time periods when the instrumentation failed.

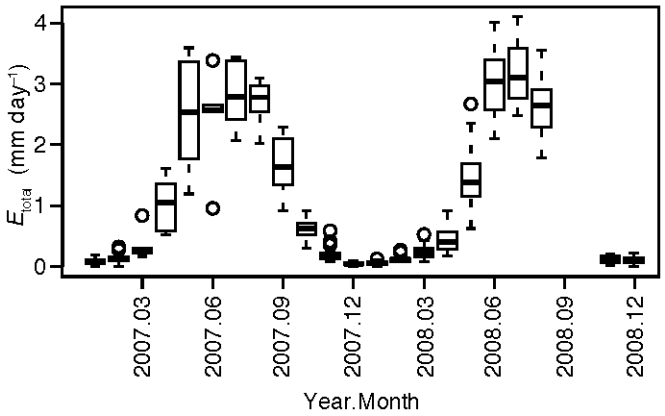

Figure 4-3. Daytime (R_S > 10 W m^{-2}) sums of ecosystem evapotranspiration (E_{total}) per month measured at the 40 m level of the KUOM tower over a suburban area of Minneapolis–Saint Paul, Minnesota. Dark lines represent median daytime sums of E_{total}, the box represents the 75th and 25th percentiles, and the dotted lines represent the maximum and minimum values. *n* varies from 4 to 20 days per month. The gap in the fall of 2008 indicates a period when the instrumentation was out of service following a lightening strike.

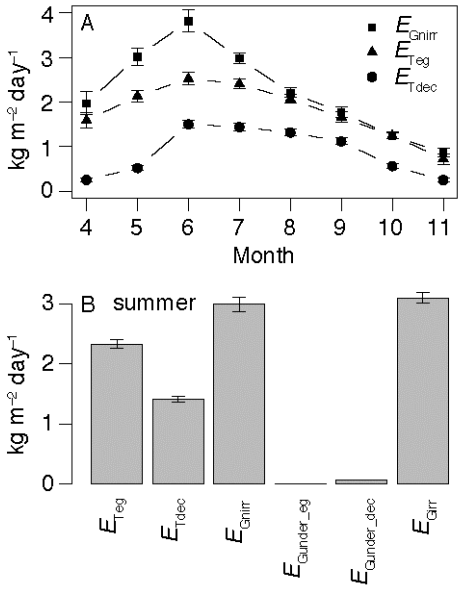

Figure 4-4. (A) Average daily sums of measured evapotranspiration per cover area for non-irrigated turfgrass (squares, E_{Gnirr}), evergreen needleleaf trees (triangles, E_{Teg}), and deciduous broadleaf trees (circles, E_{Tdec}) per month across the 2008 growing season in a suburban area of Minneapolis–Saint Paul, Minnesota. E_{Gnirr} was measured using a portable eddy covariance tower and E_{Teg} and E_{Tdec} were calculated from heat dissipation sap flow measurements and a canopy interception model. **(B)** Average summertime (June to August) daily sums of evapotranspiration per cover area in 2008 for measured and modeled vegetation components. Evapotranspiration from irrigated turfgrass (E_{Girr}) was modeled using the Priestley-Taylor equation and evapotranspiration from understory turfgrass (E_{Gunder_eg} and E_{Gunder_dec}) were modeled using the Beer-Lambert law. Error bars are ±1 standard error and n varies from 8 to 31 days per month.

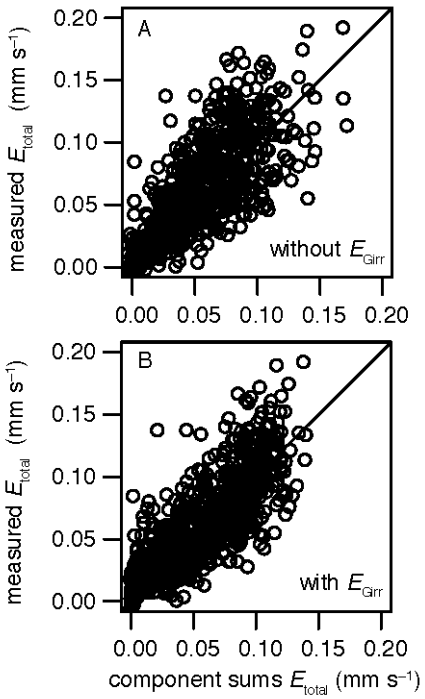

Figure 4-5. Comparison of half-hourly measured and scaled component sums of ecosystem evapotranspiration (E_{total}) in a suburban area of Minneapolis–Saint Paul, Minnesota. Component sums were constructed either **(A)** without a separate irrigated turfgrass component (E_{Girr}) or **(B)** with E_{Girr}. E_{total} was measured at the 40 m level of the KUOM tower. Data shown are from summer (June to August) in 2007 and 2008 when winds were from the southwest. Lines represent the 1:1 line.

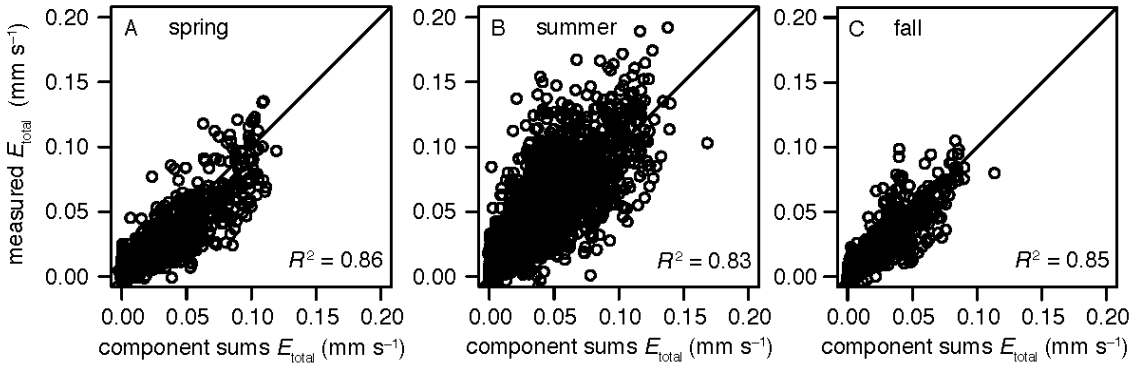

Figure 4-6. Comparison of half-hourly measured and scaled component sums of ecosystem evapotranspiration (E_{total}) in a suburban area of Minneapolis–Saint Paul, Minnesota during **(A)** spring (April and May), **(B)** summer (June to August), and **(C)** fall (September to November). E_{total} was measured at the 40 m level of the KUOM tower. Component sums were constructed as $E_T + E_G + E_W$. Data shown are from 2007 and 2008. Lines represent the 1:1 line.

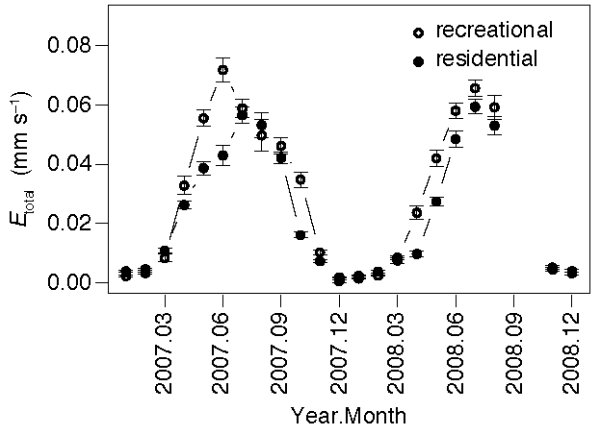

Figure 4-7. Average daytime ecosystem evapotranspiration (E_{total}) per month measured over two land-use types, recreational (open circles) and residential (closed circles), in a suburban area of Minneapolis–Saint Paul, Minnesota. E_{total} was measured at the 40 m level of the KUOM tower. Data shown were restricted to daytime (R_S > 10 W m^{-2}) periods without precipitation. Error bars are ±1 standard error and *n* varies from 17 to 270 half-hourly data points per month.

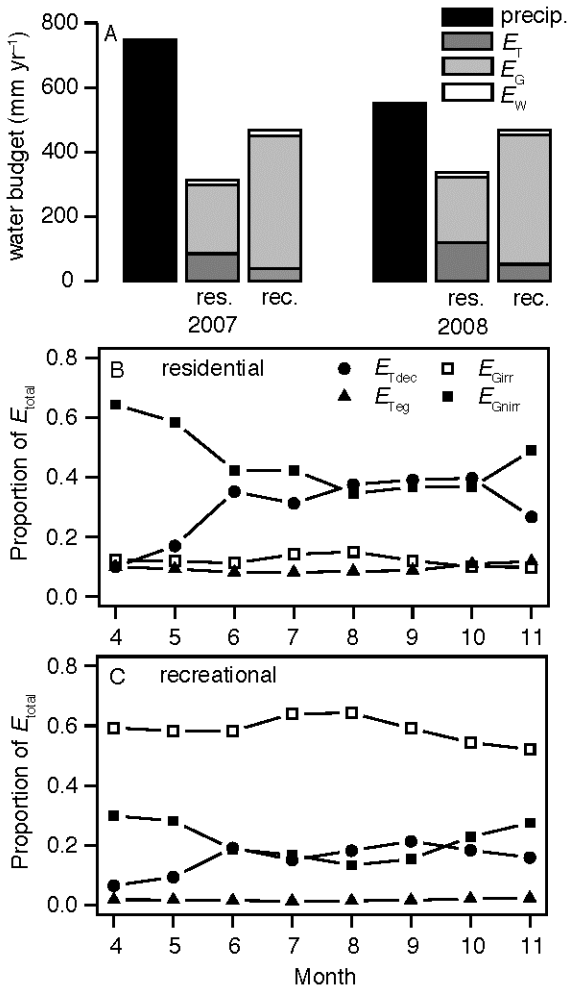

Figure 4-8. (A) Annual precipitation and annual evapotranspiration of scaled component fluxes, trees (E_T), turfgrass (E_G), and open water (E_W), from the residential (res.) and recreational (rec.) land-use areas (Figure 4-1). E_T includes evapotranspiration from evergreen needleleaf (E_{Teg}) and deciduous broadleaf trees (E_{Tdec}). E_G includes evapotranspiration from irrigated (E_{Girr}), non-irrigated (E_{Gnirr}), and understory turfgrass (E_{Gunder_eg} and E_{Gunder_dec}). The average proportional contribution of vegetation components, E_{Tdec} (circles), E_{Teg} (triangles), E_{Girr} (open squares), and E_{Gnirr} (closed squares), to ecosystem evapotranspiration (E_{total}) from **(B)** residential and **(C)** recreational land-use areas per

month. Data shown include only daytime periods (R_S > 10 W m^{-2}) in 2008 and n varies from 254 to 892 half-hourly data points per month.

Chapter 5

Conclusions

The studies presented here have quantified how different functional types of trees affect the climate and hydrology of a suburban ecosystem. The field study presented in Chapter 2 extended our previous understanding of microclimate effects of urban vegetation to show that the seasonal leaf development of trees plays a role in modulating soil and surface temperatures in urban ecosystems. The field studies presented in Chapter 3 and Appendix 1 are among the few studies to have directly measured whole-tree transpiration and canopy photosynthesis rates on urban trees, and they provide new insight into how best to scale up the tree component of urban water and carbon budgets. The field study presented in Chapter 4 is the first to directly compare measured and component-based estimates of evapotranspiration in an urban ecosystem, and provides insight into how to quantify evapotranspiration in other cities and with changes in land-use or climate. The combined results of these studies suggest that trees play a large role in reducing local surface and soil temperatures in urban areas, while contributing a smaller proportion than turfgrass to the total evaporative water loss from a suburban ecosystem in Minneapolis–Saint Paul, Minnesota. The tree contribution to suburban evapotranspiration, however, varies with plant functional type and fractional cover. Therefore, caution should be used in extrapolating the results of these studies to cities in different geographical regions with a different species composition and climate.

Research Summary

In Chapter 2, I showed that urban forest types have distinct seasonal patterns of soil and surface temperature that are largely explained by differences in tree cover and changes in LAI, rather than by plant functional type. I demonstrated that sites with higher percent tree cover and greater LAI reduced soil temperatures by up to 7˚C and surface temperatures by up to 6˚C relative to open lawns with near-zero LAI. Additionally, I found that site differences in soil temperature and turfgrass ground cover were better predicted by LAI, while percent tree cover better predicted surface temperature. For scaling up to larger metropolitan areas, I showed that field-based estimates of tree cover were better than 2.4 m resolution satellite imagery at predicting mid-summer LAI and temperature values under the urban forest canopy because they take into account gaps within individual tree canopies.

In Chapter 3 and Appendix 1, I showed that common urban tree species differed significantly in magnitude and seasonality of transpiration and canopy photosynthesis according to differences in plant functional type. I found evergreen needleleaf trees had significantly higher annual transpiration (307 kg H_2O m^{-2} yr^{-1}) and canopy photosynthesis (1.02 kg C m^{-2} yr^{-1}) per unit canopy area than deciduous broadleaf trees (153 kg H_2O m^{-2} yr^{-1} and 0.38 kg C m^{-2} yr^{-1}, respectively), largely due to their smaller projected canopy area (31.1 and 73.6 m^2, respectively), higher leaf area index (8.8 and 5.5 m^2 m^{-2}, respectively), and longer growing season (8 and 4 months, respectively). My sap flux measurements also showed species' differences in sap flux that were consistent with dif-

ferences in xylem anatomy found in previous studies. The results of this study served as the framework for scaling up species' differences in tree transpiration to estimate ecosystem evaporative water losses in the study presented in Chapter 4.

In Chapter 4, I showed that a plant functional type-based approach to estimating ecosystem evapotranspiration is useful for predicting measured water vapor fluxes from suburban landscapes. Overall, I found component-based estimates underestimated measured fluxes by 3%, although this imbalance varied seasonally from +20% to –11%. I showed that turfgrass-dominated recreational land-use areas had higher annual evapotranspiration (467 mm yr^{-1}) than deciduous tree-dominated residential areas (324 mm yr^{-1}). Seasonal patterns of evapotranspiration from recreational and residential land-use areas were consistent with the dominant plant functional type. I determined that turfgrass was the major component to annual evapotranspiration from both recreational and residential land-uses types (87% and 64%, respectively) due to its high fractional cover and high daily water use, yet the contribution of different plant functional types varied seasonally.

Implications for future research

While I have identified several factors that directly and indirectly control land–atmosphere exchanges of energy, water, and carbon in suburban ecosystems, there are many others that potentially limit the extrapolation of these results to other urban ecosystems and should be examined in future research. In Chapter 2, I showed that variability in canopy structure can influence suburban microclimates; however, impervious surfaces

with different surface energy balances also can play a role in creating microclimate variability in urban areas. Future studies should examine how tree transpiration and photosynthesis rates vary with exposure to different microclimates. The trees studied in Chapter 3 were all grown under park-like conditions. Our understanding of the controls on urban tree transpiration and photosynthesis would be improved by expanding this in future studies to street trees grown near impervious surfaces. As was demonstrated in Chapter 4, microclimate variability is a large source of uncertainty in scaling up component-based water fluxes. Therefore, an assessment of the importance of microclimate variation is needed to more accurately predict total evapotranspiration rates in other cities.

Species diversity can be high in urban areas, greatly complicating the extrapolation of measurements made on only a few species or sites. Therefore, future studies will need to assess the variation among a broader range of common urban tree species. Species composition also differs among cities, limiting the extrapolation of results from these studies to other cities, particularly those located in different geographical regions and climate zones. While I found species' differences in transpiration and canopy photosynthesis could largely be explained by plant functional type in a suburban neighborhood of Minneapolis–Saint Paul, Minnesota, this may not be the case in other cities with differing species composition or level of diversity. Plant functional types that were not present in my study system, such as C_4 warm-season turfgrasses, should be the focus of future studies in cities where these species are common.

Conclusion

This dissertation on the impact of trees to the temporal variability in urban carbon and water budgets advances our understanding of how urban ecosystems function through biophysical effects of and feedbacks on urban trees. This research has important implications for managing urban ecosystem services and for evaluating the effects of changes in land-use, vegetation composition, management practices, and climate on land–atmosphere exchanges of energy, water, and carbon in urban and suburban ecosystems. The conclusions from this work will serve as a foundation for future basic research in urban forestry and urban ecology, as well as applied research in using trees as "green infrastructure" components to manage urban ecosystem services.

References

Abramoff, M. D., P. J. Magelhaes, and S. J. Ram. 2004. Image processing with ImageJ. Biophotonics International **11**:36-42.

Abrams, M. D. 1988. Comparative water relations of 3 successional hardwood species in central Wisconsin. Tree Physiology **4**:263-273.

Arora, V. K. and G. J. Boer. 2005. A parameterization of leaf phenology for the terrestrial ecosystem component of climate models. Global Change Biology **11**:39-59.

Asbjornsen, H., M. D. Tomer, M. Gomez-Cardenas, L. A. Brudvig, C. M. Greenan, and K. Schilling. 2007. Tree and stand transpiration in a Midwestern bur oak savanna after elm encroachment and restoration thinning. Forest Ecology and Management **247**:209-219.

Baldocchi, D. D., B. B. Hicks, and T. P. Meyers. 1988. Measuring biosphere-atmosphere exchanges of biologically related trace gases with micrometeorological methods. Ecology **69**:1331–1340.

Baldocchi, D. D., B. E. Law, and P. M. Anthoni. 2000. On measuring and modeling energy fluxes above the forest floor of a homogeneous and heterogeneous conifer forest. Agriculture and Forest Meteorology **102**:187-206.

Baldocchi, D. D. and L. K. Xu. 2007. What limits evaporation from Mediterranean oak woodlands - The supply of moisture in the soil, physiological control by plants or the demand by the atmosphere? Advances in Water Resources **30**:2113-2122.

Balogun, A. A., J. O. Adegoke, S. Vezhapparambu, M. Mauder, J. P. McFadden, and K. Gallo. 2009. Surface Energy Balance Measurements Above an Exurban Residential Neighbourhood of Kansas City, Missouri. Boundary-Layer Meteorology **133**:299-321.

Barcza, Z., A. Kern, L. Haszpra, and N. Kljun. 2009. Spatial representativeness of tall tower eddy covariance measurements using remote sensing and footprint analysis. Agricultural and Forest Meteorology **149**:795-807.

Bartens, J., S. D. Day, J. R. Harris, J. E. Dove, and T. M. Wynn. 2008. Can urban tree roots improve infiltration through compacted subsoils for stormwater management? Journal of Environmental Quality **37**:2048-2057.

Bonan, G. B. 2000. The microclimates of a suburban Colorado (USA) landscape and implications for planning and design. Landscape and Urban Planning **49**:97–114.

Bonan, G. B., S. Levis, S. Sitch, M. Vertenstein, and K. W. Oleson. 2003. A dynamic global vegetation model for use with climate models: concepts and description of simulated vegetation dynamics. Global Change Biology **9**:1543-1566.

Bovard, B. D., P. S. Curtis, C. S. Vogel, H. B. Su, and H. P. Schmid. 2005. Environmental controls on sap flow in a northern hardwood forest. Tree Physiology **25**:31-38.

Bowden, J. D. and W. L. Bauerle. 2008. Measuring and modeling the variation in species-specific transpiration in temperate deciduous hardwoods. Tree Physiology **28**:1675-1683.

Breda, N. J. J. 2003. Ground-based measurements of leaf area index: a review of methods, instruments and current controversies. Journal of Experimental Botany **54**:2403-2417.

Brezonik, P. L. and T. H. Stadelmann. 2002. Analysis and predictive models of stormwater runoff volumes, loads, and pollutant concentrations from watersheds in the Twin Cities metropolitan area, Minnesota, USA. Water Research **36**:1743-1757.

Broadhead, J. S., A. R. Muxworthy, C. K. Ong, and C. R. Black. 2003. Comparison of methods for determining leaf area in tree rows. Agricultural and Forest Meteorology **115**:151-161.

Brown, P. W., C. F. Mancino, M. H. Young, T. L. Thompson, P. J. Wierenga, and D. M. Kopec. 2001. Penman Monteith crop coefficients for use with desert turf systems. Crop Science **41**:1197-1206.

Bush, S. E., D. E. Pataki, K. R. Hultine, A. G. West, J. S. Sperry, and J. R. Ehleringer. 2008. Wood anatomy constrains stomatal responses to atmospheric vapor pressure deficit in irrigated, urban trees. Oecologia **156**:13-20.

Byrne, L. B., M. A. Bruns, and K. C. Kim. 2008. Ecosystem properties of urban land covers at the aboveground-belowground interface. Ecosystems **11**:1065-1077.

Campbell, G. S. and J. M. Norman. 1998. An introduction to environmental biophysics. 2nd edition. Springer-Verlag, New York.

Carrow, R. N. 1995. Drought resistance aspects of turfgrasses in the southeast - Evapotranspiration and crop coefficiencts. Crop Science **35**:1685-1690.

Catovsky, S., N. M. Holbrook, and F. A. Bazzaz. 2002. Coupling whole-tree transpiration and canopy photosynthesis in coniferous and broad-leaved tree species. Canadian Journal of Forest Research-Revue Canadienne De Recherche Forestiere **32**:295-309.

Chen, J. M., A. Govind, O. Sonnentag, Y. Q. Zhang, A. Barr, and B. Amiro. 2006. Leaf area index measurements at Fluxnet-Canada forest sites. Agricultural and Forest Meteorology **140**:257-268.

Churkina, G. 2008. Modeling the carbon cycle of urban systems. Ecological Modelling **216**:107-113.

Clark, J. R. and R. Kjelgren. 1990. Water as a limiting factor in the development of urban trees. Journal of Arboriculture **16**:203-208.

Clearwater, M. J., F. C. Meinzer, J. L. Andrade, G. Goldstein, and N. M. Holbrook. 1999. Potential errors in measurement of nonuniform sap flow using heat dissipation probes. Tree Physiology **19**:681-687.

Cook, B. D., K. J. Davis, W. G. Wang, A. Desai, B. W. Berger, R. M. Teclaw, J. G. Martin, P. V. Bolstad, P. S. Bakwin, C. X. Yi, and W. Heilman. 2004. Carbon exchange and venting anomalies in an upland deciduous forest in northern Wisconsin, USA. Agricultural and Forest Meteorology **126**:271-295.

Coutts, A. M., J. Beringer, and N. J. Tapper. 2007. Characteristics influencing the variability of urban CO_2 fluxes in Melbourne, Australia. Atmospheric Environment **41**:51-62.
Craul, P. J. 1985. A description of urban soils and their desired characteristics. Journal of Arboriculture **11**:330-339.
Cregg, B. M. 1994. Carbon allocation, gas exchange, and needle morphology of Pinus ponderosa genotypes known to differ in growth and survival under imposed drought. Tree Physiology **14**:883-898.
Cregg, B. M. 1995. Plant moisture stress of green ash trees in contrasting urban sites. Journal of Arboriculture **21**:271-276.
Cregg, B. M. and M. E. Dix. 2001. Tree moisture stress and insect damage in urban areas in relation to heat island effects. Journal of Arboriculture **27**:8-17.
Danielson, R. E. and C. M. Feldhake. 1981. Urban lawn irrigation and management practices for water saving with minimum effect on lawn quality. Completion Report No. 106. Department of the Interior Office of Water Research and Technology, Washington D.C.
Dufrene, E. and N. Breda. 1995. Estimation of deciduous forest leaf-area index using direct and indirect methods. Oecologia **104**:156-162.
Eastham, J. and C. W. Rose. 1988. Pasture evapotranspiration under varying tree planting density in an agroforestry experiment. Agricultural Water Management **15**:87-105.
Ervin, E. H. and A. J. Koski. 1998. Drought avoidance aspects and crop coefficients of Kentucky bluegrass and tall fescue turfs in the semiarid west. Crop Science **38**:788-795.
Eugster, W. and W. Senn. 1995. A cospectral correction model for measurement of turbulent NO2 flux. Boundary-Layer Meteorology **74**:321-340.
Ewers, B. E., D. S. Mackay, S. T. Gower, D. E. Ahl, S. N. Burrows, and S. S. Samanta. 2002. Tree species effects on stand transpiration in northern Wisconsin. Water Resources Research **38**:1103-1114.
Ewers, B. E., R. Oren, K. H. Johnsen, and J. J. Landsberg. 2001. Estimating maximum mean canopy stomatal conductance for use in models. Canadian Journal of Forest Research-Revue Canadienne De Recherche Forestiere **31**:198-207.
Feldhake, C. M., J. D. Butler, and R. E. Danielson. 1985. Turfgrass evapotranspiration - responses to shade preconditioning. Irrigation Science **6**:265-270.
Feldhake, C. M., R. E. Danielson, and J. D. Butler. 1983. Turfgrass evapotranspiration 1. Factors influencing rate in urban environments. Agronomy Journal **75**:824-830.
Feldhake, C. M., R. E. Danielson, and J. D. Butler. 1984. Turfgrass evapotranspiration 2. Responses to deficit irrigation. Agronomy Journal **76**:85-89.
Foken, T. and B. Wichura. 1996. Tools for quality assessment of surface-based flux measurements. Agricultural and Forest Meteorology **78**:83–105.
Foley, J. A., M. H. Costa, C. Delire, N. Ramankutty, and P. Snyder. 2003. Green surprise? How terrestrial ecosystems could affect earth's climate. Front Ecol. Environment **1**:38–44.

Foley, J. A., S. Levis, I. C. Prentice, D. Pollard, and S. L. Thompson. 1998. Coupling dynamic models of climate and vegetation. Global Change Biology **4**:561-579.

Ford, C. R., R. M. Hubbard, B. D. Kloeppel, and J. M. Vose. 2007. A comparison of sap flux-based evapotranspiration estimates with catchment-scale water balance. Agricultural and Forest Meteorology **145**:176-185.

Ford, C. R., M. A. McGuire, R. J. Mitchell, and R. O. Teskey. 2004. Assessing variation in the radial profile of sap flux density in Pinus species and its effect on daily water use. Tree Physiology **24**:241-249.

Frey, C. M., E. Parlow, R. Vogt, M. Harhash, and M. M. Abdel Wahab. 2010. Flux measurements in Cairo. Part 1: in situ measurements and their applicability for comparison with satellite data. International Journal of Climatology.

Fry, J. and B. Huang. 2004. Applied turfgrass science and physiology. J. Wiley, Hoboken, N.J.

Gebauer, T., V. Horna, and C. Leuschner. 2008. Variability in radial sap flux density patterns and sapwood area among seven co-occurring temperate broad-leaved tree species. Tree Physiology **28**:1821-1830.

Givnish, T. J. 2002. Adaptive significance of evergreen vs. deciduous leaves: Solving the triple paradox. Silva Fennica **36**:703-743.

Granier, A. 1987. Evaluation of transpiration in a Douglas-fir stand by means of sap flow measurements. Tree Physiology **3**:309-319.

Granier, A., P. Biron, B. Kostner, L. W. Gay, and G. Najjar. 1996. Comparisons of xylem sap flow and water vapour flux at the stand level and derivation of canopy conductance for Scots pine. Theoretical and Applied Climatology **53**:115-122.

Gregg, J. W., C. G. Jones, and T. E. Dawson. 2003. Urbanization effects on tree growth in the vicinity of New York City. Nature **424**:183-187.

Grimmond, C. S. B., B. Crawford, J. Hom, B. D. Offerle, M. Patterson, and D. Golub. 2006. Carbon dioxide fluxes in a suburban area of a North American City. Geophysical Research Abstracts **8**.

Grimmond, C. S. B. and T. R. Oke. 1999. Evapotranspiration rates in urban areas. Impacts of Urban Growth on Surface Water and Groundwater Quality (Proceedings of IUGG 99 Symposium HS5).

Grimmond, C. S. B. and T. R. Oke. 2002. Turbulent heat fluxes in urban areas: observations and a local-scale urban meteorological parameterization scheme (LUMPS). Journal of Applied Meteorology **41**:792–810.

Grimmond, C. S. B., J. A. Salmond, T. R. Oke, B. Offerle, and A. Lemonsu. 2004. Flux and turbulence measurements at a densely built-up site in Marseille: Heat, mass (water and carbon dioxide), and momentum. Journal of Geophysical Research-Atmospheres **109**.

Grimmond, C. S. B., C. Souch, R. Grant, and G. Heisler. 1994. Local scale energy and water exchanges in a Chicago neighborhood. Pages 41-51 *in* E. G. McPherson, D. J. Nowak, and R. A. Rowntree, editors. Chicago's Urban Forest Ecosystem: Results of the Chicago Urban Forest Climate Project. Gen. Tech. Rep. NE-186. U.S. Department of Agriculture, Forest Service, Northeastern Forest Experiment Station Radnor, PA.

Grimmond, C. S. B., C. Souch, and M. D. Hubble. 1996. Influence of tree cover on summertime surface energy balance fluxes, San Gabriel valley, Los Angeles. Climate Research **6**:45–57.

Grimmond, S. 2007. Urbanization and global environmental change: local effects of urban warming. Geographical Journal **173**:83-88.

Haase, D. 2009. Effects of urbanisation on the water balance - A long-term trajectory. Environmental Impact Assessment Review **29**:211-219.

Hacke, U. G., J. S. Sperry, J. K. Wheeler, and L. Castro. 2006. Scaling of angiosperm xylem structure with safety and efficiency. Tree Physiology **26**:689-701.

Hagishima, A., K. I. Narita, and J. Tanimoto. 2007. Field experiment on transpiration from isolated urban plants. Hydrological Processes **21**:1217-1222.

Hahs, A. K., M. J. McDonnell, M. A. McCarthy, P. A. Vesk, R. T. Corlett, B. A. Norton, S. E. Clemants, R. P. Duncan, K. Thompson, M. W. Schwartz, and N. S. G. Williams. 2009. A global synthesis of plant extinction rates in urban areas. Ecology Letters **12**:1165-1173.

Hardin, P. J. and R. R. Jensen. 2007. The effect of urban leaf area on summertime urban surface kinetic temperatures: A Terre Haute case study. Urban Forestry & Urban Greening **6**:63-72.

Havranek, W. M. and W. Tranquillini. 1995. Physiological processes during winter dormancy and their ecological significance.*in* W. K. Smith and T. M. Hinckley, editors. Ecophysiology of coniferous forests. Academic Press Inc., New York, NY.

Hogg, E. H., T. A. Black, G. denHartog, H. H. Neumann, R. Zimmermann, P. A. Hurdle, P. D. Blanken, Z. Nesic, P. C. Yang, R. M. Staebler, K. C. McDonald, and R. Oren. 1997. A comparison of sap flow and eddy fluxes of water vapor from a boreal deciduous forest. Journal of Geophysical Research–Atmospheres **102**:28929–28937.

Holscher, D., O. Koch, S. Korn, and C. Leuschner. 2005. Sap flux of five co-occurring tree species in a temperate broad-leaved forest during seasonal soil drought. Trees-Structure and Function **19**:628-637.

Hornbeck, J. W., C. W. Martin, and C. Eagar. 1997. Summary of water yield experiments at Hubbard Brook Experimental Forest, New Hampshire. Canadian Journal of Forest Research-Revue Canadienne De Recherche Forestiere **27**:2043-2052.

Huang, L. M., H. T. Li, D. H. Zha, and J. Y. Zhu. 2008. A fieldwork study on the diurnal changes of urban microclimate in four types of ground cover and urban heat island of Nanjing, China. Building and Environment **43**:7-17.

Imhoff, M. L., L. Bounoua, R. DeFries, W. T. Lawrence, D. Stutzer, C. J. Tucker, and T. Ricketts. 2004. The consequences of urban land transformation on net primary productivity in the United States. Remote Sensing of Environment **89**:434-443.

Jackson, R. B., J. Canadell, J. R. Ehleringer, H. A. Mooney, O. E. Sala, and E. D. Schulze. 1996. A global analysis of root distributions for terrestrial biomes. Oecologia **108**:389-411.

Jenerette, G. D., S. L. Harlan, A. Brazel, N. Jones, L. Larsen, and W. L. Stefanov. 2007. Regional relationships between surface temperature, vegetation, and human settlement in a rapidly urbanizing ecosystem. Landscape Ecology **22**:353-365.

Kjelgren, R. and T. Montague. 1998. Urban tree transpiration over turf and asphalt surfaces. Atmospheric Environment **32**:35-41.
Kljun, N., P. Calanca, M. W. Rotachhi, and H. P. Schmid. 2004. A simple parameterisation for flux footprint predictions. Boundary-Layer Meteorology **112**:503-523.
Kotani, A. and M. Sugita. 2005. Seasonal variation of surface fluxes and scalar roughness of suburban land covers. Agricultural and Forest Meteorology **135**:1-21.
Kramer, P. J. 1987. The role of water stress in tree growth. Journal of Arboriculture **13**:33-38.
Kumagai, T., H. Nagasawa, T. Mabuchi, S. Ohsaki, K. Kubota, K. Kogi, Y. Utsumi, S. Koga, and K. Otsuki. 2005. Sources of error in estimating stand transpiration using allometric relationships between stem diameter and sapwood area for Cryptomeria japonica and Chamaecyparis obtusa. Forest Ecology and Management **206**:191-195.
Lagergren, F. and A. Lindroth. 2002. Transpiration response to soil moisture in pine and spruce trees in Sweden. Agricultural and Forest Meteorology **112**:67-85.
Larson, K. L., D. Casagrande, S. L. Harlan, and S. T. Yabiku. 2009. Residents' Yard Choices and Rationales in a Desert City: Social Priorities, Ecological Impacts, and Decision Tradeoffs. Environmental Management **44**:921-937.
Leuzinger, S., R. Vogt, and C. Kˆrner. 2010. Tree surface temperature in an urban environment. Agricultural and Forest Meteorology **150**:56-62.
Lindroth, A., F. Lagergren, M. Aurela, B. Bjarnadottir, T. Christensen, E. Dellwik, A. Grelle, A. Ibrom, T. Johansson, H. Lankreijer, S. Launiainen, T. Laurila, M. Molder, E. Nikinmaa, K. Pilegaard, B. D. Sigurdsson, and T. Vesala. 2008. Leaf area index is the principal scaling parameter for both gross photosynthesis and ecosystem respiration of Northern deciduous and coniferous forests. Tellus Series B-Chemical and Physical Meteorology **60**:129-142.
Lloyd, J. and J. A. Taylor. 1994. On the temperature dependence of soil respiration. Functional Ecology **8**:315-323.
Lu, P., L. Urban, and P. Zhao. 2004. Granier's thermal dissipation probe (TDP) method for measuring sap flow in trees: Theory and practice. Acta Botanica Sinica **46**:631-646.
Ludwig, F., T. E. Dawson, H. H. T. Prins, F. Berendse, and H. de Kroon. 2004. Belowground competition between trees and grasses may overwhelm the facilitative effects of hydraulic lift. Ecology Letters **7**:623-631.
Lundblad, M. and A. Lindroth. 2002. Stand transpiration and sap flow density in relation to weather, soil moisture and stand characteristics. Basic and Applied Ecology **3**:229-243.
Matile, P. 2000. Biochemistry of Indian summer: physiology of autumnal leaf coloration. Experimental Gerontology **35**:145-158.
Mauder, M., T. Foken, R. Clement, J. A. Elbers, W. Eugster, T. Grunwald, B. Heusinkveld, and O. Kolle. 2008. Quality control of CarboEurope flux data – Part 2: Inter-comparison of eddy-covariance software. Biogeosciences **5**:12.
McKinney, M. L. 2002. Urbanization, biodiversity, and conservation. BioScience **52**:883-890.

McLaren, J. D., M. A. Arain, M. Khomik, M. Peichl, and J. Brodeur. 2008. Water flux components and soil water-atmospheric controls in a temperate pine forest growing in a well-drained sandy soil. Journal of Geophysical Research-Biogeosciences **113**.

McPherson, E. G. 1994. Cooling urban heat islands with sustainable landscapes. Pages 151-171 *in* R. Platt, R. Rowntree, P. Muick editor. The ecological city: preserving and restoring urban biodiversity. University of Massachusetts Press, Amherst.

McPherson, G., J. R. Simpson, P. J. Peper, S. E. Maco, and Q. F. Xiao. 2005. Municipal forest benefits and costs in five US cities. Journal of Forestry **103**:411-416.

Melcher, P. J., M. A. Zwieniecki, and N. M. Holbrook. 2003. Vulnerability of xylem vessels to cavitation in sugar maple. Scaling from individual vessels to whole branches. Plant Physiology **131**:1775-1780.

Milesi, C., S. W. Running, C. D. Elvidge, J. B. Dietz, B. T. Tuttle, and R. R. Nemani. 2005. Mapping and modeling the biogeochemical cycling of turf grasses in the United States. Environmental Management **36**:426-438.

Mitchell, V. G., H. A. Cleugh, C. S. B. Grimmond, and J. Xu. 2008. Linking urban water balance and energy balance models to analyse urban design options. Hydrological Processes **22**:2891-2900.

Montague, T. and R. Kjelgren. 2004. Energy balance of six common landscape surfaces and the influence of surface properties on gas exchange of four containerized tree species. Scientia Horticulturae **100**:229-249.

Monteith, J. L. and M. H. Unsworth. 1990. Principles of environmental physics, 2nd Edition. Edward Arnold, London.

Moore, C. J. 1986. Frequency response corrections for eddy correlation systems. Boundary-Layer Meteorology **37**:17–35.

Moriwaki, R. and M. Kanda. 2004. Seasonal and diurnal fluxes of radiation, heat, water vapor, and carbon dioxide over a suburban area. Journal of Applied Meteorology **43**:1700-1710.

Mueller, E. C. and T. A. Day. 2005. The effect of urban ground cover on microclimate, growth and leaf gas exchange of oleander in Phoenix, Arizona. International Journal of Biometeorology **49**:244-255.

National Climatic Data Center. 2004. Climatography of the United States No. 20 1971-2000. U.S. Department of Commerce, National Oceanic and Atmospheric Administration, National Environmental Satellite, Data, and Information Service, Asheville.

Nemitz, E., K. J. Hargreaves, A. G. McDonald, J. R. Dorsey, and D. Fowler. 2002a. Meteorological measurements of the urban heat budget and CO2 emissions on a city scale. Environmental Science & Technology **36**:3139-3146.

Nemitz, E., K. J. Hargreaves, A. G. McDonald, J. R. Dorsey, and D. Fowler. 2002b. Micrometeorological measurements of the urban heat budget and CO_2 emissions on a city scale. Environmental Science and Technology **36**:3139–3146.

Neumann, P. M., R. Weissman, G. Stefano, and S. Mancuso. Accumulation of xylem transported protein at pit membranes and associated reductions in hydraulic conductance. Journal of Experimental Botany **61**:1711-1717.

New, M., M. Hulme, and P. Jones. 1999. Representing twentieth-century space-time climate variability. Part I: Development of a 1961-90 mean monthly terrestrial climatology. Journal of Climate **12**:829-856.

Niinemets, U. and F. Valladares. 2006. Tolerance to shade, drought, and waterlogging of temperate Northern Hemisphere trees and shrubs. Ecological Monographs **76**:521-547.

Nowak, D. J. 1994. Atmospheric carbon dioxide reduction by Chicago's urban forest. Pages 83-94 *in* E. G. McPherson, D. J. Nowak, and R. A. Rowntree, editors. Chicago's Urban Forest Ecosystem: Results of the Chicago Urban Forest Climate Project. Gen. Tech. Rep. NE-186. U.S. Department of Agriculture, Forest Service, Northeastern Forest Experiment Station Radnor, PA.

Nowak, D. J. and D. E. Crane. 2002. Carbon storage and sequestration by urban trees in the USA. Environmental Pollution **116**:381–389.

Nowak, D. J., D. E. Crane, J. C. Stevens, R. E. Hoehn, J. T. Walton, and J. Bond. 2008. A ground-based method of assessing urban forest structure and ecosystem services. Arboriculture and Urban Forestry **34**:347-358.

Nowak, D. J., R. A. Rowntree, E. G. McPherson, S. M. Sisinni, E. R. Kerkmann, and J. C. Stevens. 1996. Measuring and analyzing urban tree cover. Landscape and Urban Planning **36**:49-57.

Offerle, B., C. S. B. Grimmond, K. Fortuniak, and W. Pawlak. 2006. Intraurban differences of surface energy fluxes in a central European city. Journal of Applied Meteorology and Climatology **45**:125-136.

Oishi, A. C., R. Oren, and P. C. Stoy. 2008. Estimating components of forest evapotranspiration: A footprint approach for scaling sap flux measurements. Agricultural and Forest Meteorology **148**:1719-1732.

Oke, T. R. 1979. Advectively-assisted evapotranspiration from irrigated urban vegetation. Boundary-Layer Meteorology **17**:167-173.

Oke, T. R. 1982. The Energetic Basis of the Urban Heat-Island. Quarterly Journal of the Royal Meteorological Society **108**:1-24.

Oke, T. R. 1989. The micrometeorology of the urban forest. Philosophical Transactions of the Royal Society of London, Series B **324**:335–349.

Oren, R., N. Phillips, G. Katul, B. E. Ewers, and D. E. Pataki. 1998. Scaling xylem sap flux and soil water balance and calculating variance: a method for partitioning water flux in forests. Annales Des Sciences Forestieres **55**:191-216.

Paco, T. A., T. S. David, M. O. Henriques, J. S. Pereira, F. Valente, J. Banza, F. L. Pereira, C. Pinto, and J. S. David. 2009. Evapotranspiration from a Mediterranean evergreen oak savannah: The role of trees and pasture. Journal of Hydrology **369**:98-106.

Pataki, D. E., R. J. Alig, A. S. Fung, N. E. Golubiewski, C. A. Kennedy, E. G. McPherson, D. J. Nowak, R. V. Pouyat, and P. R. Lankao. 2006a. Urban ecosystems and the North American carbon cycle. Global Change Biology **12**:2092-2102.

Pataki, D. E., R. J. Alig, A. S. Fung, N. E. Golubiewski, C. A. Kennedy, E. G. McPherson, D. J. Nowak, R. V. Pouyat, and P. R. Lankao. 2006b. Urban ecosystems and the North American carbon cycle. Global Change Biology **12**:1-11.

Pataki, D. E., H. R. McCarthy, E. Livtak, and S. Pincetl. In review. Transpiration of urban forests in the Los Angeles metropolitan area. Ecological Applications.

Pataki, D. E. and R. Oren. 2003. Species differences in stomatal control of water loss at the canopy scale in a mature bottomland deciduous forest. Advances in Water Resources **26**:1267-1278.

Peper, P. J. and E. G. McPherson. 2003. Evaluation of four methods for estimating leaf area of isolated trees. Urban Forestry & Urban Greening **2**:19-29.

Peters, E. B. and J. P. McFadden. 2010. Influence of seasonality and vegetation type on suburban microclimates. Urban Ecosystems.

Peters, E. B., J. P. McFadden, and R. A. Montgomery. in press. Biological and environmental controls on tree transpiration in a suburban landscape. Journal of Geophysical Research.

Phillips, N. and R. Oren. 1998. A comparison of daily representations of canopy conductance based on two conditional time-averaging methods and the dependence of daily conductance on environmental factors. Annales Des Sciences Forestieres **55**:217-235.

Pielke, R. A. and R. Avissar. 1990. Influence of landscape structure on local and regional climate. Landscape Ecology **4**:133–156.

Pielke, R. A., G. Marland, R. A. Betts, T. N. Chase, J. L. Eastman, J. O. Niles, D. D. S. Niyogi, and S. W. Running. 2002. The influence of land-use change and landscape dynamics on the climate system: relevance to climate-change policy beyond the radiative effect of greenhouse gases. Philosophical Transactions of the Royal Society of London Series a-Mathematical Physical and Engineering Sciences **360**:1705-1719.

Priestley, C. H. B. and R. J. Taylor. 1972. On the assessment of surface heat flux and evaporation using large-scale parameters. Monthly Weather Review **100**:81-92.

R Development Core Team. 2010. R: A language and environment for statistical computing. R Foundation for Statistical Computing, Vienna, Austria.

Radeloff, V. C., R. B. Hammer, and S. I. Stewart. 2005. Rural and suburban sprawl in the US Midwest from 1940 to 2000 and its relation to forest fragmentation. Conservation Biology **19**:793-805.

Rebmann, C., M. Gockede, T. Foken, M. Aubinet, M. Aurela, P. Berbigier, C. Bernhofer, N. Buchmann, A. Carrara, A. Cescatti, R. Ceulemans, R. Clement, J. A. Elbers, A. Granier, T. Grunwald, D. Guyon, K. Havrankova, B. Heinesch, A. Knohl, T. Laurila, B. Longdoz, B. Marcolla, T. Markkanen, F. Miglietta, J. Moncrieff, L. Montagnani, E. Moors, M. Nardino, J. M. Ourcival, S. Rambal, U. Rannik, E. Rotenberg, P. Sedlak, G. Unterhuber, T. Vesala, and D. Yakir. 2005. Quality analysis applied on eddy covariance measurements at complex forest sites using footprint modelling. Theoretical and Applied Climatology **80**:121-141.

Reich, P. B., D. S. Ellsworth, and M. B. Walters. 1998. Leaf structure (specific leaf area) modulates photosynthesis-nitrogen relations: evidence from within and across species and functional groups. Functional Ecology **12**:948-958.

Reich, P. B., M. B. Walters, and D. S. Ellsworth. 1997. From tropics to tundra: global convergence in plant functioning. Proceedings of the National Academy of Science **94**:13730–13734.

Rivalland, V., J. C. Calvet, P. Berbigier, Y. Brunet, and A. Granier. 2005. Transpiration and CO2 fluxes of a pine forest: modelling the undergrowth effect. Annales Geophysicae **23**:291-304.

Rowntree, R. R. 1984. Forest canopy cover and land use in four eastern united states cities. Urban Ecology **8**:55-67.

Rutter, A. J., A. J. Morton, and P. C. Robins. 1975. Predictive model of rainfall interception in forests .2. Generalization of model and comparison with observation in some coniferous and hardwood stands. Journal of Applied Ecology **12**:367-380.

Ryu, Y., O. Sonnentag, T. Nilson, R. Vargas, H. Kobayashi, R. Wenk, and D. D. Baldocchi. 2010. How to quantify tree leaf area index in an open savanna ecosystem: A multi-instrument and multi-model approach. Agricultural and Forest Meteorology **150**:63-76.

Santer, B. D., C. Mears, F. J. Wentz, K. E. Taylor, P. J. Gleckler, T. M. L. Wigley, T. P. Barnett, J. S. Boyle, W. Bruggemann, N. P. Gillett, S. A. Klein, G. A. Meehl, T. Nozawa, D. W. Pierce, P. A. Stott, W. M. Washington, and M. F. Wehner. 2007. Identification of human-induced changes in atmospheric moisture content. Proceedings of the National Academy of Sciences of the United States of America **104**:15248-15253.

Scharenbroch, B. C., J. E. Lloyd, and J. L. Johnson-Maynard. 2005. Distinguishing urban soils with physical, chemical, and biological properties. Pedobiologia **49**:283-296.

Schmid, H. P. 1994. Source areas for scalars and scalar fluxes. Boundary-Layer Meteorology **67**:293-318.

Schmid, H. P., C. S. B. Grimmond, F. Cropley, B. Offerle, and H. B. Su. 2000. Measurements of CO_2 and energy fluxes over a mixed hardwood forest in the mid-western United States. Agricultural and Forest Meteorology **103**:357–374.

Schmid, H. P., H. B. Su, C. S. Vogel, and P. S. Curtis. 2003. Ecosystem-atmosphere exchange of carbon dioxide over a mixed hardwood forest in northern lower Michigan. Journal of Geophysical Research-Atmospheres **108**:19.

Schotanus, P., F. T. M. Nieuwstadt, and H. A. R. Debruin. 1983. Temperature-measurement with a sonic anemometer and its application to heat and moisture fluxes. Boundary-Layer Meteorology **26**:81-93.

Sen Roy, S. and F. Yuan. 2009. Trends in extreme temperatures in relation to urbanization in the Twin Cities Metropolitan Area, Minnesota. Journal of Applied Meteorology and Climatology **48**:669-679.

Shashua-Bar, L., D. Pearlmutter, and E. Erell. 2009. The cooling efficiency of urban landscape strategies in a hot dry climate. Landscape and Urban Planning **92**:179-186.

Smith, D. L. and L. Johnson. 2004. Vegetation-mediated changes in microclimate reduce soil respiration as woodlands expand into grasslands. Ecology **85**:3348-3361.

Snyder, K. A. and D. G. Williams. 2007. Root allocation and water uptake patterns in riparian tree saplings: Responses to irrigation and defoliation. Forest Ecology and Management **246**:222-231.

Sobrado, M. A. 1997. Embolism vulnerability in drought-deciduous and evergreen species of a tropical dry forest. Acta Oecologica-International Journal of Ecology **18**:383-391.

Soegaard, H. and L. Møller-Jensen. 2003. Towards a spatial CO2 budget of a metropolitan region based on textural image classification and flux measurements. Remote Sensing of Environment **87**:283-294.

Solomon, S., D. Qin, M. Manning, R. B. Alley, T. Berntsen, N. L. Bindoff, Z. Chen, A. Chidthasisong, J. M. Gregory, G. C. Hergerl, M. Heimann, B. Hewitson, B. J. Hoskins, F. Joos, J. Jouzel, V. Kattsov, U. Lohmann, T. Matsuno, M. Molina, N. Nicholls, J. Overpeck, G. Raga, V. Ramaswamy, J. Ren, M. Rusticucci, R. Somerville, T. F. Stocker, P. Whetton, R. A. Wood, and D. Wratt. 2007. 2007: Technical Summary. In: Climate Change 2007: The Physical Science Basis. Contribution of Working Group I to the Fourth Assessment Report of the Intergovermental Panel on Climate Change. [Solomon,S., D. Qin, M. Manning, Z. Chen, M. Marquis, K.B. Averyt, M. Tignor and H.L. Miller (eds.)]. Cambridge, United Kingdom and New York, NY, USA.

Sperry, J. S., U. G. Hacke, and J. Pittermann. 2006. Size and function in conifer tracheids and angiosperm vessels. American Journal of Botany **93**:1490-1500.

Spronken-Smith, R. A. 2002. Comparison of summer- and winter-time suburban energy fluxes in Christchurch, New Zealand. International Journal of Climatology **22**:979–992.

Spronken-Smith, R. A., T. R. Oke, and W. P. Lowry. 2000. Advection and the surface energy balance across an irrigated urban park. International Journal of Climatology **20**:1033–1047.

State of Minnesota. 2006. Ramsey County. Department of Administration, Land Management Information Center, Saint Paul, MN.

Tanaka, K. and S. Hashimoto. 2006. Plant canopy effects on soil thermal and hydrological properties and soil respiration. Ecological Modelling **196**:32-44.

Taneda, H. and J. S. Sperry. 2008. A case-study of water transport in co-occurring ring-versus diffuse-porous trees: contrasts in water-status, conducting capacity, cavitation and vessel refilling. Tree Physiology **28**:1641-1651.

Tang, J. W., P. V. Bolstad, B. E. Ewers, A. R. Desai, K. J. Davis, and E. V. Carey. 2006. Sap flux-upscaled canopy transpiration, stomatal conductance, and water use efficiency in an old growth forest in the Great Lakes region of the United States. Journal of Geophysical Research-Biogeosciences **111**.

Taylor, J. R. 1982. An introduction to error analysis: the study of uncertainities in physical measurements. 2nd edition. University Science Books, Sausalito.

Todhunter, P. E. 1996. Environmental indices for the Twin Cities Metropolitan Area (Minnesota, USA) urban heat island - 1989. Climate Research **6**:59-69.

Tooke, T. R., N. C. Coops, N. R. Goodwin, and J. A. Voogt. 2009. Extracting urban vegetation characteristics using spectral mixture analysis and decision tree classifications. Remote Sensing of Environment **113**:398-407.

United Nations. 2005. Fact Sheet 1. Department of Economic and Social Affairs, Population Division. World Urbanization Prospects: The 2005 Revision.

USDA Forest Service. 2005. Forest inventory and analysis national core field guide, volume 2: FIA field methods for Phase 3 measurements, version 3.0. U.S. Department of Agriculture, Washington D.C.

Valente, F., J. S. David, and J. H. C. Gash. 1997. Modelling interception loss for two sparse eucalypt and pine forests in central Portugal using reformulated Rutter and Gash analytical models. Journal of Hydrology **190**:141-162.

Vesala, T., L. Jarvi, S. Launiainen, A. Sogachev, U. Rannik, I. Mammarella, E. Siivola, P. Keronen, J. Rinne, A. Riikonen, and E. Nikinmaa. 2008a. Surface-atmosphere interactions over complex urban terrain in Helsinki, Finland. Tellus Series B-Chemical and Physical Meteorology **60**:188-199.

Vesala, T., N. Kljun, U. Rannik, J. Rinne, A. Sogachev, T. Markkanen, K. Sabelfeld, T. Foken, and M. Y. Leclerc. 2008b. Flux and concentration footprint modelling: State of the art. Environmental Pollution **142**:14.

Vickers, D. and L. Mahrt. 1997. Quality control and flux sampling problems for tower and aircraft data. Journal of Atmospheric and Oceanic Technology **14**:512-526.

Villalobos, F. J., F. Orgaz, and L. Mateos. 1995. Non-destructive measurement of leaf-area in olive (Olea-europaea L) trees using a gap inversion method. Agricultural and Forest Meteorology **73**:29-42.

Walker, J. S., N. B. Grimm, J. M. Briggs, C. Gries, and L. Dugan. 2009. Effects of urbanization on plant species diversity in central Arizona. Frontiers in Ecology and the Environment **7**:465-470.

Walton, J. T., D. J. Nowak, and E. J. Greenfield. 2008. Assessing urban forest canopy cover using airborne or satellite imagery. Arboriculture and Urban Forestry **34**:334-340.

Wang, J., T. A. Endreny, and D. J. Nowak. 2008. Mechanistic simulation of tree effects in an urban water balance model. Journal of the American Water Resources Association **44**:75-85.

Waring, R. H., W. H. Emmingham, H. L. Gholz, and C. C. Grier. 1978. Variation in maximum leaf area of coniferous forests in Oregon and its ecological significance. Forest Science **24**:131-140.

Waring, R. H. and S. W. Running. 1997. Forest ecosystems: analysis at multiple scales. Academic Press, New York.

Webb, E. K., G. I. Pearman, and R. Leuning. 1980. Correction of flux measurements for density effects due to heat and water vapour transfer. Quarterly Journal of the Royal Meteorological Society **106**:85–100.

Whitlow, T. H. and N. L. Bassuk. 1988. Ecophysiology of urban trees and their management - the North American experience. HortScience **23**:542-546.

Whitlow, T. H., N. L. Bassuk, and D. L. Reichert. 1992. A 3-year study of water relations of urban street trees. Journal of Applied Ecology **29**:436-450.

Willson, C. J. and R. B. Jackson. 2006. Xylem cavitation caused by drought and freezing stress in four co-occurring Juniperus species. Physiologia Plantarum **127**:374-382.

Wilson, K., A. Goldstein, E. Falge, M. Aubinet, D. Baldocchi, P. Berbigier, C. Bernhofer, R. Ceulemans, H. Dolman, C. Field, A. Grelle, A. Ibrom, B. E. Law, A. Kowalski, T. Meyers, J. Moncrieff, R. Monson, W. Oechel, J. Tenhunen, R. Valentini, and S. Verma. 2002. Energy balance closure at FLUXNET sites. Agricultural and Forest Meteorology **113**:223-243.

Wilson, K. B., P. J. Hanson, P. J. Mulholland, D. D. Baldocchi, and S. D. Wullschleger. 2001. A comparison of methods for determining forest evapotranspiration and its components: sap-flow, soil water budget, eddy covariance and catchment water balance. Agricultural and Forest Meteorology **106**:153-168.

Winkler, J. A., R. H. Skaggs, and D. G. Baker. 1981. Effect of temperature adjustments on the Minneapolis-St. Paul urban heat-island. Journal of Applied Meteorology **20**:1295-1300.

Wullschleger, S. D. and P. J. Hanson. 2006. Sensitivity of canopy transpiration to altered precipitation in an upland oak forest: evidence from a long-term field manipulation study. Global Change Biology **12**:97-109.

Wullschleger, S. D., P. J. Hanson, and D. E. Todd. 2001. Transpiration from a multi-species deciduous forest as estimated by xylem sap flow techniques. Forest Ecology and Management **143**:205-213.

Zhang, L., W. R. Dawes, and G. R. Walker. 2001. Response of mean annual evapotranspiration to vegetation changes at catchment scale. Water Resources Research **37**:701-708.

Zhang, X., L. Hu, X. Bian, B. Zhao, F. Chai, and X. Sun. 2007. The most economical irrigation amount and evapotranspiration of the turfgrasses in Beijing City, China. Agricultural Water Management **89**:98-104.

Zhang, X. Y., M. A. Friedl, C. B. Schaaf, A. H. Strahler, J. C. F. Hodges, F. Gao, B. C. Reed, and A. Huete. 2003. Monitoring vegetation phenology using MODIS. Remote Sensing of Environment **84**:471-475.

Appendix 1

Estimating canopy photosynthesis using leaf gas-exchange and sap flow measurements

Introduction

Cities represent large sources of CO_2 to the atmosphere, yet vegetation, through the processes of photosynthesis and carbon storage in biomass, can act as a significant sink of CO_2 in urban areas (Soegaard and Møller-Jensen 2003, Grimmond et al. 2006). In the United States, cities are increasingly using forest inventories to evaluate the potential carbon storage of urban trees (Nowak and Crane 2002, Nowak et al. 2008). While these methods estimate net carbon storage by trees at time scales of years to decades, they cannot provide a mechanistic understanding of canopy carbon uptake at shorter time scales. To predict urban ecosystem responses to climate change, it is necessary to know how canopy photosynthesis of urban trees responds to changes in environmental drivers at diurnal, seasonal, and inter-annual time scales. In addition, tree species vary in the magnitude and seasonality of carbon uptake rates (Catovsky et al. 2002, Givnish 2002), complicating efforts to scale up species' differences in carbon uptake in species-rich urban ecosystems.

In this study, I combined continuous measurements of sap flow with species-specific leaf-level gas exchange measurements to model canopy photosynthesis during the 2008 growing season for the dominant tree species in a suburban neighborhood of

Minneapolis–Saint Paul, Minnesota. My objectives were 1) to determine how suburban tree species vary in their canopy photosynthesis rates across the growing season; and 2) to evaluate the ability of plant functional types to predict the tree component of urban and suburban carbon budgets.

Methods

During the 2008 growing season, I collected leaf-level gas exchange measurements in tree canopies at the Lauderdale and Saint Paul sites (described in Chapter 3) and at two Minneapolis parks, Logan Park and Windom Park (5 and 4 km, respectively, from our study area). Logan Park and Windom Park were both located in a residential area similar to the other two sites. The Lauderdale site was sampled on one day in each of the months of July and September, at the Saint Paul site in June, August, and September, at the Logan Park site in August and October, and at the Windom Park site in August and September. Table A1-1 describes the number of trees in each species that were sampled at each site. To maximize the number of high quality measurements, the sampling days were restricted to weather conditions with clear skies and low winds. On each sampling date, gas exchange measurements were made throughout the day (08:00–15:00 h) on leaves that were accessible from an aerial lift truck. Leaves were sampled throughout the canopy of each tree. Most of the leaves sampled were exposed to direct sunlight during part of the day because all trees had open canopies and were grown under park-like conditions. Six to 43 leaves were sampled within each canopy on each sampling day depend-

ing on the size of the canopy and the ability to access different parts of the canopy from the aerial lift truck.

In-situ measurements of leaf-level photosynthesis and stomatal conductance were made using a portable infrared gas-exchange system (LI-6400, LI-Cor, Lincoln, Nebraska, USA) that was set to match existing environmental conditions of air temperature, irradiance, and water vapor concentration. Ambient air was drawn through a dry empty carboy to stabilize air temperature and water vapor concentrations in the LI-6400 leaf cuvette. The clear LI-6400 leaf cuvette provided ambient light conditions. The conifer chamber (LI-6400-05) was used to measure leaves on evergreen needleleaf trees. CO_2 cartridges were used to provide a constant reference CO_2 concentration of 390 ppm, which was representative of local CO_2 concentrations at the study sites. For deciduous broadleaf species, the measuring area of the standard LI-6400 leaf cuvette determined the sampled leaf area. For evergreen needleleaf trees, sampled needles were collected and scanned to determine their area using ImageJ (version 1.36b) software (Abramoff et al. 2004).

Canopy-level conductance (G_C) in m s^{-1} was determined from continuous sap flow measurements at the Lauderdale and Saint Paul site (described in Chapter 3) using a simplified form of the Penman-Monteith equation that assumes an aerodynamically well-mixed canopy (Monteith and Unsworth 1990):

$$G_C = \frac{\lambda \gamma E_C}{c_p \rho D} \qquad (1)$$

where λ is the latent heat of vaporization (MJ kg^{-1}), γ is the psychrometric constant (kPa $ºC^{-1}$), ρ is the density of air (kg m^{-3}), E_C is tree transpiration per canopy area (kg H_2O m^{-2} s^{-1}), and D is the vapor pressure deficit between the leaf interior and the bulk air (kPa). D was calculated using measurements of air temperature and relative humidity within tree canopies at each site, as leaf and air temperature were assumed to be similar due to a well-mixed canopy. It is reasonable to assume a well-mixed canopy in this study area due to the diversity of surface types likely creating a high surface roughness. E_C was calculated from sap flow measurements, as described in Chapter 3. G_C was converted to mol m^{-2} s^{-1} using the Ideal Gas Law:

$$G_{Cmol} = \frac{G_C P}{RT} \qquad (2)$$

where P is air pressure (Pa), T is air temperature (K), and R is the ideal gas law constant (m^3 Pa K^{-1} mol^{-1}).

To convert G_{Cmol} to canopy-level photosynthesis (A_C) per canopy area (g C m^{-2} s^{-1}), or gross primary productivity (GPP), I developed species-specific linear regression models between leaf-level photosynthesis and stomatal conductance, following Catovsky et al. (2002). Linear regression models were fit through the origin in the form $y = ax$. A_C was calculated by multiplying G_{Cmol} by the slope, or parameter a, of the linear regression model for each species. I separately tested each tree species for significant differences in the regression slopes among seasons, canopy positions, and sites to evaluate the need for specialized regression equations.

Results

The relationship between stomatal conductance and leaf-level photosynthesis varied among the nine species sampled during the 2008 growing season (Figure A1-1). For those species measured at more than one site, there were no significant differences in this relationship among sites ($F_{[1,97]} = 0.84$ for *F. pennsylvanica*; $F_{[1,27]} = 0.02$ for *P. glauca*; $F_{[1,73]} = 2.53$ for *P. sylvestris*; $F_{[2,105]} = 1.00$ for *T. americana*, all $P > 0.16$). The relationship was also not significantly different between summer (June to August) and fall (September and October) sampling dates for all species except *Fraxinus pennsylvanica*, where the slope of the relationship was slightly higher on average in fall than summer ($F_{[1,97]} = 29.6$, $P < 0.001$ for *F. pennsylvanica*; $P > 0.10$ for all other species). In addition, the relationship did not differ between upper and lower canopy layers (all species $P > 0.15$, Figure A1-1).

The parameter used to convert G_{Cmol} to A_C was generated by the linear regression analysis shown in Table A1-1. Although leaves were sampled throughout the height of the tree canopies, access restrictions due to the aerial lift truck meant that most of the measured leaves were in the outer canopy and thus were exposed to more direct sunlight. Consequently, the linear regression models may be more representative of sun-adapted than shade-adapted leaves, which could lead to a potential overestimate of A_C.

Seasonal patterns of A_C per canopy area (g C m^{-2} day^{-1}) varied among the six tree genera studied in 2008 (Figure A1-2). Evergreen needleleaf genera (*Picea* and *Pinus*) had higher daily A_C across the entire growing season than deciduous broadleaf genera (*Frax-*

inus, *Ulmus*, *Tilia* and *Juglans*), reaching maximum A_C rates of >10 g C m^{-2} day^{-1} in May and June. Daily A_C of three of the deciduous genera (*Fraxinus*, *Ulmus*, and *Juglans*) remained <5 g C m^{-2} day^{-1} across the entire growing season. *Tilia*, however, had daily A_C >8 g C m^{-2} day^{-1}, particularly in early summer.

Annual sums of A_C per canopy area ranged from 0.25 to 1.13 kg C m^{-2} yr^{-1} across genera, and differed significantly between plant functional types (P = 0.002, Figure A1-3). Evergreen needleleaf trees had greater annual A_C than deciduous broadleaf trees (1.01 and 0.38 kg C m^{-2} yr^{-1}, respectively). The actual difference in annual A_C between evergreen needleleaf and deciduous broadleaf trees could be slightly larger because our spring sap flow measurements began after evergreen needleleaf trees were already physiologically active (Figure 3-2).

Discussion

Annual sums of canopy photosynthesis per canopy area (A_C) found in this study (0.25–1.13 kg C m^{-2} yr^{-1}) were similar to those found in a forest ecosystem in the northeastern USA, where annual A_C ranged from 0.30–1.06 kg C m^{-2} yr^{-1} for two deciduous broadleaf and one evergreen needleleaf species (Catovsky et al. 2002). However, in contrast, Catovsky et al. (2002) results showed that the evergreen needleleaf species they measured, hemlock (*Tsuga canadensis*), had lower annual and daily A_C across the middle of the growing season than the two deciduous broadleaf species, red maple (*Acer rubrum*) and red oak (*Quercus rubra*). This difference can be partly attributed to the relatively low LAI of hemlock trees, compared to most evergreen needleleaf species (Waring et al.

1978). While the average annual A_C of the deciduous trees measured by Catovksy et al. (2002) was higher (0.84 kg C m^{-2} yr^{-1}) than values observed in this study (0.38 kg C m^{-2} yr^{-1}), no tree species were the same in both studies. Another way of evaluating the annual A_C estimates in this study is to compare them to predictions generated by an urban forest growth model based on allometric equations (Nowak and Crane 2002, Nowak et al. 2008). Nowak et al. (2002) found that net productivity of urban forests in the United States ranged from 0.18 to 0.66 kg C m^{-2} yr^{-1} on a canopy area basis. Assuming net productivity is a constant 50% of GPP (Waring and Running 1997), these values are also similar to the carbon uptake rates observed in this study.

Overall, my results suggest that plant functional types offer a useful approach to scale up species' differences in A_C in suburban landscapes, as was found for species' differences in tree transpiration in Chapter 3. With the availability of ecosystem fluxes of CO_2 from the KUOM eddy covariance tower, data from this study will be used to evaluate the tree component on a suburban carbon budget, as was done for ecosystem evapotranspiration in Chapter 4.

Table A1-1. Number of trees measured, site, and parameters from the linear regression model, $y = ax$, between leaf-level photosynthesis and stomatal conductance for nine tree species. Numbers in parentheses represent ±1 standard error.

Species	*n*	Site	*a*	R^2
Fraxinus penn-sylvanica	3 2 5	Lauderdale Saint Paul	40.03 (2.05)	0.79
Juglans nigra	1	Saint Paul	45.13 (1.40)	0.94
Picea abies	2	Lauderdale	58.72 (6.26)	0.83
Picea glauca	2 2 4	Logan Saint Paul	94.96 (2.02)	0.99
Pinus nigra	2	Lauderdale	79.10 (3.36)	0.95
Pinus sylvestris	2 3 5	Logan Saint Paul	68.06 (1.68)	0.93
Tilia americana	1 1 1 3	Lauderdale Saint Paul Windom	56.07 (2.12)	0.85
Ulmus pumila	2	Lauderdale	30.60 (1.94)	0.79
Ulmus thomasii	4	Saint Paul	43.09 (1.74)	0.85

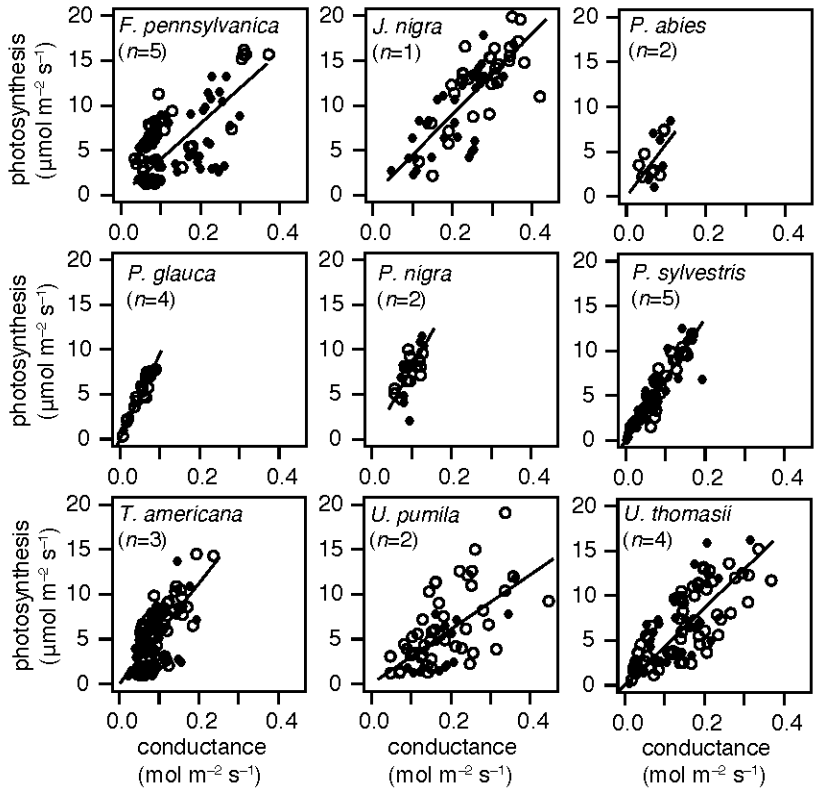

Figure A1-1. Relationship between leaf-level photosynthesis (µmol m^{-2} s^{-1}) and stomatal conductance (mol m^{-2} s^{-1}) for nine tree species in a suburban neighborhood of Minneapolis–Saint Paul, Minnesota. Data shown were from upper (open circles) and lower (closed circles) canopy layers and were collected from June to October, 2008 from Saint Paul, Lauderdale, Windom Park, and Logan Park sites. Each panel represents all trees measured for a given species with the number of trees shown in parentheses. Lines are linear regressions of the form: $y = ax$. Regression slopes and sites for each species are given in Table A1-1.

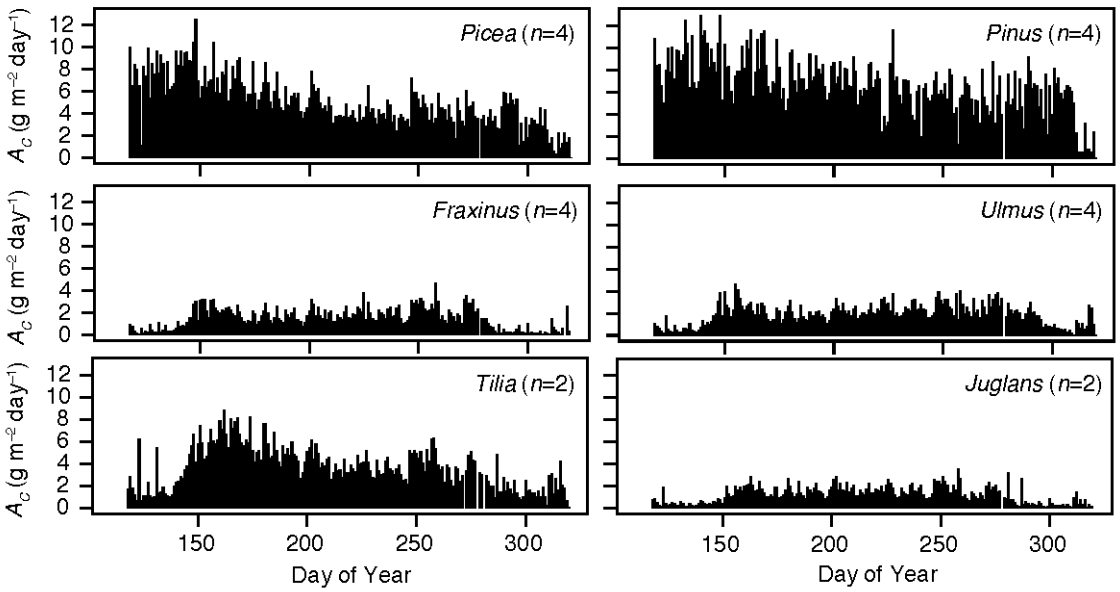

Figure A1-2. Daily sums of canopy photosynthesis per unit canopy area (A_C) for six tree genera in a suburban neighborhood of Minneapolis–Saint Paul, Minnesota. Each panel represents the mean of all trees per genus. Data shown are from the 2008 growing season. Numbers in parentheses are the number of trees per genus.

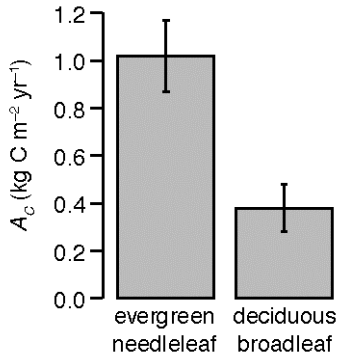

Figure A1-3. Annual sums of canopy photosynthesis per unit canopy area (A_C) in evergreen needleleaf and deciduous broadleaf plant functional types in a suburban neighborhood of Minneapolis–Saint Paul, Minnesota. Cumulative carbon uptake was summed from April to November 2008. Error bars represent ±1 standard error.